ERDC/CHL TR-11-1

US Army Corps
of Engineers®
Engineer Research and
Development Center

ERDC
INNOVATIVE SOLUTIONS
for a safer, better world

FEMA Region III Storm Surge Study

Coastal Storm Surge Analysis: Storm Surge Results

Report 5: Intermediate Submission No. 3

Jeffrey L. Hanson, Michael F. Forte, Brian Blanton,
Mark Gravens, and Peter Vickery

November 2013

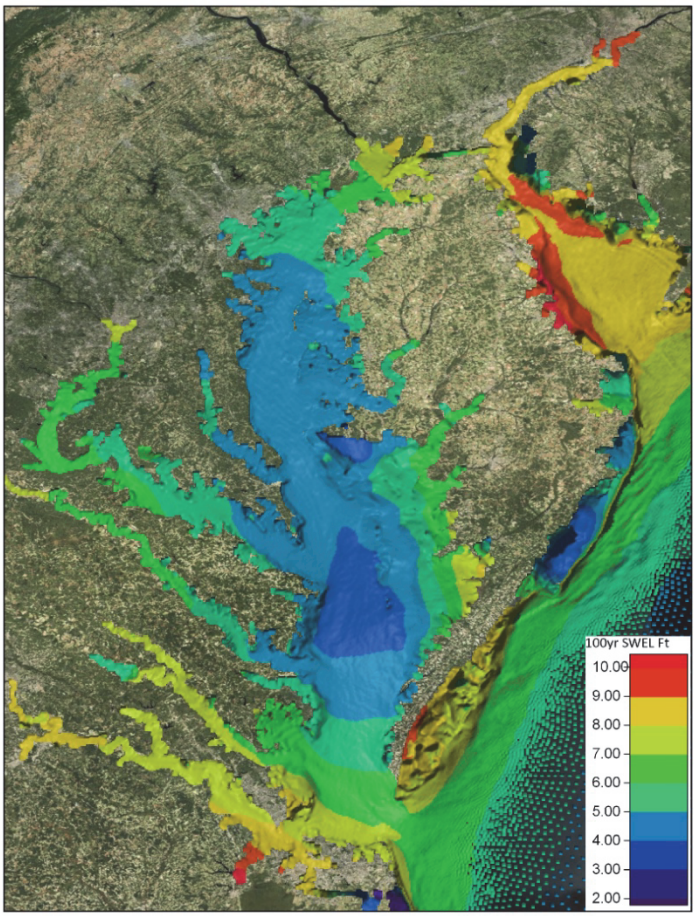

Approved for public release; distribution is unlimited.

Coastal and Hydraulics Laboratory

The US Army Engineer Research and Development Center (ERDC) solves the nation's toughest engineering and environmental challenges. ERDC develops innovative solutions in civil and military engineering, geospatial sciences, water resources, and environmental sciences for the Army, the Department of Defense, civilian agencies, and our nation's public good. Find out more at www.erdc.usace.army.mil.

To search for other technical reports published by ERDC, visit the ERDC online library at http://acwc.sdp.sirsi.net/client/default.

Coastal Storm Surge Analysis: Storm Surge Results

Report 5: Intermediate Submission No. 3

Jeffrey L. Hanson and Michael F. Forte

Field Research Facility
US Army Engineer Research and Development Center
1261 Duck Rd
Kitty Hawk, NC 27949

Brian Blanton

Renaissance Computing Institute
100 Europa Drive, Suite 540
Chapel Hill, NC 27517

Mark Gravens

Coastal and Hydraulics Laboratory
US Army Engineer Research and Development Center
3909 Halls Ferry Road
Vicksburg, MS 39180-6199

Peter Vickery

Applied Research Associates
8537 Six Forks Road, Suite 600
Raleigh, NC 27615

Report 5 of a series

Approved for public release; distribution is unlimited.

Prepared for Federal Emergency Management Agency
615 Chestnut Street
One Independence Mall, Sixth Floor
Philadelphia, PA 19106-4404

Under US Army Corps of Engineers Work Unit J64C87

Abstract

The Federal Emergency Management Agency (FEMA), Region III office, has initiated a study to update the coastal storm surge elevations within the states of Virginia, Maryland, and Delaware, including the Atlantic Ocean, Chesapeake Bay (including its tributaries), and the Delaware Bay. This effort is one of the most extensive coastal storm surge analyses to date, encompassing coastal floodplains in three states and including the largest estuary in the world. The study will replace outdated coastal storm surge stillwater elevations for all Flood Insurance Studies in the study area, and serve as the basis for new coastal hazard analyses and ultimately updated Flood Insurance Rate Maps (FIRMs). Study efforts were initiated in August of 2008, and were concluded in 2013.

The storm surge study utilized the ADvanced CIRCulation Model for Oceanic, Coastal, and Estuarine Waters (ADCIRC) for simulation of two-dimensional hydraulics. ADCIRC was coupled with two-dimensional wave models to calculate the combined effects of surge and wind-induced waves. A seamless modeling grid was developed to support the storm surge modeling efforts.

This report is the fifth and final in a series for the project. It provides a detailed overview of the extratropical and tropical storm statistical analyses, treatment of tidal influences, and final water level recurrence interval results. Furthermore, the similarities and differences between the new results and earlier study findings are explored.

DISCLAIMER: The contents of this report are not to be used for advertising, publication, or promotional purposes. Citation of trade names does not constitute an official endorsement or approval of the use of such commercial products. All product names and trademarks cited are the property of their respective owners. The findings of this report are not to be construed as an official Department of the Army position unless so designated by other authorized documents.

DESTROY THIS REPORT WHEN NO LONGER NEEDED. DO NOT RETURN IT TO THE ORIGINATOR.

Contents

Figures and Tables

Figures

Tables

Preface

This study was conducted for the Federal Emergency Management Agency (FEMA) under Project HSFE03-06-X-0023, NFIP Coastal Storm Surge Model for Region III and Project HSFE03-09-X-1108, Phase II Coastal Storm Surge Model for FEMA Region III. The FEMA technical monitor was Robin Danforth.

The work was performed by the Coastal Processes Branch of the Flood and Storm Protection Division, US Army Engineer Research and Development Center (ERDC) – Coastal and Hydraulics Laboratory (CHL). At the time of publication, Mark Gravens was Chief, Coastal Processes Branch; Dr. Ty V. Wamsley was Chief, Flood and Storm Protection Division; and Dr. Jeffrey L. Hanson was the Project Manager. The Deputy Director of CHL was Dr. Richard B. Styles and the Director was Jose E. Sanchez.

COL Jeffrey R. Eckstein was the ERDC Commander, and Dr. Jeffery P. Holland was the Director.

1 Study Overview

A comprehensive coastal storm surge risk assessment for the US Mid-Atlantic coast has been conducted for the Federal Emergency Management Agency (FEMA Region III) Risk Mapping, Assessment, and Planning program (Risk MAP). As indicated by Figure 1.1, the study area includes five major population centers and covers all tidal waters within the states of Virginia, Maryland, and Delaware including the Atlantic Ocean, Delaware Bay, and the third largest estuary in the world, Chesapeake Bay and associated tributaries. The primary objective of this ambitious undertaking was to produce detailed maps of the 100-yr recurrence interval coastal storm surge water levels resulting from extratropical and tropical storms. The study required developing a high-resolution representation of the regional topography and bathymetry; assembling and testing a coupled storm surge modeling system for winds, waves, tides, and currents; establishing a representative set of historical and synthetic storm events, and performing an extreme value analysis on the study results. Study methods and results are presented in a series of 5 submittal reports, of which this is the final.

Figure 1.1. Population density map of the FEMA Region III study region.

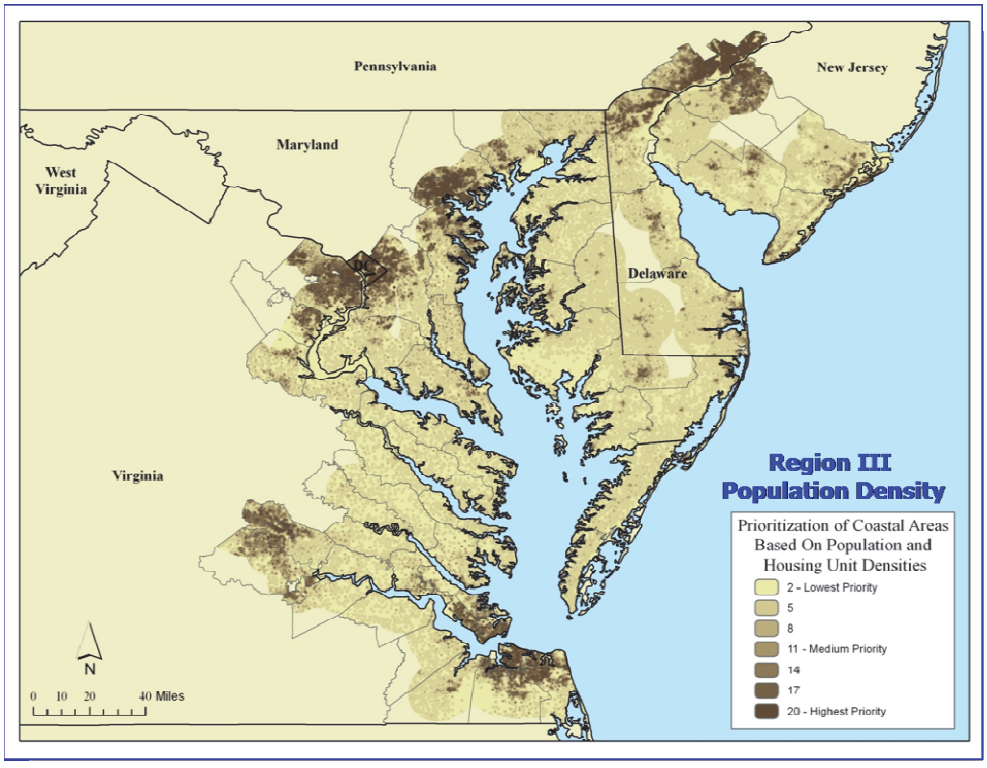

An end-to-end storm surge modeling system has been assembled around the ADvanced CIRCulation Model for Oceanic, Coastal, and Estuarine Waters (ADCIRC) for simulation of two-dimensional hydrodynamics. As described in Submittal 1.2 (Blanton et al. 2011), ADCIRC was dynamically coupled to the unstructured numerical wave model Simulating WAves Nearshore (UnSWAN) to calculate the contribution of waves to total storm surge. A 10-m horizontal resolution Digital Elevation Model (DEM) was constructed using the most recent topographic and bathymetric data available for the region, including coastal LIDAR surveys where available. Development of the Region III DEM is fully described in Submittal 1.1 (Forte et al. 2011). To facilitate the selected SWAN+ADCIRC system, the DEM was converted into a seamless unstructured modeling grid, appearing in Figure 1.2 (Blanton et al. 2011). The resulting grid contains minimum node-to-node spacing of 30-m horizontal resolution in the nearshore regions.

Figure 1.2. FEMA Region III unstructured modeling mesh, showing the overall modeling domain (left), and topographic detail within Region III (right).

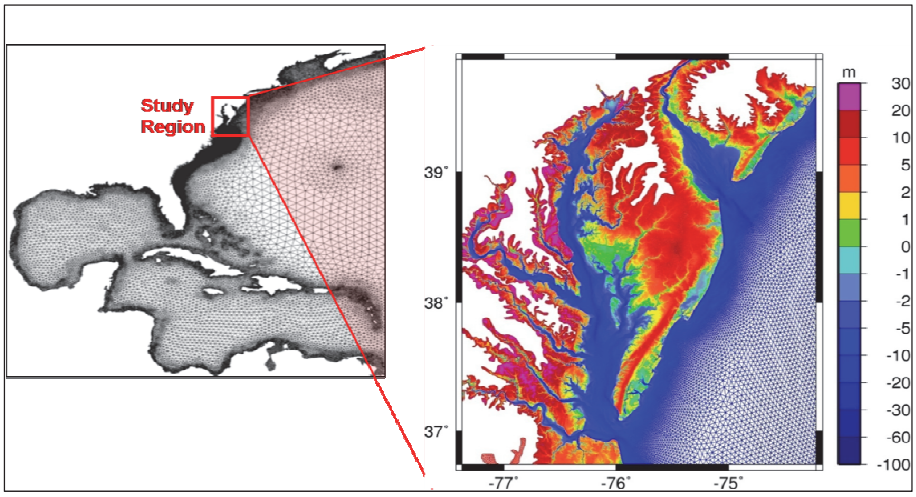

Modeling system skill was assessed through a comprehensive tidal calibration as well as event hindcasting using carefully reconstructed wind and pressure fields from three major flood events in the Mid-Atlantic: Hurricane Isabel, Hurricane Ernesto, and extratropical storm Ida (Nor'Ida). Using National Ocean Service (NOS) water-level observations from 18 stations as ground-truth, the modeling system is shown to replicate peak water levels with an overall bias of 0.02 m, root mean square error (RMSE) of 0.16 m and scatter index (SI) of 0.13. The validation results, appearing in Submittal 2 (Hanson et al. 2012) and summarized in Figure 1.3, suggest that the modeling system can be used with confidence to assess storm surge risk in the Mid-Atlantic region.

Figure 1.3. Validation of FEMA Region III coastal storm surge modeling system with NOS water level observations. Multi-station peak water level modeling results from Hurricanes Isabel and Ernesto and extratropical storm Nor'Ida are included.

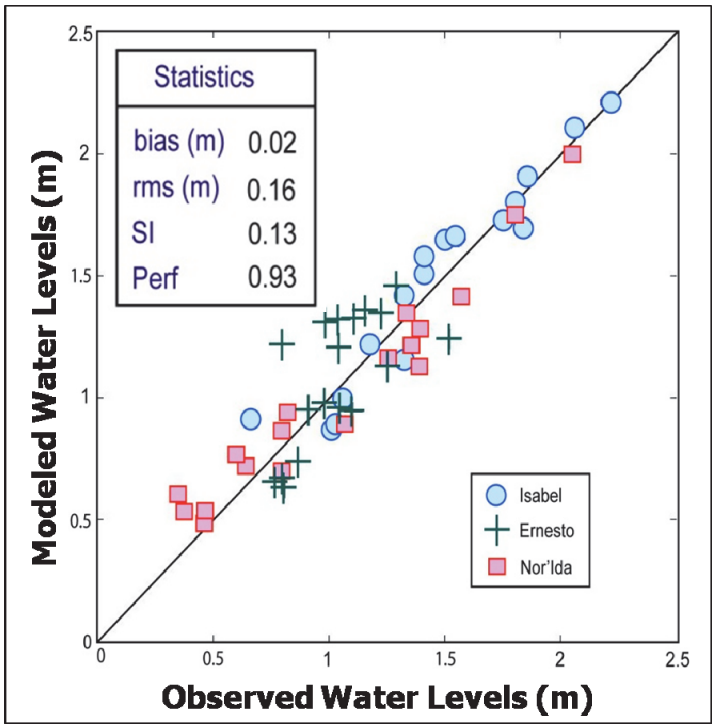

Atmospheric forcing for the study, fully described in Submittal 1.3 (Vickery et al. 2012), is derived from both extratropical and tropical storms. Wind and pressure fields from the 29 top-ranked extratropical storms from 1975-2009 (including Nor'Ida) were carefully reconstructed for the study by Oceanweather, Inc. As the historic record of 20 hurricanes in the past 60 years is insufficient for a 100-yr-recurrence interval analysis, a synthetic storm set was required. The tropical storm track and intensity parameters from a total of 156 representative events were extracted from a 100,000-yr synthetic storm set developed by Applied Research Associates, Inc., for establishing American Society of Civil Engineers (ASCE) wind-loading standards. A Hurricane Boundary Layer (HBL) model was used to convert the storm track parameters to wind and pressure fields. Validity of the approach was established through statistical comparison of resulting storm surges with the historic record.

This report focuses on the production-run modeling and results of 186 storm events (29 extratropical and 156 tropical), producing a region-wide set of storm-response water levels that include the combined effects of winds, waves, tides, and currents. A summary flow chart for the study

appears in Figure 1.4. Extreme value analyses were conducted using the Empirical Simulation Technique (EST) for the extratropical storm surge events and the Joint Probability Method (JPM) for tropical storm surges. Furthermore, the resulting water levels are placed in historical context through comparison with previous study results.

Figure 1.4. Top-level overview of the Region III coastal storm surge study.

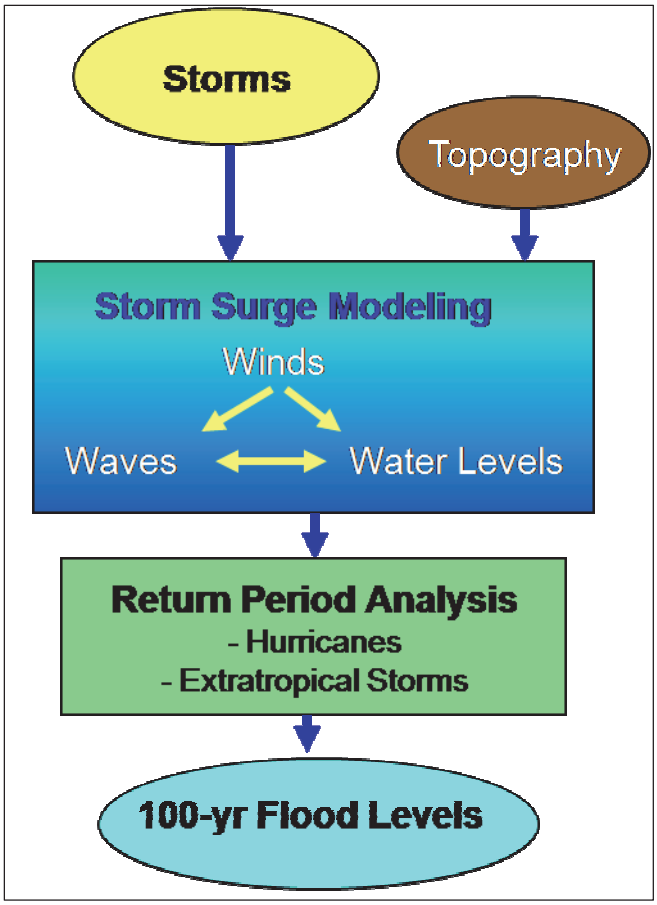

2 Extratropical Storm Approach

This chapter describes the analysis undertaken to quantify the contribution of extratropical storm events to combined (total) stage frequency relationships developed in support of the FEMA Region III coastal storm surge study. Significant extratropical storm events influencing the primary study area of the Chesapeake Bay and Delaware Bay were identified based on the available historical record between January 26, 1975, and August 31, 2008. For each of the identified storms, a detailed hindcast of sea level pressures and wind fields was generated. These hindcast results in turn provided input to ADCIRC which was used to estimate water levels throughout the Region III study area. Peak water levels associated with each storm, as determined from the ADCIRC results, served as input combined with representative tide information to the Empirical Simulation Technique (EST) which allowed for the estimation of stage frequency information associated with extratropical storms. This chapter will summarize the extratropical storm selection methodology, describe the EST statistical analysis approach including accounting for astronomical tide contributions to total stage, and present the results from validation tests to demonstrate the robustness and reliability of the statistical analysis.

Storm selection

The extratropical storm selection process is fully described in Submittal 1.3 (Vickery et al. 2012). A storm surge ranking method, using long-term NOS water level records, resulted in the selection of 30 extratropical storms over the period January 26, 1975, to August 31, 2008. At each selected NOS station, the water level peaks greater than the 99th percentile residual water level and were identified individually as candidate storm events. Storm peaks were then ranked by station and the top-ranked events matched with those from the other NOS stations within a 3-day window. The population of 30 events was obtained by taking the top-ranked storms from each of the NOS stations sequentially and removing storms found to be tropical in nature as determined by historical tropical storm/hurricane tracks. During this period, the tropical cyclones of David (1979), Gloria (1985), Josephine (1986), Isabel (2003), and Ernesto (2006) were identified and removed from the storm list. Furthermore, multiple storm peaks at a single NOS site within a 3-day period were merged into a single storm event.

The occurrence of extratropical storm Nor'Ida in November 2009 resulted in that storm being added to the list. Subsequently, two of the lowest-ranked storms were eliminated, resulting in a total population of 29 extratropical storms used in the study recurrence interval calculations.

Statistical analysis approach

The statistical analysis approach applied for the extratropical storms involved the application of the Empirical Simulation Technique (EST) (Scheffner et al. 1999). The EST is a life-cycle approach to frequency-and error-associated risk analysis. Universal applicability of the EST has been demonstrated through implementation to projects located along all coasts of the United States to develop frequency-of-occurrence relationships for storm-related impacts such as storm-surge elevation, vertical erosion of dredged-material mounds, and horizontal recession of coastal beaches and dunes. As a result of this demonstrated capability, the EST is one of several approaches that has been recommended by the Headquarters, US Army Corps of Engineers, Washington, DC, for developing risk-based design criteria.

The EST utilizes observed and/or computed parameters associated with site-specific historical events as a basis for developing a methodology for generating multiple life-cycle simulations of storm activity and the effects associated with each simulated event. The technique uses joint probability relationships inherent in the local site-specific database. Therefore, probabilities are site-specific, do not depend on fixed, parametric relationships, and do not assume parameter independence. Thus, the EST is "distribution free" and nonparametric.

EST is a statistical procedure for simulating nondeterministic, multi-parameter systems such that frequency-of-occurrence relationships for storm-related response parameters (e.g., volume of erosion above datum or change in dune-crest elevation) can be determined. The EST is a generalized procedure for generating N repetitions of a T-yr simulation based on a re-sampling-with-replacement, nearest neighbor interpolation procedure. A statistical analysis of the resulting simulations is used to develop frequency relationships for any storm response as a function of input parameters that are descriptive of the storm event but have unknown joint probabilities.

The EST is based on a "Bootstrap" re-sampling-with-replacement, interpolation and subsequent smoothing technique in which a random sampling of a finite length database is used to generate a larger database. An assumption is that future events will be statistically similar in magnitude and frequency to past events. The EST begins with an analysis of historical events that have impacted a specific locale. The selected database of events is then parameterized to define the characteristics of each event and the impacts of that event. Parameters that define the storm are referred to as input vectors. Response vectors define storm-related impacts such as inundation and shoreline/dune erosion. These input and response vectors are then used as a basis for generating life-cycle simulations of storm-event activity. The present study employed a univariate EST analysis where the input vector is total surge and the response vector is total surge.

Input vectors

Input vectors describe the physical characteristics of the storm event and the location of the event with respect to the area of interest. These values are defined as an N-dimensional vector space as follows:

$$v = \left(v_1, v_2, v_3, \ldots, v_N\right) \tag{1}$$

For the present study, the one-dimensional input vector is total water level or storm surge. For the development of stage frequency relationships, modeled peak water elevation plus the astronomical tide contribution were used to estimate the total peak water surface elevation.

Response vectors

The response vectors describe any response that can be attributed to the passage of the storm. This M-dimensional space is defined as the following:

$$r = \left(r_1, r_2, r_3, \ldots, r_M\right) \tag{2}$$

Response vectors can include parameters such as maximum surge elevation, shoreline erosion, and/or dune recession. In the present study the response vector is the maximum total water surface elevation.

Although response vectors are related to input vectors,

$$v \rightarrow r \tag{3}$$

the interrelationship is highly nonlinear and involves correlation relationships that cannot be directly defined, i.e., a nonparametric relationship. For example, in addition to storm input parameters, storm surge is a function of local bathymetry, shoreline slope and exposure, ocean currents, temperature, etc., as well as their spatial and temporal gradients. It is assumed, however, that these combined effects are reflected by the response vectors even though their individual contribution to the response is unknown.

Response vectors define storm effects such as the maximum surge elevation, shoreline erosion, or dune recession. These parameters are usually not available from post-storm records at the spatial density required for a frequency analysis. Therefore, response vectors are generally computed via numerical models. For example, as in the present study, if the response of interest is maximum surge elevation, long-wave hydrodynamic models are coupled to databases containing extratropical wind fields. If the response of interest involves storm-related erosion, additional models are used that access the hydrodynamic model surge elevation and current hydrographs to compute, for example, berm/dune erosion.

The historical data for storms can be characterized as follows:

$$\left[v_i;\ i = 1, \ldots, I\right] \tag{4}$$

where I is the number of historical storm events. Events of the historical database v_i contain d_v-components such that

$$V_i = R^{d_v} \tag{5}$$

where R^{d_v} denotes a d_v–dimensional space.

Ideally, there are an adequate number of historic event parameters to fill the d_v–dimensional vector space. An adequate number refers to both the number of events and the severity of events as measured by their descriptive parameters. If the number of historic events is sparse, then some event augmentation may be necessary. If the historic population contains redundant events, i.e., similar events with respect to input and response vector space, then some events may be omitted from the set of historic

events. In the present study, because of the significant computational effort associated with the development of appropriate wind fields and simulation of storm surges over the rather vast computational domain of interest, a representative training set of storms was used. In Section 2.4 the validity of the selected representative training set of storms is demonstrated by comparing the stage frequency outcome from the representative training set of storms to the stage frequency outcome obtained for the full historical record of storms.

EST implementation

The goal of the EST is summarized as follows:

- Given the following:
    - The historical data
    - The "training set"
    - The response vectors calculated from the training set
- Produce N simulations of a T-yr sequence of events, each with their associated input vectors and response vectors.

Two criteria are required of the T-yr sequence of events. The first criterion is that the individual events must be similar in behavior and magnitude to the historical events, i.e., the interrelationships among the input and response vectors must be realistic. The second criterion is that the frequency of storm events has remained the same.

Storm consistency with past events

The first major assumption in the EST is that hypothetical events will be similar to past events. This criterion is maintained by ensuring that the input/response vectors for simulated events have similar values and joint probabilities to those of the training set of historical or historically based events. The simulation of realistic events is accounted for in the nearest neighbor interpolation/bootstrap/re-sampling technique developed by Borgman et al. (1992). By using the training set as a basis for defining future events, unrealistic events are not included in the life cycle of events generated by the EST. Events that are output by the EST are similar to those in the training set with some degree of variability from the historic/historically based events. This variability is a function of the

nearest neighbor; therefore, the deviation from historic conditions is limited to natural variability of the system.

The EST is not simply a re-sampling of historical events technique, but rather an approach intended to simulate the vector distribution contained in the training-set database population. The EST approach is to select a sample storm based on a random number selection from 0 to 1 and then perform a random walk from the event X_i with x_1 and x_2 response vectors to/from the nearest neighbor vectors. The walk is based on independent uniform random numbers on (-1, 1) and has the effect of simulating responses that are not identical to the historical events but are similar to events that have historically occurred.

The process can be summarized by selecting a specific storm event from the training set and proceeding to the location in the multi-dimensional input vector space corresponding to the event. From that location, perform a nearest neighbor random walk to define a new set of input vectors. This defines a new multi-dimensional input vector space that is different from that of the specific event initially selected but not substantially unlike it since it was developed from the random-walk procedure starting from the selected events. This new input vector defines a new storm, similar to the original but with some variability in parameters. Finally, use this new input vector to interpolate a corresponding response.

Storm frequency

The second criterion to be satisfied is that the total number of storm events selected per year must be statistically similar to the number of historical events that have occurred at the area of concern. Given the mean frequency of storm events for a particular region, a Poisson distribution is used to determine the average number of expected events in a given year. For example, the Poisson distribution can be written in the following form:

$$\Pr\left(s;\lambda\right)=\frac{\lambda^{s}\ e^{-\lambda}}{s!} \tag{6}$$

For s = 0, 1, 2, 3,... the probability, $Pr(s\ ;\ \lambda)$, defines the probability of having s events per year where λ is a measure of the historically based number of events per year.

Output of the EST program is multiple life-cycle simulations, i.e., N-repetitions of T-yrs of simulated storm-event responses. It is from these responses that frequency-of-occurrence relationships can be computed. Because EST output is of the form of multiple time-series simulations, post-processing of the output yields mean-value frequency relationships with definable error estimates. The computational procedure followed is based on the generation of a cumulative distribution function corresponding to each of the T-yr sequence of simulated data.

Risk-based frequency analysis

The methodology for post-processing the life-cycle simulation to generate estimates of frequency and associated variability is presented in the following. The procedures for computing mean-value frequency-of-occurrence relationships from the N-repetitions of T-yrs of storm-event impact are presented along with an error analysis in the form of a standard deviation from the mean value. Finally, the mechanics for computing frequency relationships for combined storm types (tropical storms and extratropical storms) are presented.

Frequency-of-occurrence computations

Estimates of frequency of occurrence begin with a calculation of a Cumulative Distribution Function (CDF) for the response vector of interest. Let $X_1, X_2, X_3,..., X_n$ be n identically distributed random response variables with a CDF

$$F_x(x) = \Pr[X \le x] \tag{7}$$

where $Pr[\ \ ]$ represents the probability that the random variable X is less than or equal to some value x, and $F_x(x)$ is the cumulative probability distribution function ranging from 0.0 to 1.0. The problem is to estimate the value of F_x without introducing some parametric relationship for probability. The following procedure is adopted because it makes use of the probability laws defined by the data and does not incorporate any prior assumptions concerning probability.

Assume a set of n observations of x data. The n values of x are first ranked in order of increasing size such that

$$x_{(1)} \leq x_{(2)} \leq x_{(3)} \leq \ldots \leq x_n \tag{8}$$

where the parentheses surrounding the subscript indicate that the data have been rank-ordered. The value $x(1)$ is the smallest in the series and $x(n)$ represents the largest. Let r denote the rank of the value $x(r)$ such that rank 1 is the smallest and rank $r = n$ is the largest.

An empirical estimate of $F_x(x(r))$, denoted by $\hat{F}_x(x(r))$, is given by Gumbel (1954) (see also Borgman and Scheffner 1991 or Scheffner and Borgaman 1992):

$$\hat{F}_x\left(x_{(r)}\right) = \frac{r}{(n+1)} \tag{9}$$

for $\{x(r), r = 1,2,3,\ldots,n\}$. This form of estimate allows for probabilities of future values of x to be less than the smallest observation $x(1)$ with probability of $1/(n+1)$, and to be larger than the largest value $x(n)$ also with probability $r/(n+1)$.

Consider that the CDF for some storm impact corresponding to an n-yr return period event can be approximated. The cdf as defined by Equation 9 is used to develop stage-frequency relationships in the following manner:

$$F\left(x_{(n)}\right) = 1 - \frac{1}{n} \tag{10}$$

where $F\left(x_{(n)}\right)$ is the simulated CDF for the n-yr impact. Frequency-of-occurrence relationships are obtained by computing a simulated CDF for an n-yr event according to Equation 10, and using that value for a CDF from Equation 9 and the rank ordered observations linearly interpolating a stage. Equations 9 and 10 are applied to each of the N-repetitions of T-yrs of storm events simulated via the EST. Therefore, there are N frequency-of-occurrence relationships generated. Then, for each return period year, the standard deviation is computed to define an error band of ± one standard deviation corresponding to each mean value curve.

Application

The procedures outlined above for a single response analysis for coastal storm surge have been applied to projects along all coasts of the United

States and for a variety of applications. The approach has been shown to be accurate, relatively easy to implement. However, as with any numerical methodology, accurate results require accurate input.

Treatment of astronomical tides

The production-run simulation of extratropical storm surge was performed in the absence of tidal forcing. Consequently, in order to develop stage-frequency relationships reflecting total water-surface elevation it is necessary to include the contribution of astronomical tides in the final solution. As the typical duration of extratropical storms exceeds the duration of the tidal cycle, it was assumed that high tide will coincide with peak storm surge. This assumption eliminates the need to consider tide phase and aligning peak surge at various phases of the tide such as high tide, mean tide falling, low tide, etc. However, consideration of the spring-neap tidal amplitude cycle is required.

The first step in this process involved computing statistically valid estimates of the spring, neap, and mean tidal amplitude. The spring tidal amplitude was estimated as the mean tidal amplitude of the highest 25th percentile of all predicted tides within a 19-yr tidal epoch. The mean tidal amplitude was estimated as the mean tidal amplitude of the central 50 percent of all predicted tides within a 19-yr tidal epoch. The neap tidal amplitude was estimated as the mean tidal amplitude of the lowest 25^{th} percentile of all predicted tide within a 19-yr tidal epoch. These calculations were performed at all computational nodes within the study domain based on the previously established tidal constituents.

To reflect the inclusion of tidal contributions to total water level in the EST analysis, the training set of storms was expanded by a factor of 4. For each storm, the peak surge elevation was increased by the estimated high-tide amplitude corresponding to spring tide, mean tide, and neap tide. Those storms associated with mean high-tide amplitude were weighted double to those associated with spring and neap high-tide amplitude.

By adding the high-tide amplitudes associated with statistically valid tidal ranges to the simulated peak surge values, the training set of storms, and their associated response vectors (peak total water elevations) now include the contribution of astronomical tides. The results of the EST analysis procedure therefore include the contribution of astronomical tides to the total predicted stage-frequency relationships produced in this study.

Examples of the magnitude of the tidal contribution to the predicted stage frequency are illustrated in Figures 2.1 and 2.2. In Figure 2.1, the response points represent the response vectors that were input to the EST analysis whereas the solid lines represent the computed stage-frequency relationship at the NOS station at Chesapeake Bay Bridge Tunnel, VA. Plotted in Figure 2.2 are the computed stage-frequency relationships with and without the tidal contribution at the NOS station at Cape May, NJ. Note that the tidal contribution to the stage-frequency relationship is different at these two stations. The reason for these differences is the relative magnitude of the tidal contribution as related to the magnitude of the storm surge contribution to the total water level. At the Chesapeake Bay Bridge Tunnel station, the statistically representative tidal amplitudes range between 0.27 m and 0.49 m and are small as compared to the magnitude of the storm surges, particularly at the low-frequency (high return period) end of the stage-frequency relationship. As a consequence, the magnitude of the tidal contribution to total water level drops off as there is movement from high-frequency events to low-frequency events (left to right on the figure). At Cape May, the magnitude of the tidal contribution to the total water level stage-frequency relationship is nearly uniform across all return periods. This is a result of the relatively large tidal amplitudes, which range between 0.52 m and 0.88 m, as compared to the magnitude of the storm surges. Consequently, the magnitude of the tidal contribution to the total water level stage frequency is nearly constant at ~0.65 m across all return periods.

EST Comparison with GPD

A set of three comparison tests were performed in this study. The first test compared results from of the EST analysis procedure to the parametric Generalized Pareto Distribution (GPD). These comparisons employed the available long-term measurements at six NOS recording stations at which long-term measurements were available (Atlantic City, NJ; Baltimore, MD; Chesapeake Bay Bridge Tunnel, VA; Cape May, NJ; Lewes, DE; and Sewells Point, VA). The results of these comparisons are shown in Figures 2.3 through 2.8.

The red points in these figures represent the available measured water levels that provided the input to the two statistical extremal analysis procedures. The solid blue line is the resulting stage-frequency relationship generated by the parametric analysis procedure whereas the solid green line is the resulting stage-frequency relationship generated by the EST analysis procedure. The dashed lines represent the 90 percent confidence interval

Figure 2.1. Tide contribution to stage-frequency relationship at Chesapeake Bay Bridge Tunnel, MD, NOS station.

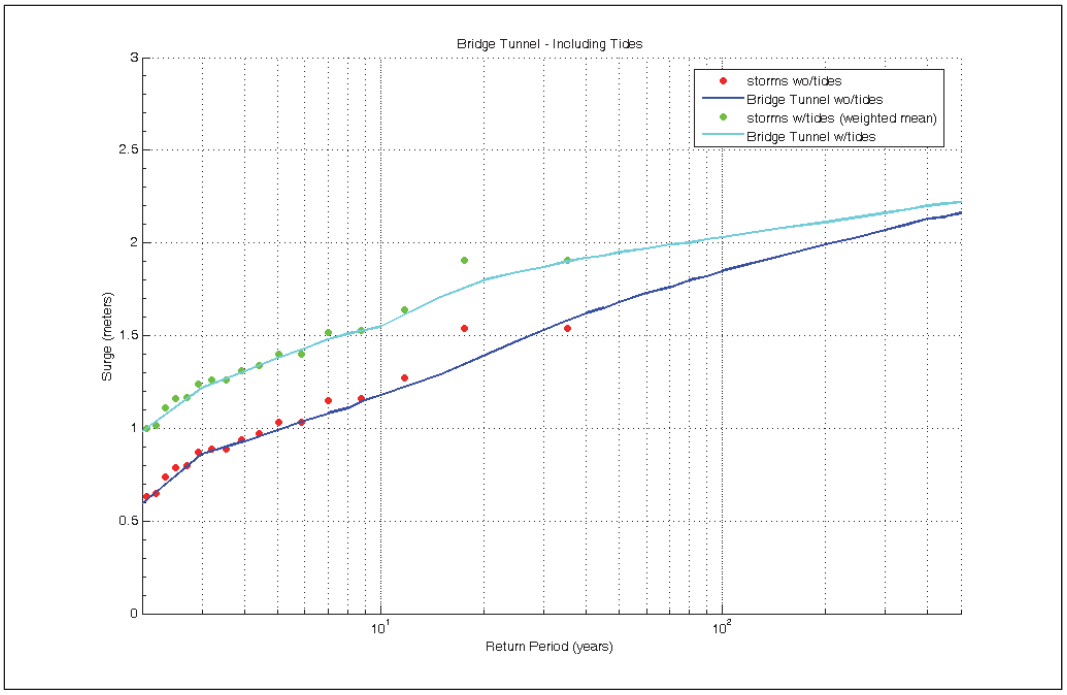

Figure 2.2. Tide contribution to stage-frequency relationship at Cape May, NJ, NOS station.

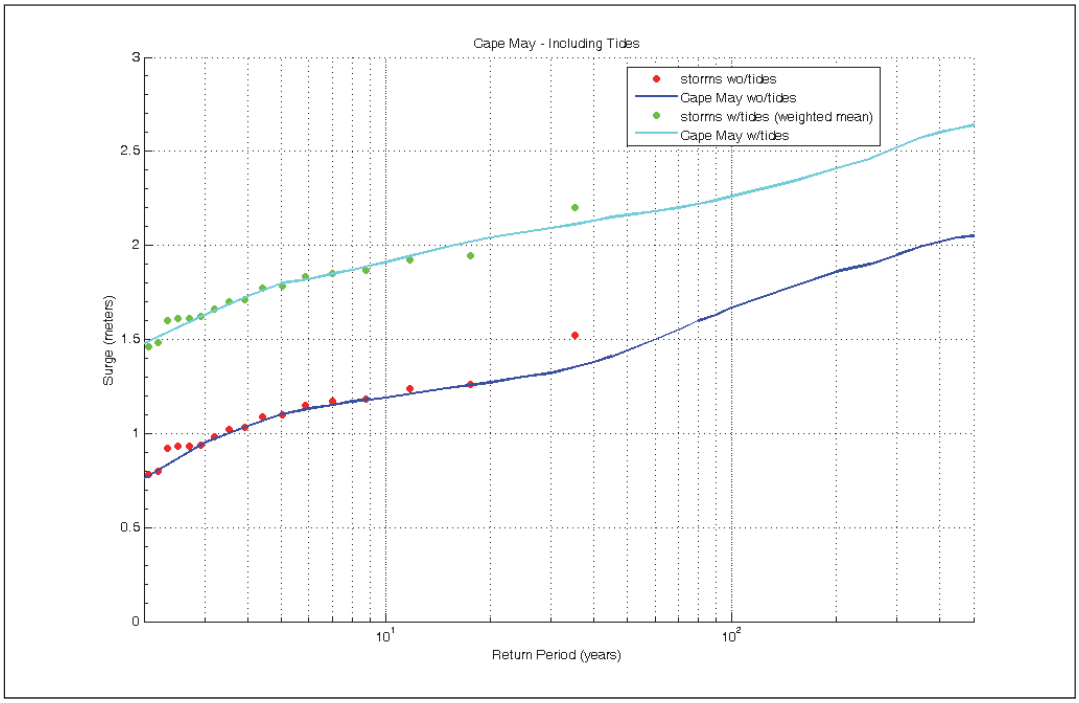

Figure 2.3. Comparison of EST and GPD (parametric) stage-frequency relationships based on long-term measurements at NOS recording station Atlantic City, NJ.

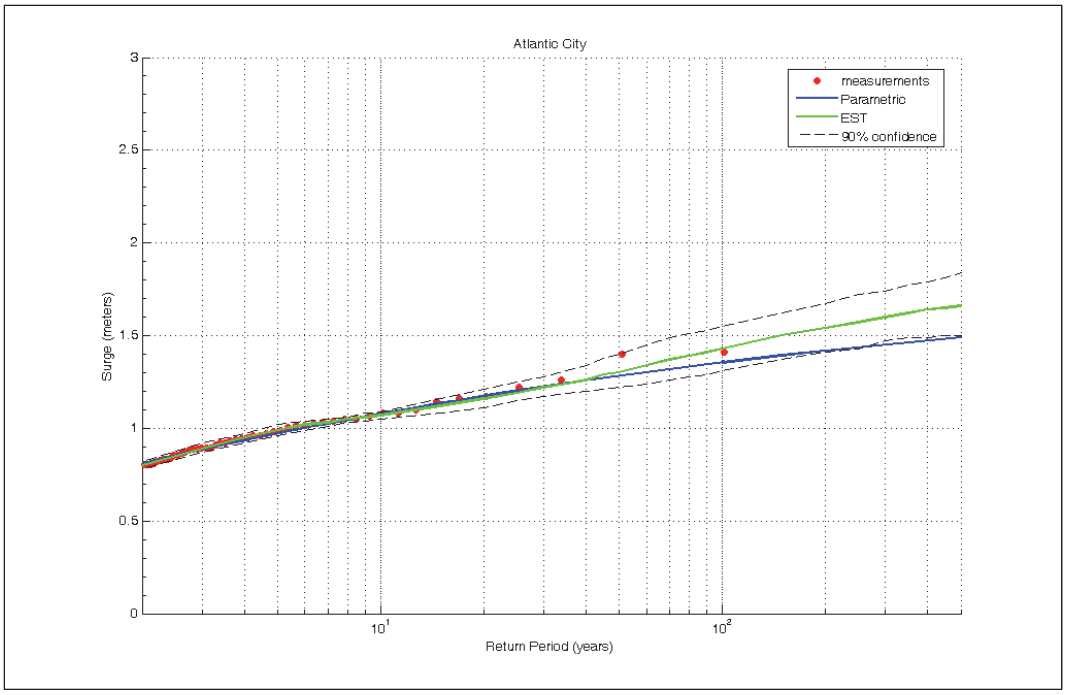

Figure 2.4. Comparison of EST and GPD (parametric) stage-frequency relationships based on long-term measurements at NOS recording station Baltimore, MD.

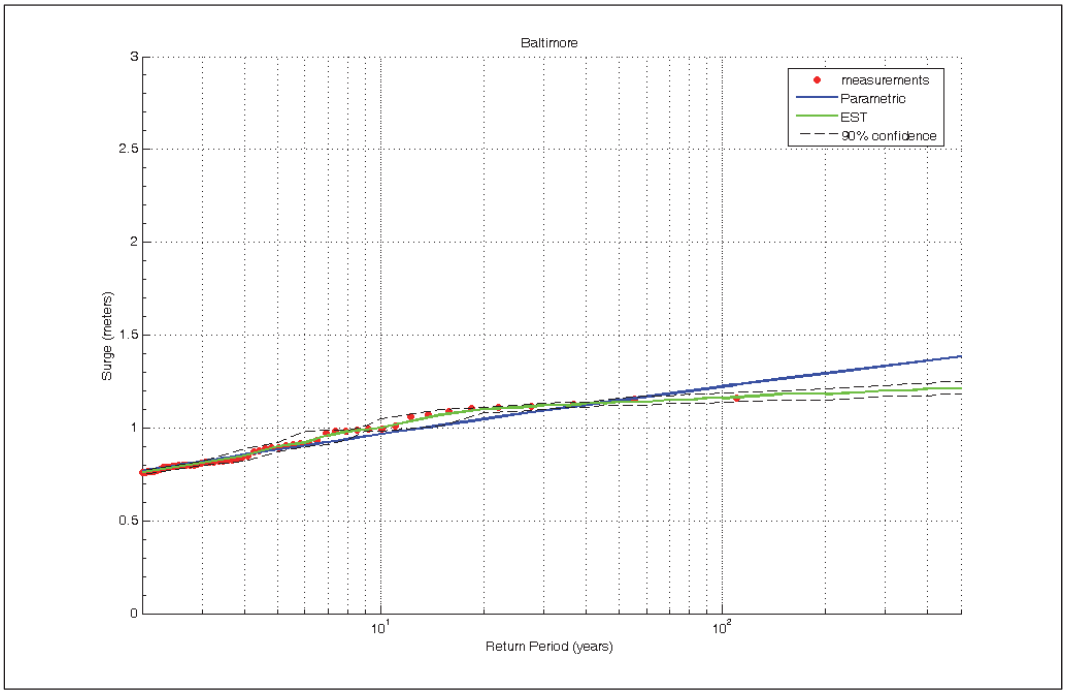

Figure 2.5. Comparison of EST and GPD (parametric) stage-frequency relationships based on long-term measurements at NOS recording station Chesapeake Bay Bridge Tunnel, VA.

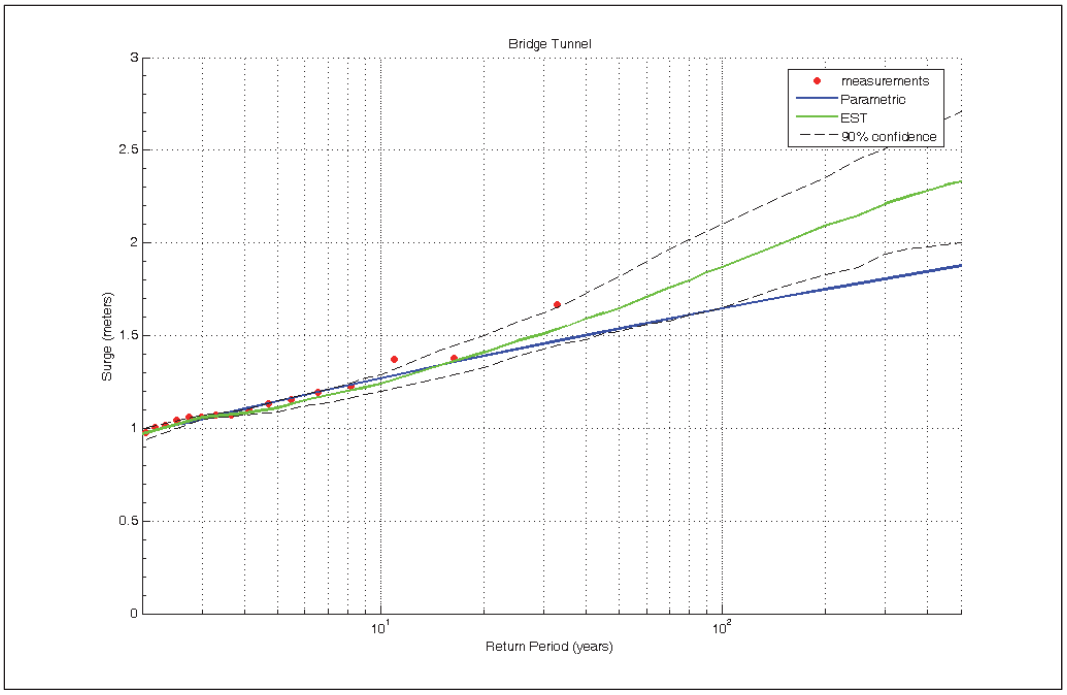

Figure 2.6. Comparison of EST and GPD (parametric) stage-frequency relationships based on long-term measurements at NOS recording station Cape May, NJ.

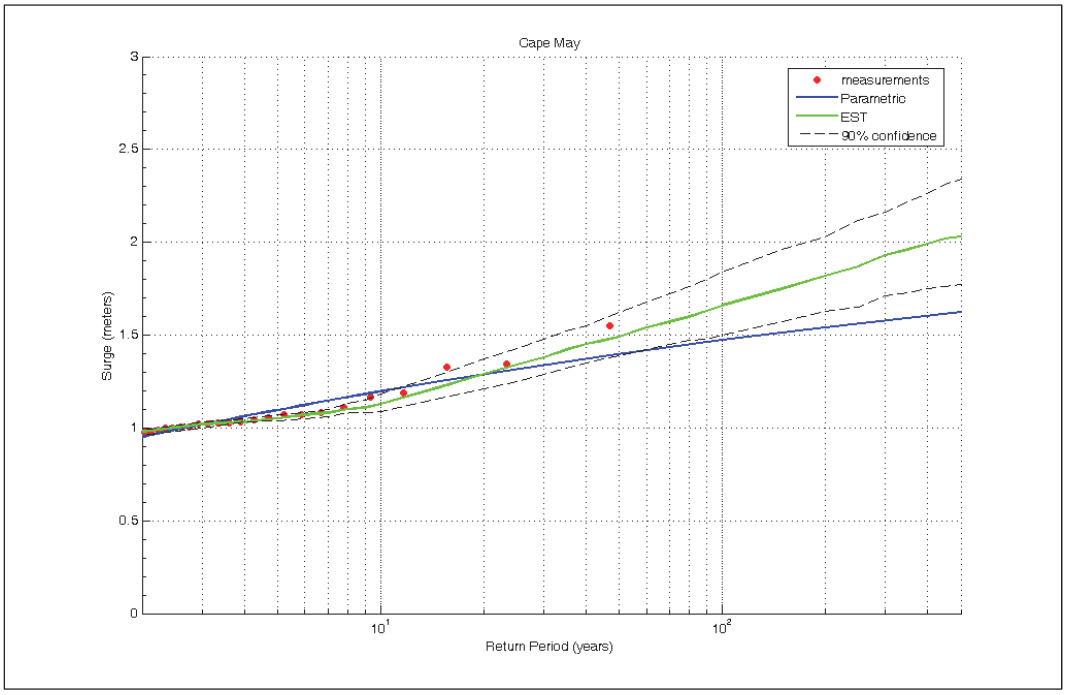

Figure 2.7. Comparison of EST and GPD (parametric) stage-frequency relationships based on long-term measurements at NOS recording station Lewes, DE.

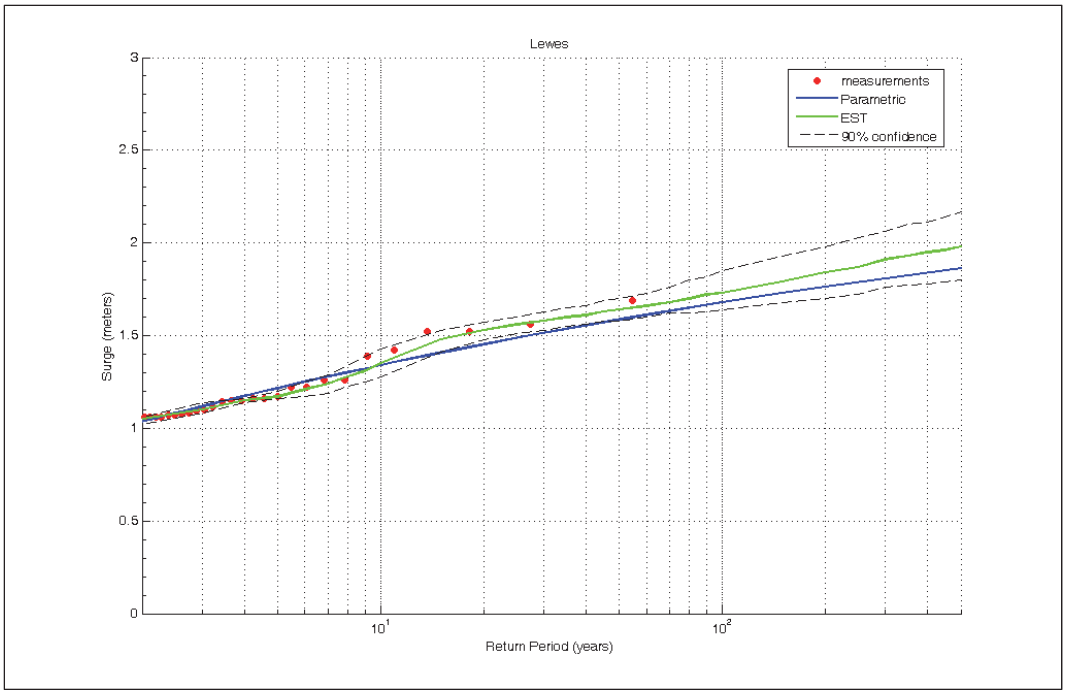

Figure 2.8. Comparison of EST and GPD (parametric) stage-frequency relationships based on long-term measurements at NOS recording station Sewells Point, VA.

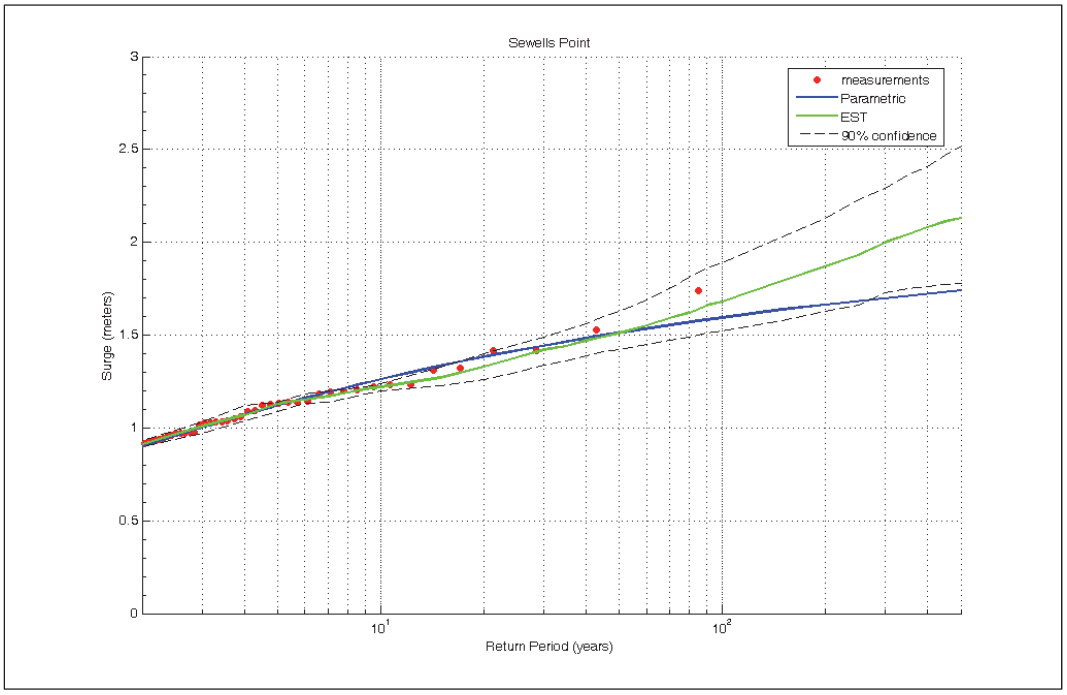

based on the EST analysis procedure. As the measurements fall within the 90-percent confidence interval, the EST analysis provides a reasonable prediction of the measured stage-frequency distributions. Furthermore, for most of the long-term recording stations, the parametric result is within or very near the 90-percent confidence interval generated by the EST procedure.

The second set of tests compared return-period results from the selected subset of extratropical storms to the available long-term measurements. Again, this validation test relied on measured data alone. Figures 2.9 through 2.14 display the measured data points and the resulting stage-frequency relationships generated by the EST analysis procedure. The red points represent the available long-term measurements and the solid blue line is the associated EST-generated stage-frequency curve. The green points are the measured surge for the selected subset of storms (the training set of storms) and the light blue line is the associated EST-generated stage-frequency curve.

Figure 2.9. Comparison of long-term measurements and selected subset of storms at NOS recording station Atlantic City, NJ.

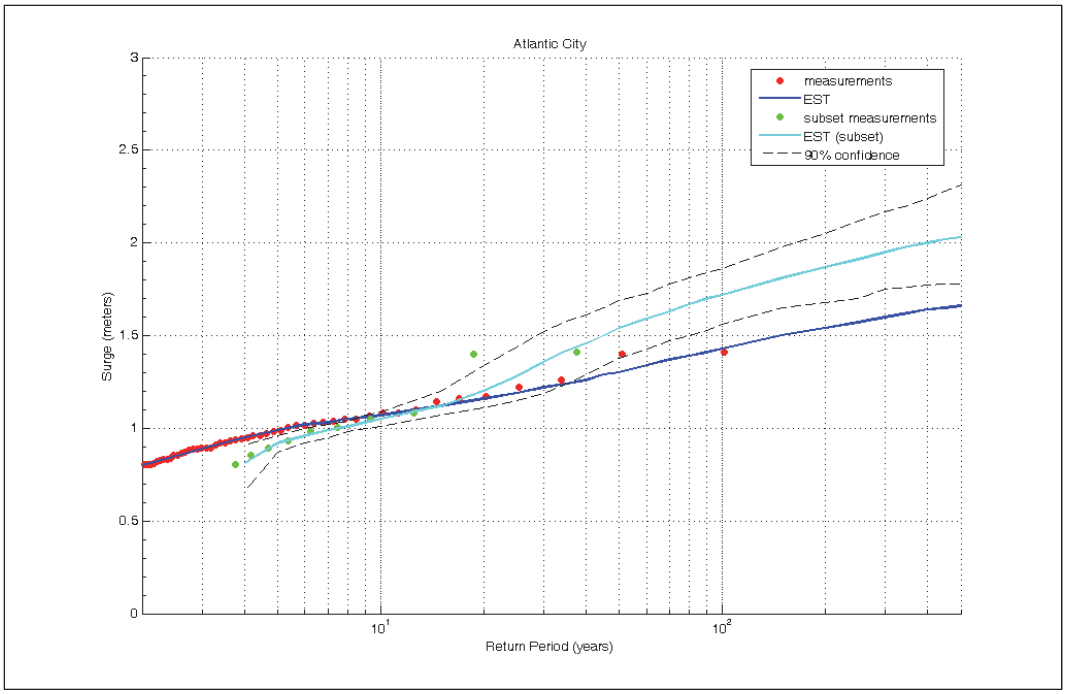

Figure 2.10. Comparison of long-term measurements and selected subset of storms at NOS recording station Baltimore, MD.

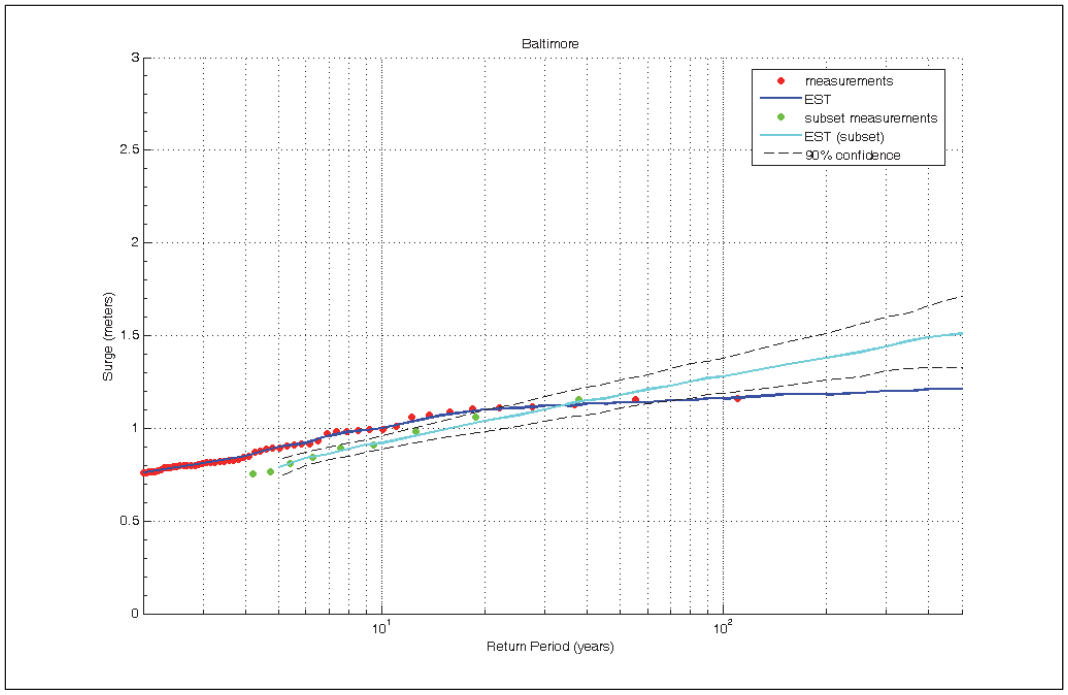

Figure 2.11. Comparison long-term measurements and selected subset of storms at NOS recording station Chesapeake Bay Bridge Tunnel, VA.

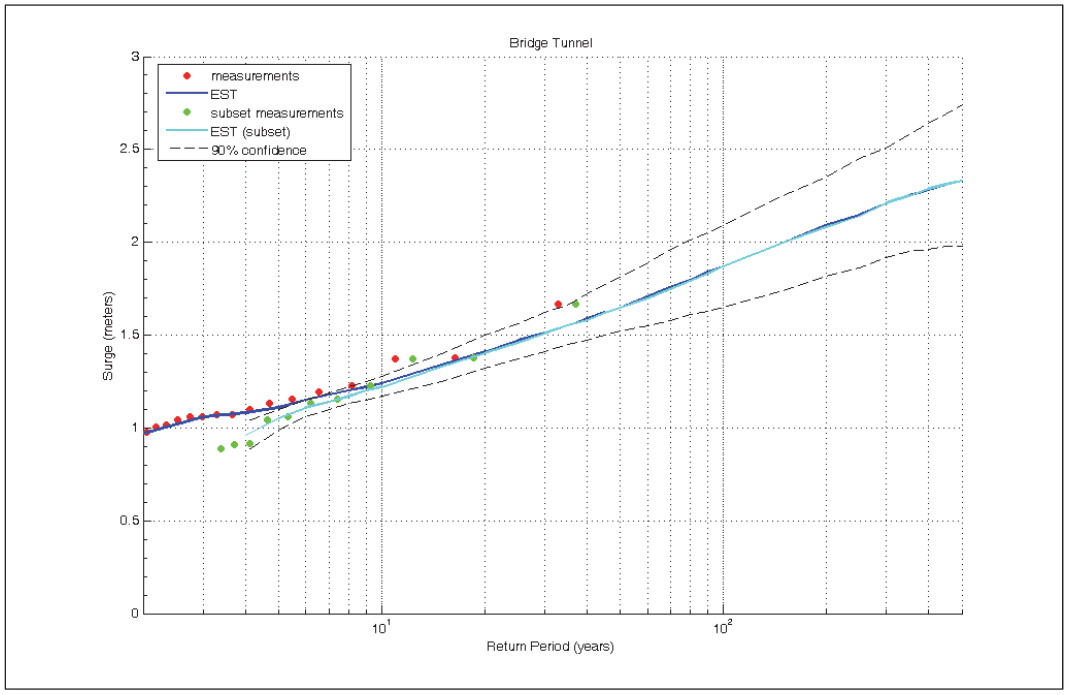

Figure 2.12. Comparison long-term measurements and selected subset of storms at NOS recording station Cape May, NJ.

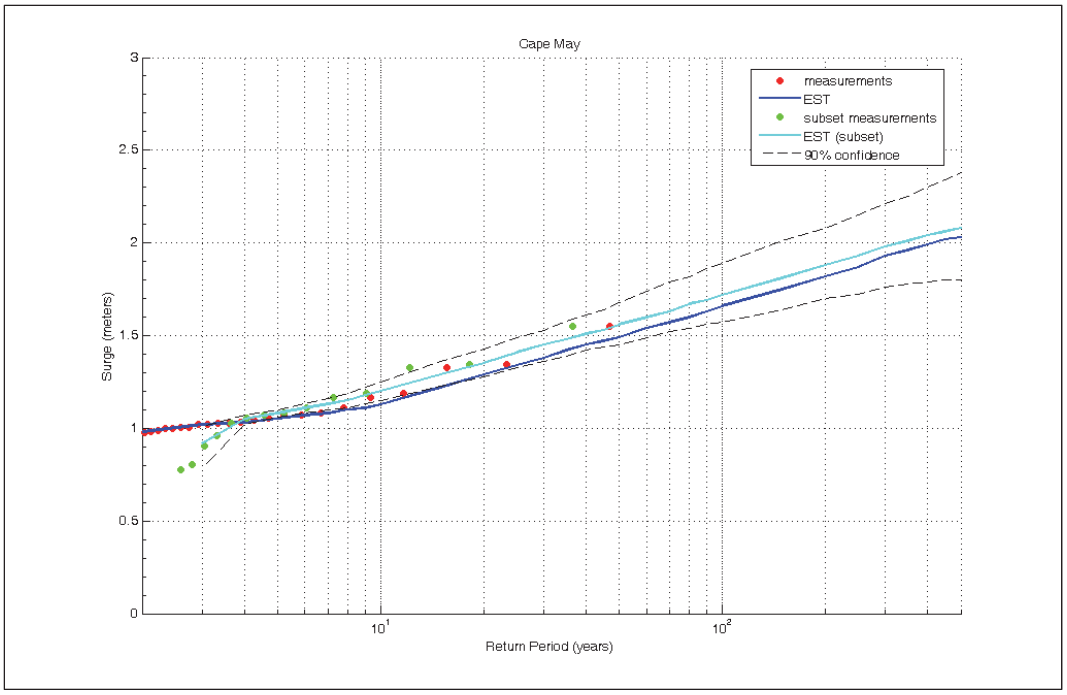

Figure 2.13. Comparison long-term measurements and selected subset of storms at NOS recording station Lewes, DE.

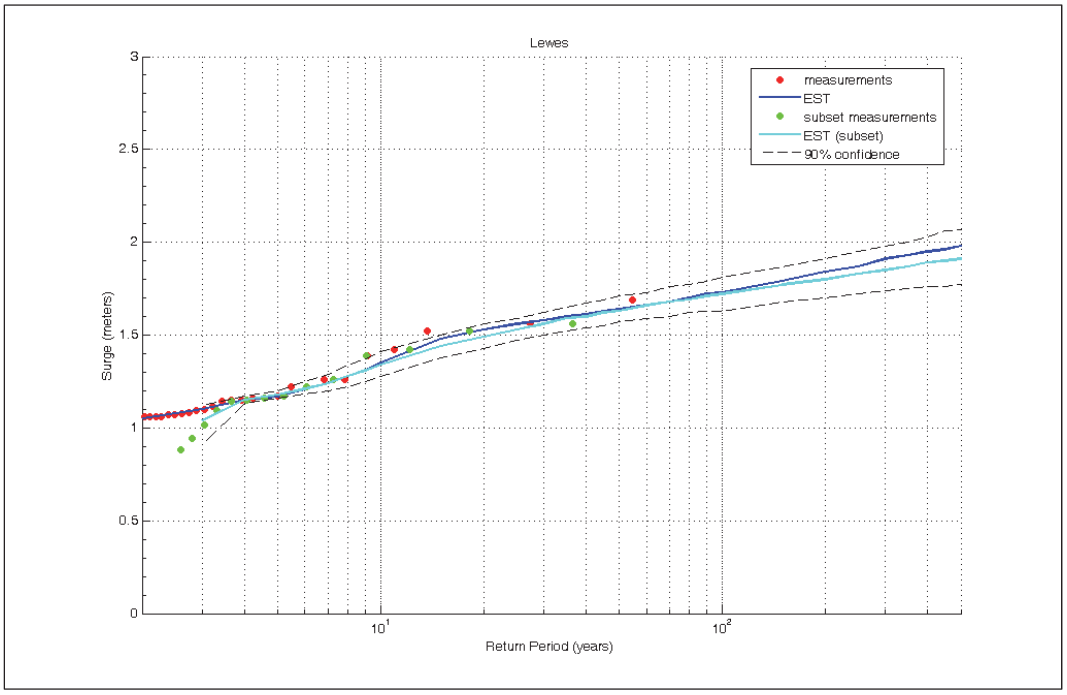

Figure 2.14. Comparison long-term measurements and selected subset of storms at NOS recording station Sewells Point, VA.

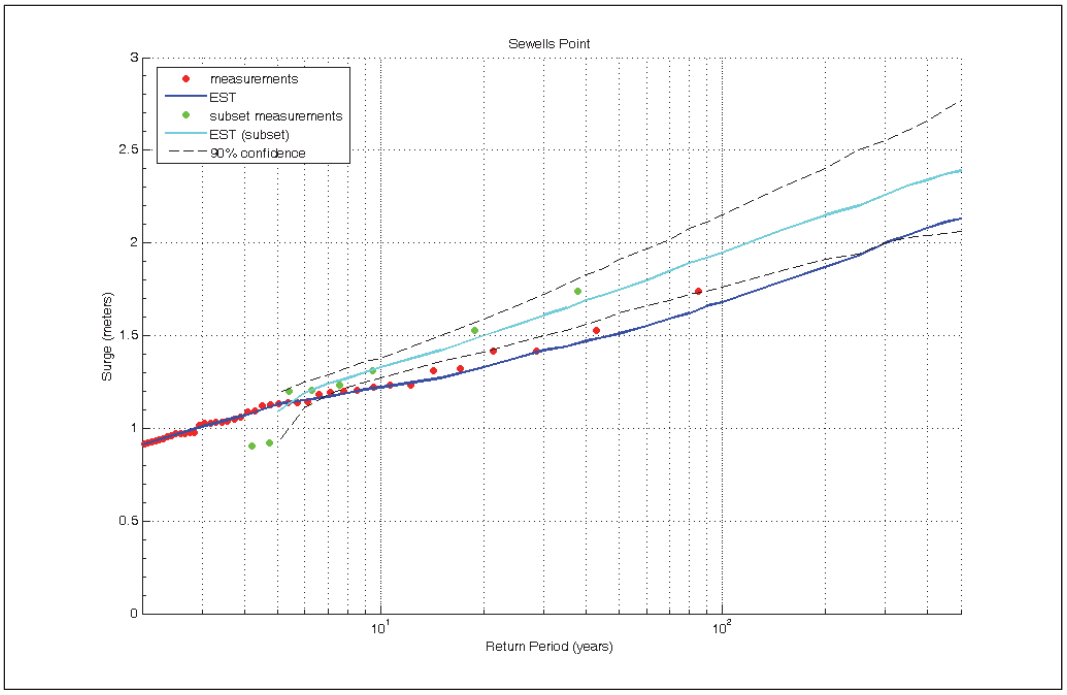

The stage-frequency curves for the selected subset of storms nearly identically match the stage frequency based on the full long-term record of storms at three of the six validation stations (Chesapeake Bay Bridge Tunnel, VA; Cape May, NJ; and Lewes, DE). At the other three validation stations (Atlantic City, NJ; Baltimore, MD; and Sewells Point, VA) the stage-frequency curve based on the subset of storms is moderately higher than the stage-frequency curve based on the full long-term record of storms. The reason for this is the significantly shorter period of record associated with the subset of storms and the existence of the top two or three storm events in the shorter period of record associated with the subset of storms. Nevertheless, the deviation of the subset of storms is generally less than about 0.5 m at the 500-yr return period and 0.3 m at the 100-yr return period.

A third series of validation tests employed peak storm surge values predicted through numerical simulation of the selected subset of storms as compared to the available long-term measurements. These validation tests provide insight into both the validity of the selected subset of storms and the quality of the numerical estimation of peak surge values as compared to the long-term record of measured storms at the validation stations. The results of this series of validation tests are illustrated in Figures 2.15 through 2.20.

Figure 2.15. Comparison of long-term measurements and selected subset of storms at NOS recording station Atlantic City, NJ.

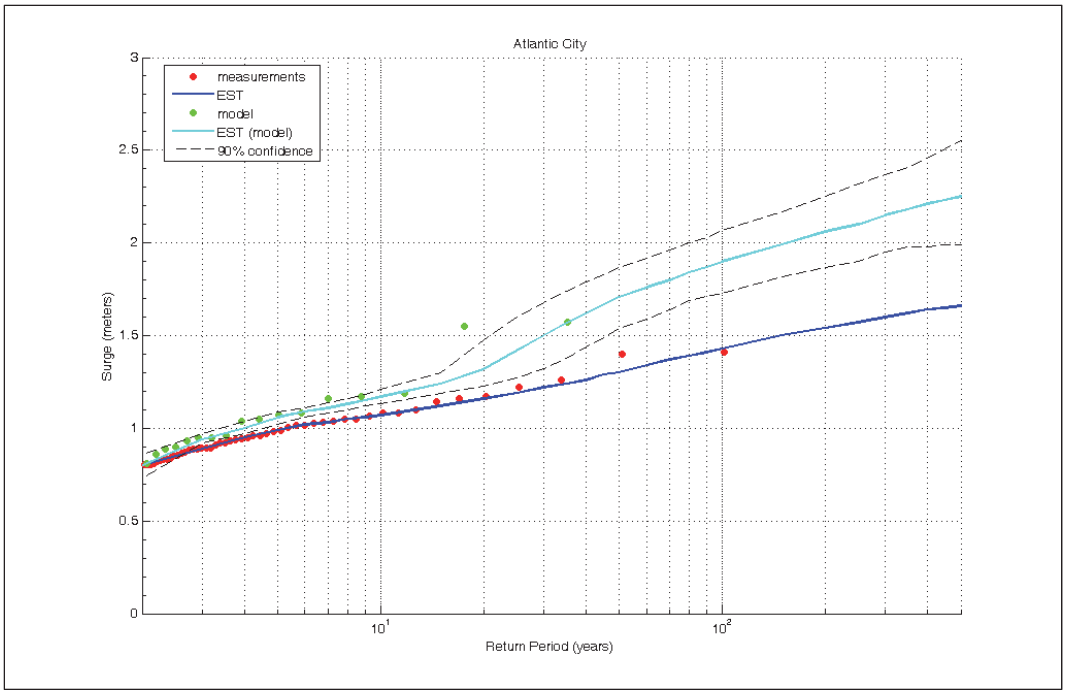

Figure 2.16. Comparison of long-term measurements and simulated subset of storms at NOS recording station Baltimore, MD.

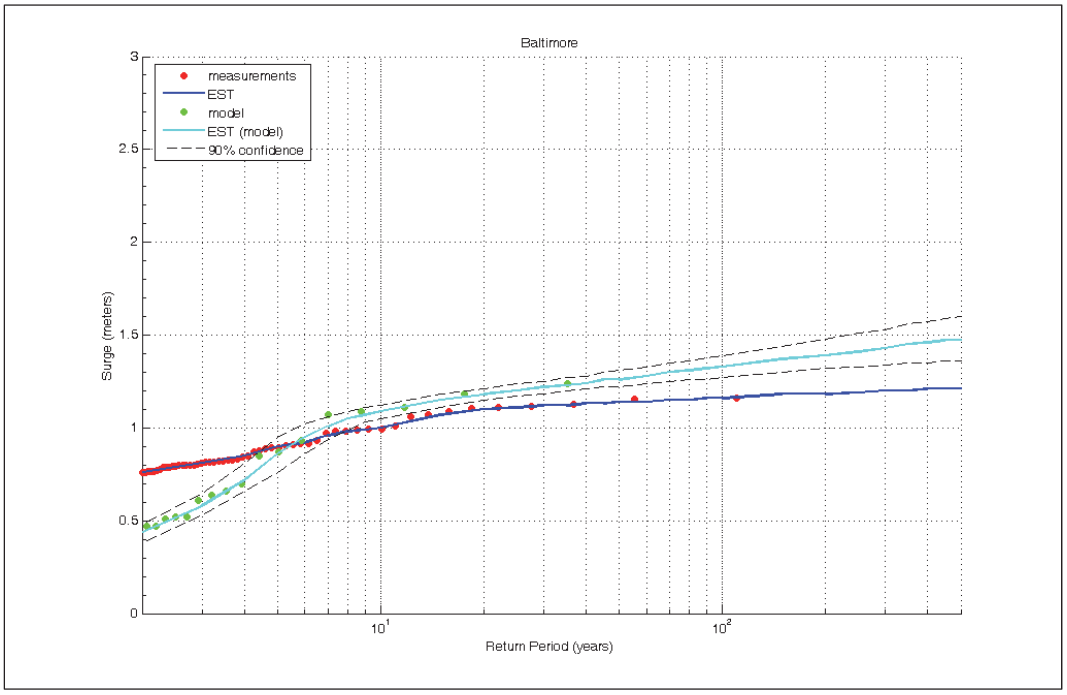

Figure 2.17. Comparison of long-term measurements and simulated subset of storms at NOS recording station Chesapeake Bay Bridge Tunnel, VA.

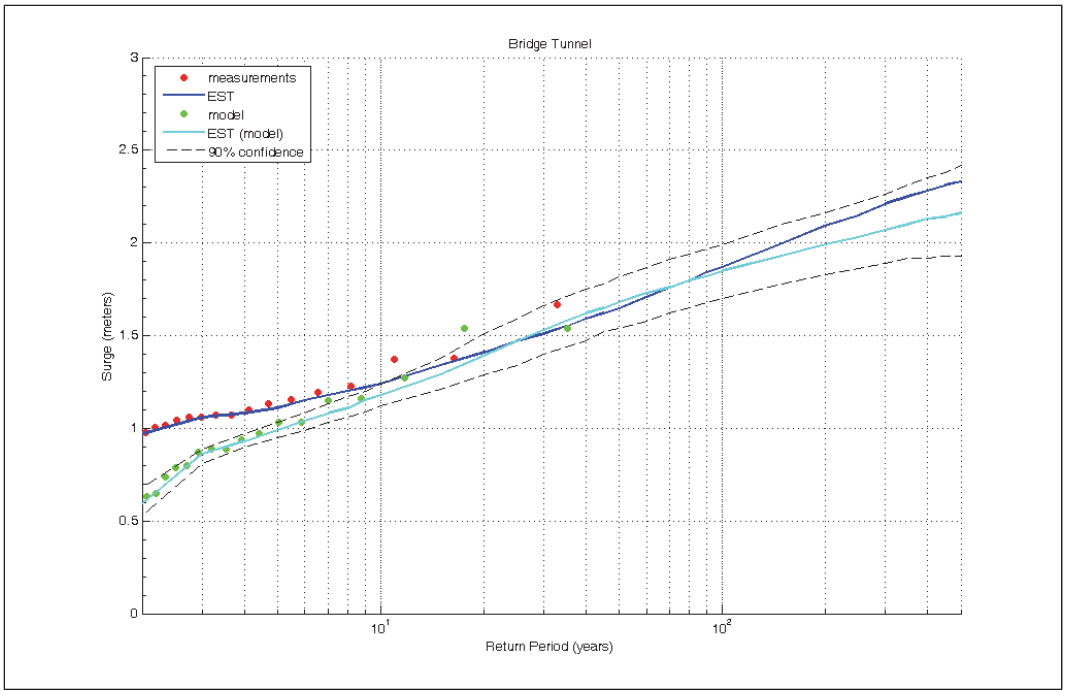

Figure 2.18. Comparison of long-term measurements and simulated subset of storms at NOS recording station Cape May, NJ.

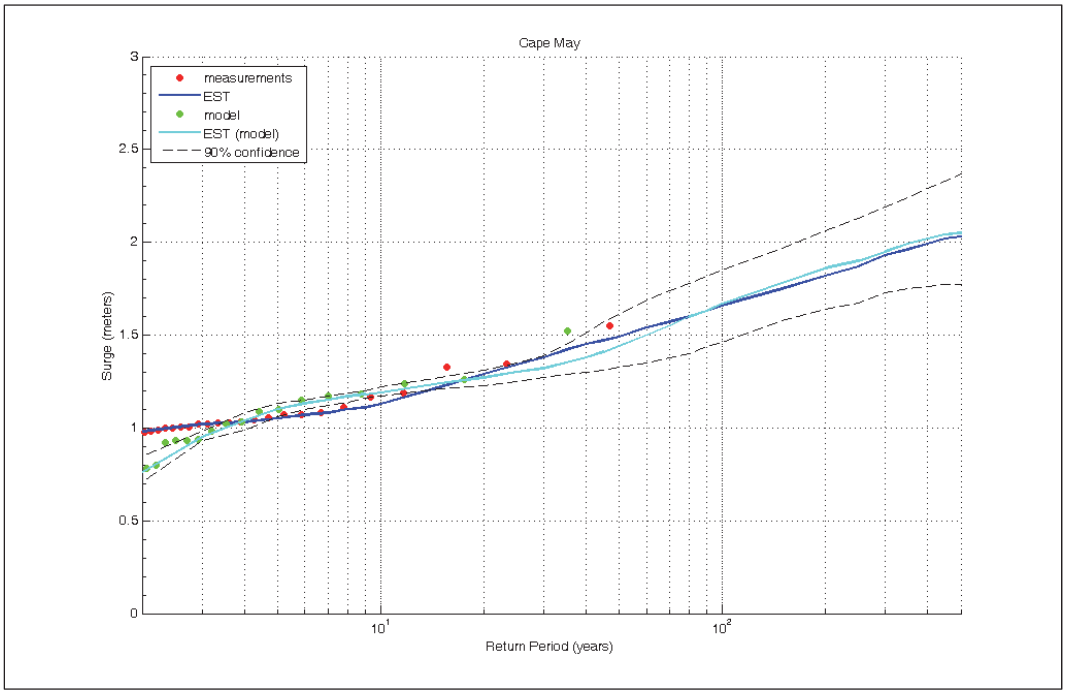

Figure 2.19. Comparison of long-term measurements and simulated subset of storms at NOS recording station Lewes, DE.

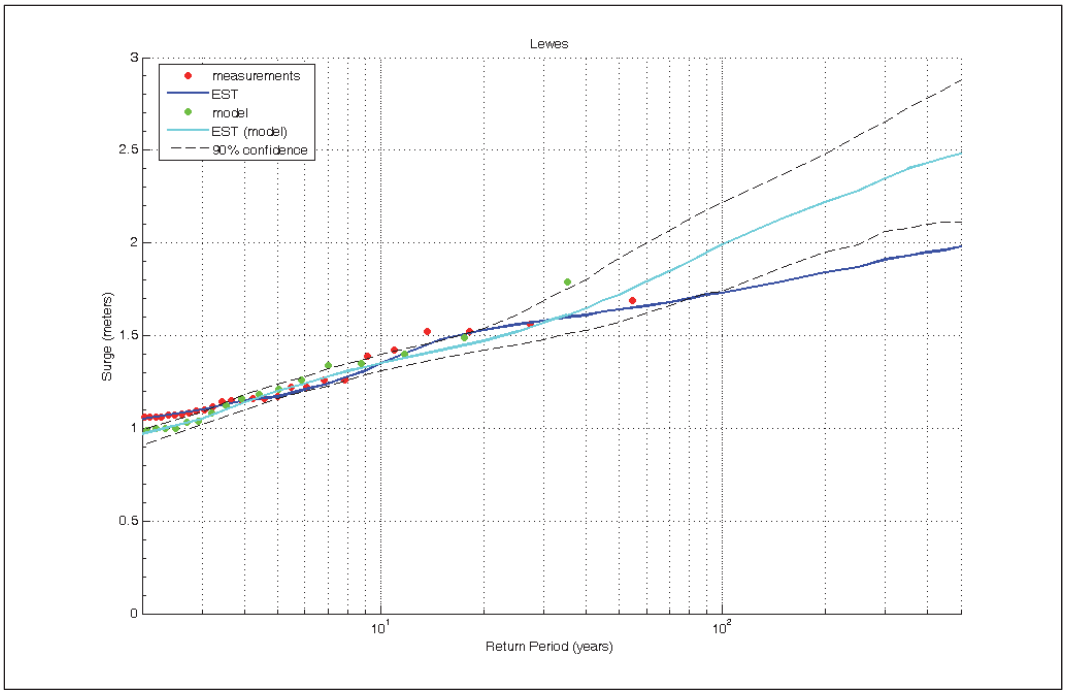

Figure 2.20. Comparison of long-term measurements and simulated subset of storms at NOS recording station Sewells Point, VA.

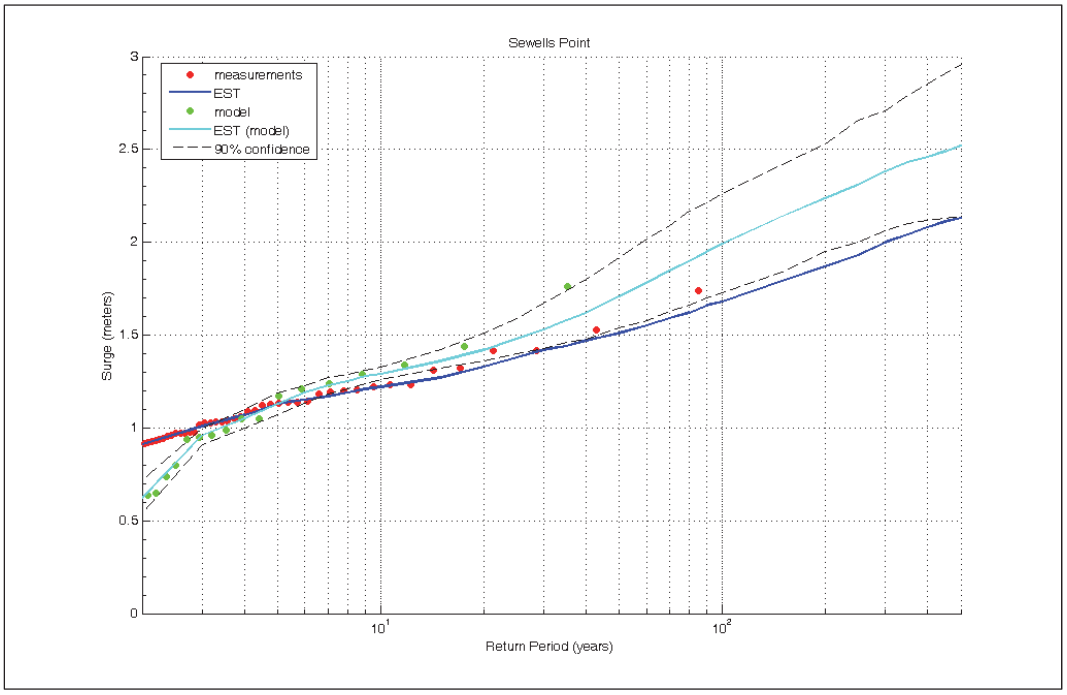

The results of the third series of validation tests are similar in nature to those of the second set of validation tests. The difference here is that the peak surge values for the subset of storms were generated through numerical simulation of the selected subset of storms. At three of the validation stations (Chesapeake Bay Bridge Tunnel, VA; Cape May, NJ; and Lewes, DE) the stage-frequency curve based on the full long-term measurements at the validation stations is largely contained within the EST-predicted 90-percent confidence interval of the stage-frequency curve for the simulated subset of storms. At the other three stations (Atlantic City, NJ; Baltimore, MD; and Sewells Point, VA), the stage-frequency curve is moderately higher than the stage-frequency curve based on the full long-term record of measured surge.

Figures 2.21 and 2.22 provide summary statistical error information at 100-yr return period and at the 500-yr return period, respectively, at each of the validation stations. These error estimates are considered acceptable with the 100-yr return period bias at 0.2 m with an RMSE less than 0.3 m and the 500-yr return period bias less than 0.3 m with an RMSE less than 0.4 m.

Figure 2.21. 100-yr return period scatter plot with error estimates at validation stations.

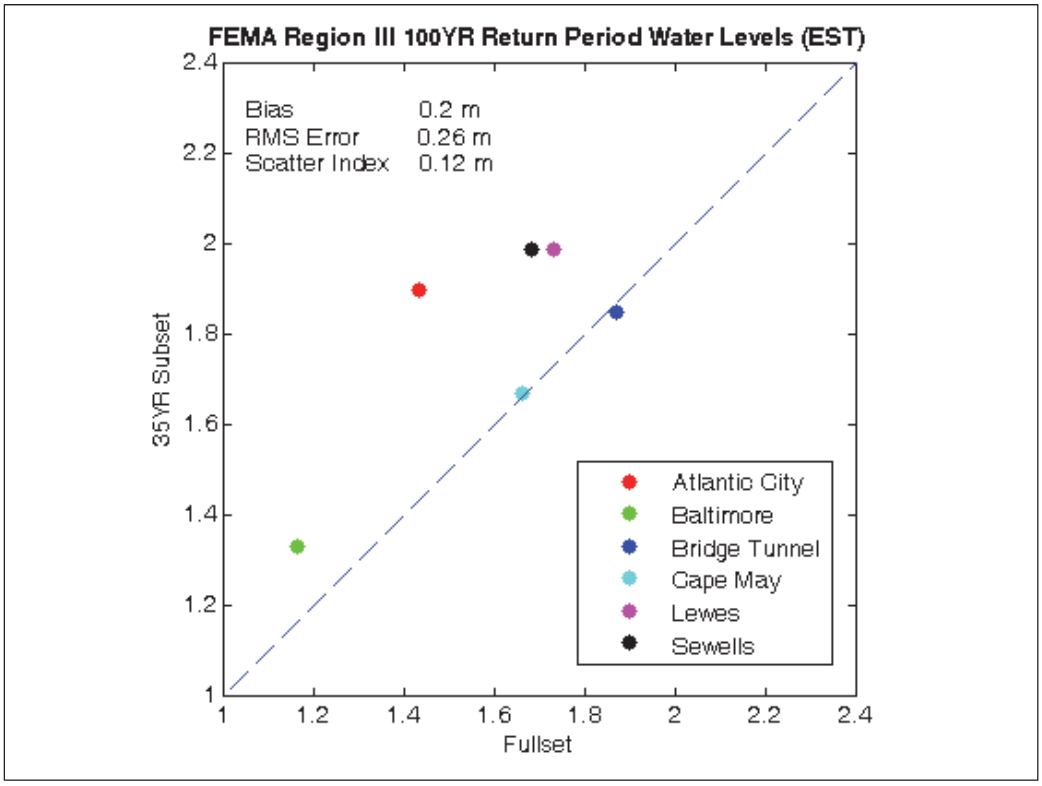

Figure 2.22. 500-yr return period scatter plot with error estimates at validation stations.

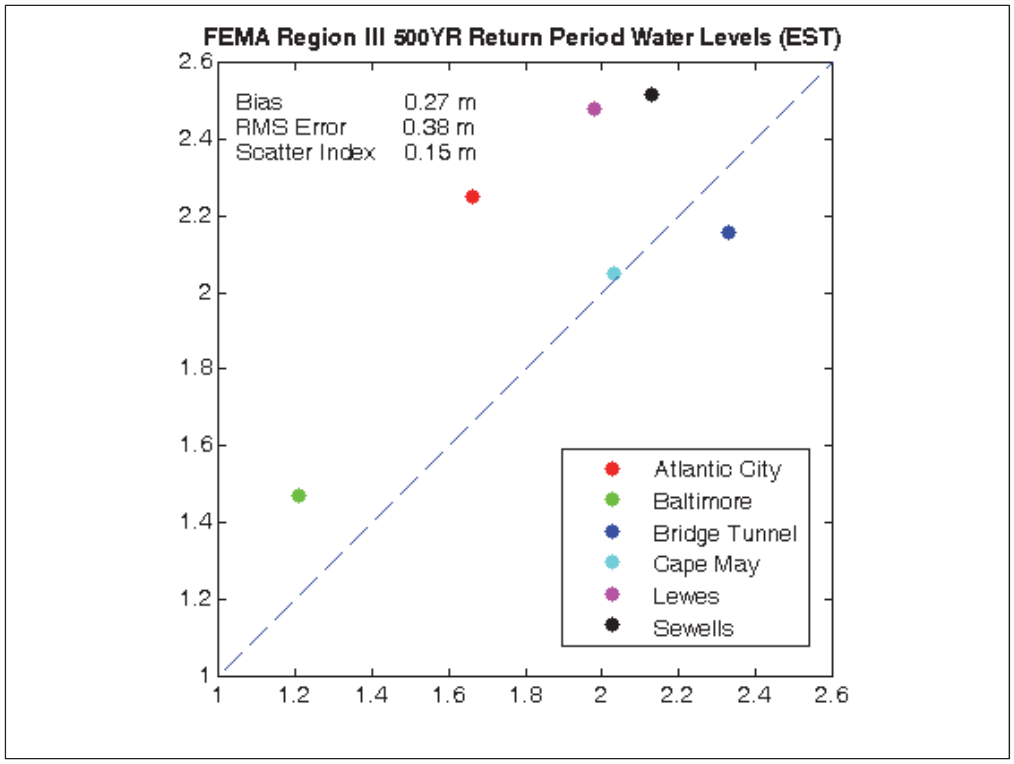

3 Tropical Storm Approach

FEMA Region III coastal areas are impacted by both tropical and extratropical coastal storms. To accurately account for the storm surge contributions from each, this project uses different statistical approaches to address the storm surge and wave hazard from tropical and extratropical storms. As described in Submittal 1.3 (Vickery et al. 2012), tropical storms can be parametrically represented via the Joint Probabilities Method (JPM). This produces a set of candidate tropical storms that are likely to occur over some long time periods. In the Region III case, 156 storms were specified (Figure 3.1) with an annual occurrence rate of .156 storms/yr. The storms were divided into three classes:

- Virginia, Delaware, and New Jersey Landfalling
- North Carolina Landfalling
- by-passing.

Figure 3.1. Hurricane Tracks for the project JPM storm suite.

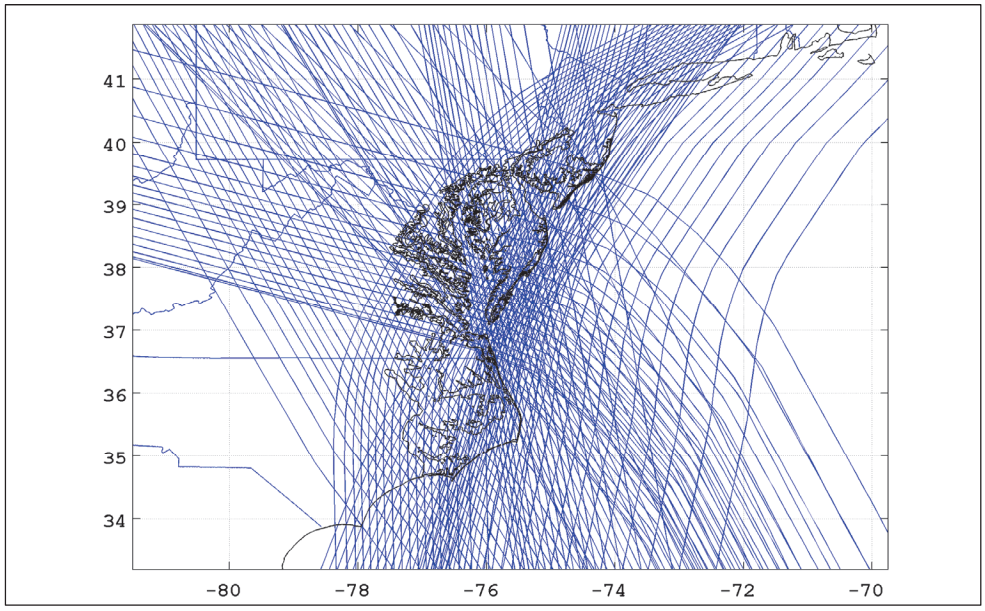

Each storm is assigned a statistical weight, which is the product of the probabilities of the storm parameters that define that storm (the joint probability). Tables 3.1-3.3 provide the track parameters and statistical weights for all storms in each of the three categories. Three different radius to maximum wind (RMW) uniformly weighted values were also applied to each event scenario.

Table 3.1. Hurricane Parameter Values and Weights for Virginia, Delaware, and New Jersey Landfalling Hurricanes.

Heading Degrees CW from North	Weight	Central Pressure Difference (mbar)	Weight	Trans Speed (m/sec)	Weight
-75	0.09	34, 51, 65	0.44, 0.35, 0.21	4.0, 7.2	0.60, 0.40
-45	0.06	34, 51, 65	0.44, 0.35, 0.21	4.7, 9.5	0.65, 0.35
-30	0.12	34, 51, 65	0.44, 0.35, 0.21	4.7, 9.5	0.65, 0.35
-10	0.27	34, 51, 65	0.44, 0.35, 0.21	4.8, 10.5	0.57, 0.43
-15	0.47	34, 51, 65	0.44, 0.35, 0.21	5.0, 13.0	0.45, 0.55

Table 3.2. Hurricane Parameter Values and Weights for North Carolina Landfalling Hurricanes.

Heading Degrees CW from North	Weight	Central Pressure Difference (mbar)	Weight	Trans Speed (m/sec)	Weight
-35	0.37	38, 56, 75	0.52, 0.40, 0.08	4.6, 11.5	0.66, 0.34
0	0.20	38, 56, 75	0.47, 0.42, 0.11	4.6, 11.5	0.66, 0.34
22	0.43	38, 56, 75	0.38, 0.50, 0.12	4.6, 11.5	0.66, 0.34

Table 3.3. Hurricane Parameter Values and Weights for by-passing Hurricanes.

Heading Degrees CW from North	Weight	Central Pressure Difference (mbar)	Weight	Trans Speed (m/sec)	Weight
12	1	42,67	0.75,0.25	4.0,11.4	0.65,0.35

Tropical storm intensities within the 156-storm JPM suite range from tropical storm to Category 3 Hurricane. The distribution of storm intensities, depicted in Figure 3.2, indicates that most of the storms are Cat 1 and Cat 2 in strength. This corresponds to sustained wind speeds of 64-95 kt. There are no Category 4 or 5 storms in the set, as storms of this intensity are far too infrequent to influence a 500-yr water level in this region.

Statistical Methods (Joint Probabilities Method)

The JPM development of the statistical storm probabilities, storm weights, and tracks are covered in previous project submittals. In this section, we describe the overall process for computation of the JPM return levels and associated wave heights and periods. Examples of the steps are given for one model node on the open coast. Incorporation of tides and a statistical error term are addressed in the next section.

Figure 3.2. Distribution of storm intensities in the FEMA Region III JPM tropical storm suite.

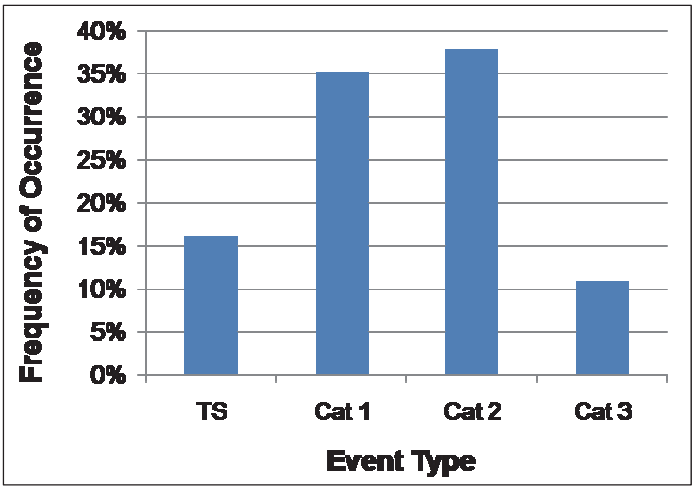

1. Load all simulation results. This includes the maximum water levels and the significant wave height that co-occurs with the maximum water level, and the peak wave period that co-occurs with the co-occurring significant wave height.
2. At each model node that wets during the simulations, rank-order the maximum surge responses (Figure 3.3, blue dotted line and green dotted line).
3. Permute the storm weights according to the surge ranking in Step 2. This results in a Cumulative Distribution Function (CDF) for the response at this node (Figure 3.3, red dotted line).
4. From the CDF, compute the return period according to the following equation:

$$R = \frac{1}{1 - e^{-\alpha(1-CDF)}} \tag{11}$$

where R is the return period in years, α is the annual occurrence rate of tropical storms (0.156 storms/year), and CDF is the cumulative distribution function computed in step 3. This results in the relationship between the return period and the storm-surge response. The return levels associated with the 10-, 25-, 50-, 100-, 500-, and 1000-yr periods are then interpolated from this relationship (Figure 3.4);

5. From Step 4, find the storm that is closest to the computed 100-yr surge level and get the co-occurring wave height and period from the table generated in the post-processing step 1. This step associates a wave height and period that co-occurs with the 100-yr storm surge value at every model node.

Figure 3.3. Storm surge response at example node along the lower Maryland open coast. The blue dots are the unranked maximum surge by storm number. The green dots are the ranked storm surge. The red line is the cumulative sum of the ranked storm weights, the CDF for this node. It is relative to the vertical axis on the right (red). There are 156 storms in the tropical storm population.

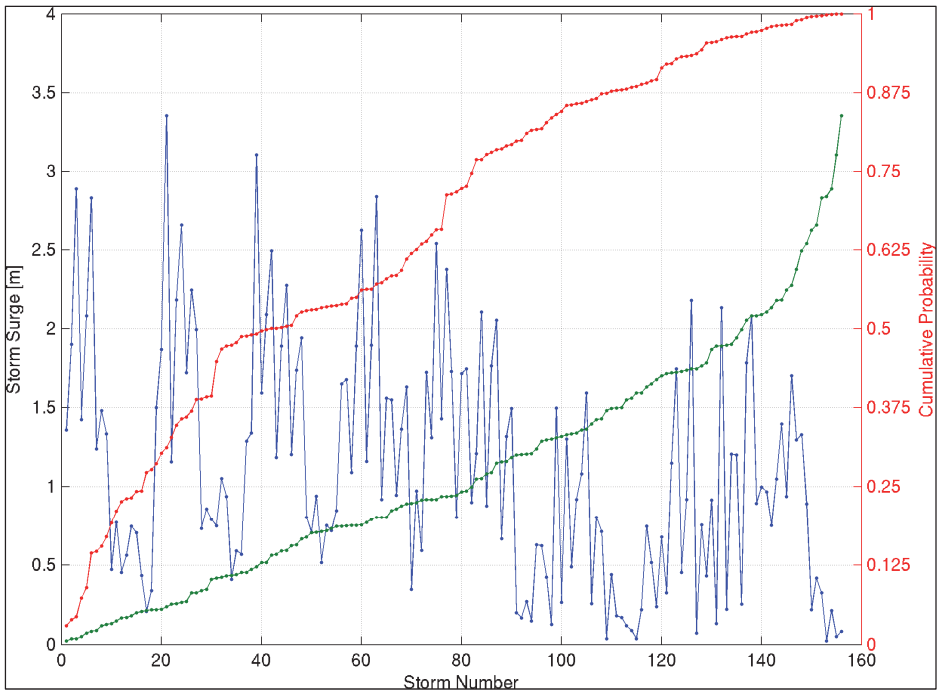

Figure 3.4. JPM return water levels at the standard return periods.

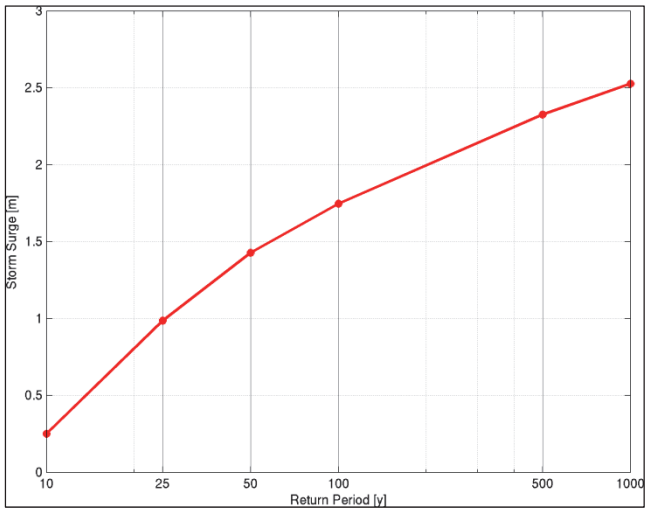

Incorporation of Tides and Errors into JPM analysis

Other projects (e.g., Niedoroda et al. 2010) have included tides as a constant (in space and time) in addition to the JPM error term. In regions where the tides are relatively the same amplitude and generally in phase, this is an

appropriate choice. However, tides along the Region III coast exhibit large changes in amplitude and phase. Tidal amplitudes, as indicated by the tidal datum *highest amplitude tide* (Figure 3.5), range from about 1.5 m in the upper/eastern Delaware Bay, to 0.75-1.0 m along the coast between the bays, to generally less than 0.60 m in Chesapeake Bay. This complexity renders using an unreasonable constant tidal value.

Figure 3.5. Highest Amplitude Tide [m above MSL] for Study area, computed from the equilibrium tidal solution used in the tidal validation.

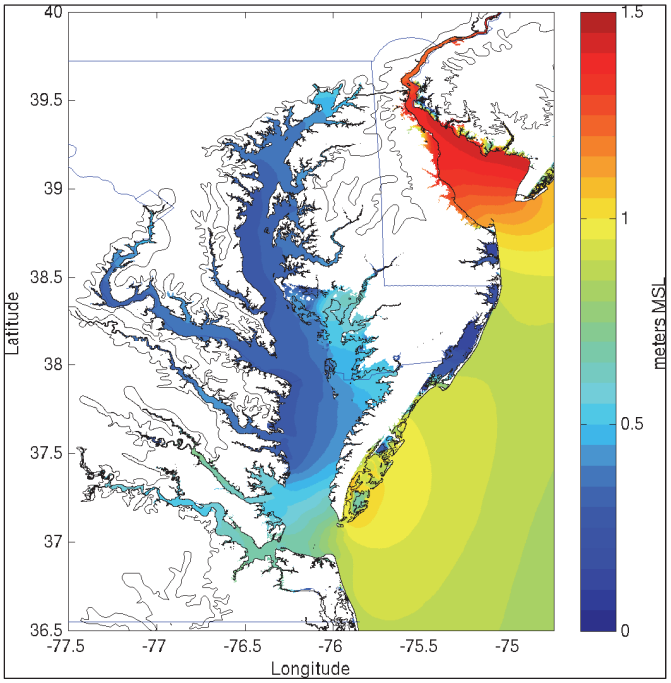

Tides are incorporated into the JPM analysis by replicating the surge response data and adding tidal heights randomly selected from the cumulative distribution functions of the tides. The level of replication, i.e., how many times the tidal CDF was sampled for each node and each storm, is N = 100. In the example analysis below, N = 12 for figure clarity. The analysis is done at each model node as follows:

1. Replicate surge responses at each node N times. As used in the final project statistics N = 100. This results in N replicates for the 156 surge responses. The weights of the storms are also replicated and normalized by N so that the sum of the probabilities is still 1.0.
2. For each storm, sample the tidal CDF N times (Figure 3.6, where N = 12 for clarity) and add this tidal value to the surge value. If the resulting combined tides + surge value is lower than the topography/bathymetry,

set this tides + surge value to 0, meaning that this storm at this location (node) and at the selected tide level did not produce a positive water level. The results of this step are shown in Figure 3.6, where the surge-only response is in blue, and the N (=12) tides + surge levels are drawn with the red dots. The full statistical results are computed with N = 100.

3. Rank-order the new water levels and reorder the weights, accordingly. This is shown in Figure 3.7.
4. Finally, compute the return period in the same manner as above and interpolate the resulting period/levels to the standard return periods (Figure 3.8). Also shown in Figure 3.8 is the result for N = 100.

Concurrent with the addition of the random tides, an error term is also included that represents errors in modeling skill. This is similar to the error model described in Niedoroda et al. (2010), except that only the modeling skill term is included. In the Region III project, tides are directly incorporated (their error component 1), and Holland-B (their error component 2) is explicitly represented in the storm parameter distributions used to generate the JPM storm population.

The project high water mark analysis (reported on in Submittal Number 2) indicates that the overall error distribution is relatively Gaussian, with a mean (bias) of 0.02 m and a standard deviation of 0.16 m. For each of the tidal replicates, a modeling error is sampled from the error distribution and added to the total surge response (modeled + tidal + error). An example of the effect of this term is shown in Figure 3.8.

Figure 3.6. Unranked, surge only (blue) and unranked surge + random tides (red). In this example, *N* = 12 for clarity. The full statistical results are computed with *N* = 100. The surge-only data is the same as in Figure 3.3 above.

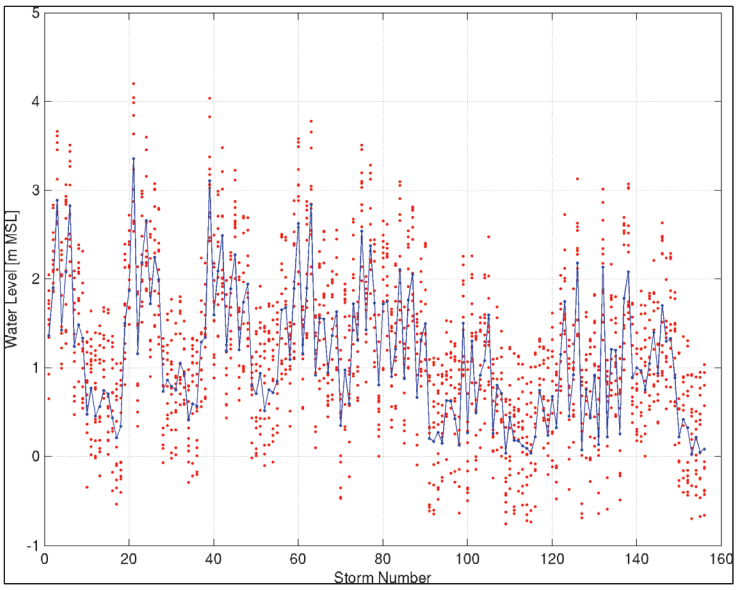

Figure 3.7. Replicated surge response with each replicate shown separately (i.e., end-to-end). The replicated surge-only response is shown with blue dots and the surge + tides are shown with red dots. This is the same data as in Figure 3.6. The ranked surge + tides are shown with the green dots.

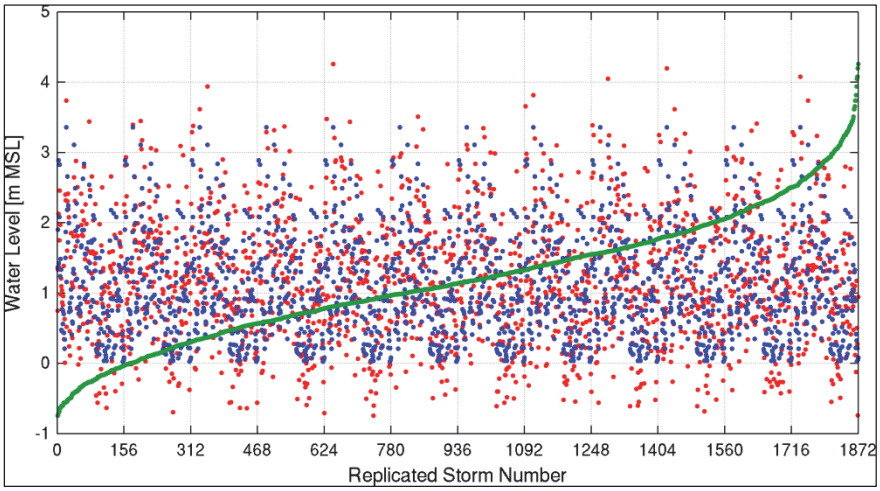

Figure 3.8. JPM return levels at standard return periods for surge only (red) and surge + tide (green). Also shown is the result for *N* = 100 (blue) and the result that includes the JPM error term in the surge + tide results.

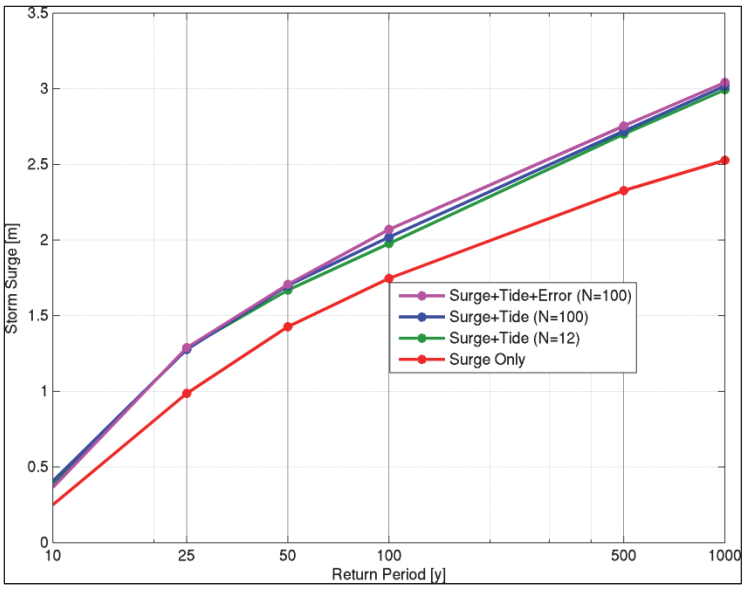

4 Computation of Storm Responses

The production simulations were conducted with the comprehensive modeling system established for the validation phase of the project and described in previous submittals. To review, this system runs the coupled unstructured surge and wave model ADCIRC (version 49.60). The system runs automatically, interacting with the computer's job scheduler to minimize the need of human intervention, thus, minimizing potential file management errors. The system is driven by a specification of a storm population to simulate. Individual storms are either an extratropical storm represented by an Oceanweather, Inc., best winds analysis, or a tropical storm computed using the Applied Research Associates hurricane boundary layer model from one of the many tropical JPM storms. The computational system itself does not distinguish between the two storm types. Production simulations started 28 April 2011, using approximately 1024 cores of RENCI's Blueridge Nehalem cluster. The last simulation was finished on 13 May 2011.

All production simulations were run using the project's ADCIRC grid, version FEMA_REGION III_20110303_MSL. No modifications to the grid have been made since the validation phase of the project was completed. Figure 4.1 shows the ADCIRC grid in the project region.

Each simulation produces a suite of graphical output to aide in the QA/QC procedure. Each graphical output has been examined to gain an overall perspective of the simulations. During this phase, no systematic issues were discovered. Examples of the maximum water level and maximum significant wave height are shown in Figure 4.2, for the Virginia landfalling storm VAR_dp3r3b1c2h4l1.

The final step in the overall post-processing and statistical analysis is the conversion of the water-level data from mean sea level to NAVD88. This is performed after the final, combined return levels are computed, with the same datum translation used to transform the ADCIRC mesh node elevations from NAVD88 to MSL. All results herein are in meters MSL. The NAVD88 products are provided in file form as part of the project data archive.

Figure 4.1. ADCIRC grid (version FEMA_REGION III_20110303_MSL) used for production simulations. The 10, 25, and 50 meter isobaths are shown with the black lines, and the coastline is shown in red. There are 1,875,689 nodes in the grid, 93 percent of which are in the project area.

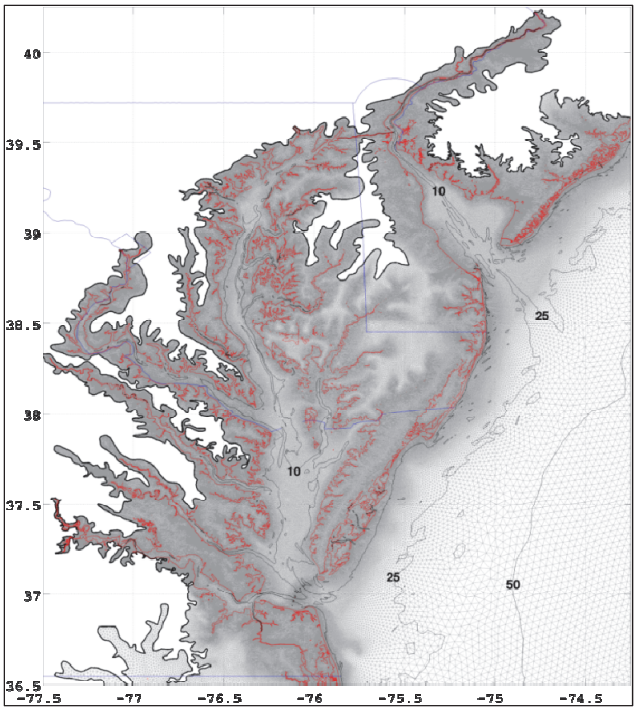

Figure 4.2. Example of Maximum Water Level (left) and Maximum Significant Wave Height (right) for project storm VAR_dp3r3b1c2h4l1. Units are meters relative to MSL. The storm track is shown with the red line at 1-hr positions.

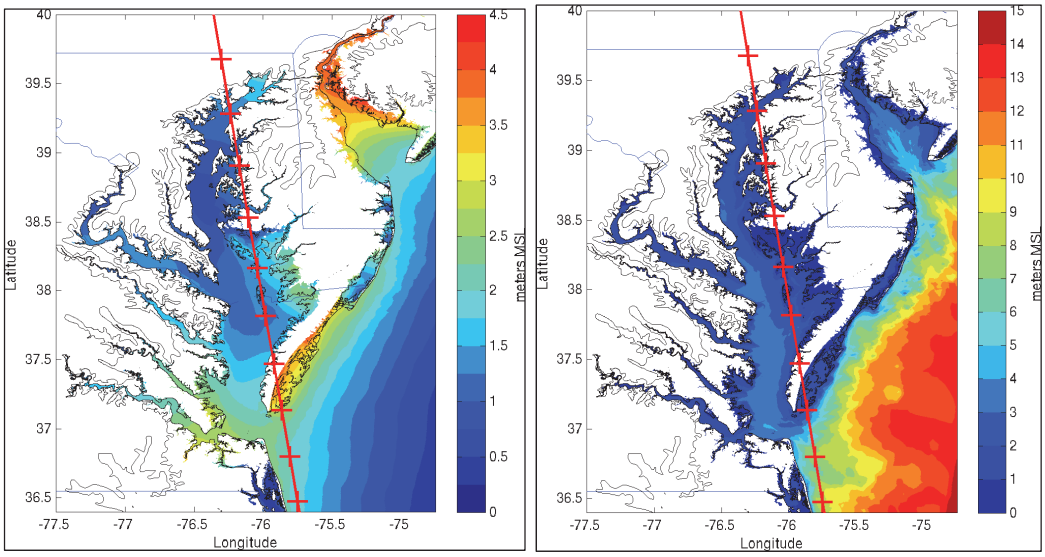

Combining return levels from JPM and EST

After the return levels are computed for each storm type (tropical/JPM and extratropical/EST), the final return levels at the 10-, 25-, 50-, 100-, and 500-yr periods are computed. Statistical independence of the separate results is assumed. The method, as follows, is described fully in the EST User's Manual (Scheffner et al. 1999). Over the range 0 to 5 meters, at an interval of 0.1 meter, the return periods (and, hence, probabilities of exceedance) at these levels are interpolated from the hazard curves for JPM and EST. The new probability of exceedance is then determined as

$$P_c = 1 - \left(1 - P_j\right)\left(1 - P_e\right) \tag{12}$$

where P_j is the probability of exceeding the specified level from the JPM return levels (P_e)is the probability of exceeding the specified level from the EST return levels, and (P_c) is the probability of exceeding the specified level in the combined levels. Since the JPM and EST probabilities are annual values, the resulting combined probability is also annual, and the annual percent chance of exceedence is the $T_c = 1/P_c$. After looping over the return level range, the result is a new hazard curve from which the new return levels are interpolated.

This process is illustrated in Figure 4.3 and Figure 4.4 using hypothetical return levels. In the first example, the JPM and EST values overlap in the 1.0 to 1.5 meter region. At the water level 1.0 m, the probability of exceedence for JPM is 0.1 (since 1.0 m is the 10-yr return level for JPM). Thus, P_j = 0.1, and, similarly, P_e = 0.01. Then, from Equation 12, the combined probability of occurrence for the 1.0 meter level is as follows:

$$\begin{aligned} Pc &= 1 - \left(1 - Pj\right)\left(1 - Pe\right) \\ &= 1 - \left(1 - 0.1\right)\left(1 - 0.01\right) \\ &= 1 - 0.9 \times 0.99 \\ &= 0.109 \end{aligned} \tag{13}$$

Last, the new return period for the 1.0-meter level is 1/0.109 = 9.2 yrs (magenta dot in Figure 4.3). At the 2.0-meter level, the EST probability is very low since 2.0 meters is substantially greater than the 1000-yr level. Thus the term (1-P_e) is essentially 1, and $P_c \sim P_j$. In this example, the combined levels are the same as the JPM levels except at the 10-yr period, which is determined by interpolating the combined curve at 10 years. In this example, the combined 10-yr level is 1.05 m.

Figure 4.3. Example of combining return levels from JPM and EST. The JPM return levels are shown in blue, the EST levels in red, and the combined levels in green. In this example, the JPM and EST curves overlap between 1.0 and 1.5 meters. The example calculation for the combined 1.0-meter level is shown with the magenta dot (at 9.2 yrs). Note that the combined values are slightly larger between 10 and 25 yrs.

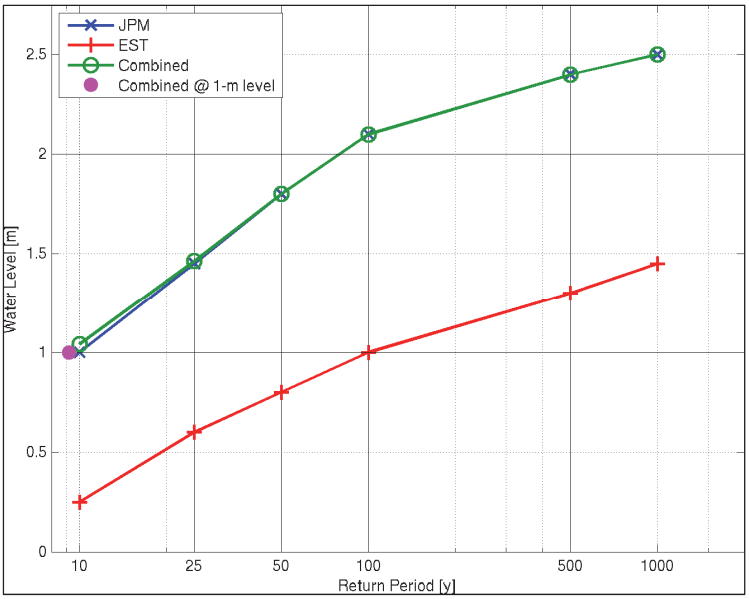

Figure 4.4. Examples of combining return levels from JPM and EST. The JPM return levels are shown in blue, the EST levels in red, and the combined levels in green. Upper: Case where the respective levels do not overlap; the largest EST level is smaller than the smallest JPM level. The resulting combined levels are the same as the JPM levels. Lower: Case where there is overlap in EST and JPM levels; combined results are higher than either the JPM or EST levels.

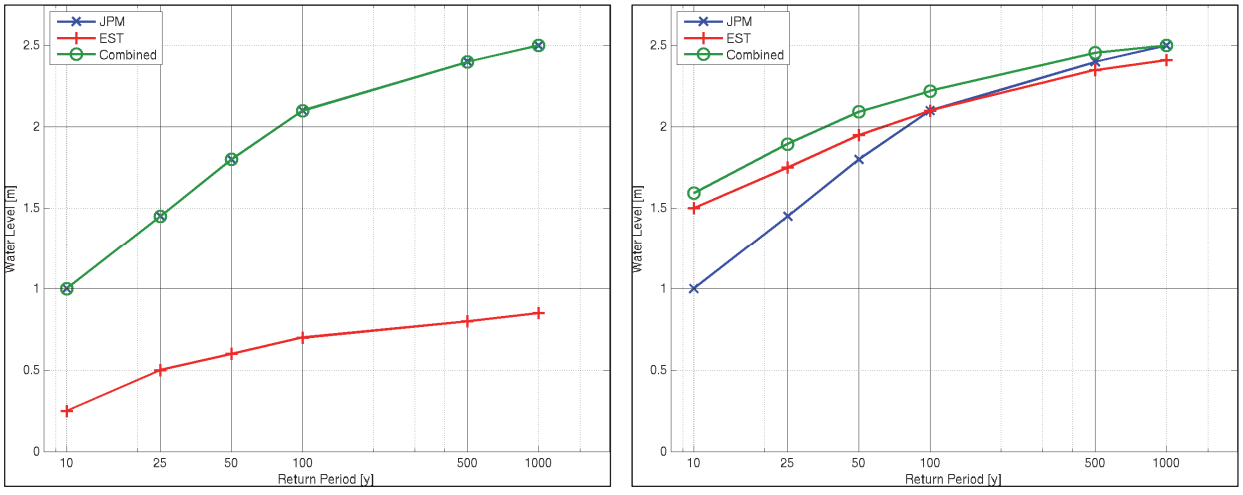

Two more illustrative examples are given in Figure 4.4. Consider that the highest EST level is lower than the lowest JPM level (Figure 4.4, top). In this case, the contributions of the EST values to the combined levels are

insignificant, and the resulting combined levels are the same as the JPM levels. This is because (P_e) is effectively 0 for all JPM levels, and, thus, $P_c = P_j$.

Next, consider the case where there is overlap between the JPM and EST curves (Figure 4.4, bottom). In this case, there is substantial contribution from both components to the combined levels. Note particularly that at the 100 yr period, *JPM* = *EST* = 2.1 m. Thus, $P_e = P_j = .01$, and $P_c = 0.0199$. The combined period for 2.1 m is then approximatley 50 yrs. This is intuitive, because the events (tropical and extratropical) are of equal magnitude (at 100 yrs) and are independent and can thus co-occur in any given year.

Note, also, that the combined levels cannot be lower than the largest of EST or JPM at a specified period.

Computed return levels

Return periods analysis results for JPM, EST, and the combined values are shown in Figure 4.5 for the periods 100 (1 percent) and 500 (0.2 percent) yrs. Note that the units are m above mean sea level in the figures. However, the data are reported in digital form relative to both MSL and NAVD88.

For the 100-yr period, the JPM and EST values range from approximately 0.5-1.0 m in the middle of Chesapeake Bay up to 2.5 m in western Delaware Bay. Since the levels are generally near each other, the combined levels are higher than either JPM or EST, particularly in Delaware Bay.

The 500-yr values are higher than the 100-yr values and range from 1.0-1.5 m in middle Chesapeake Bay to up to 3.25 m in upper Delaware Bay. In general, the JPM levels are higher than the EST levels, and JPM levels largely determine the combined results.

Determination of the Starting Wave Conditions

The primary data from each simulation for the statistical analysis is the maximum water level and significant wave height at each model node. These fields are computed by ADCIRC and output at the end of each simulation along with the time at which the local maximum occurs. The latter field is subsequently used to determine the significant wave height and periods that co-occur with the maximum water levels to develop the starting wave conditions needed in overland wave analyses. An example of this is shown in Figure 4.6, where the primary model system outputs are shown at a sheltered location in Chesapeake Bay.

Figure 4.5. 1% and 0.2% return levels for the JPM, EST, and combined statistical analyses. All color scales are the same, and the units are in meters MSL.

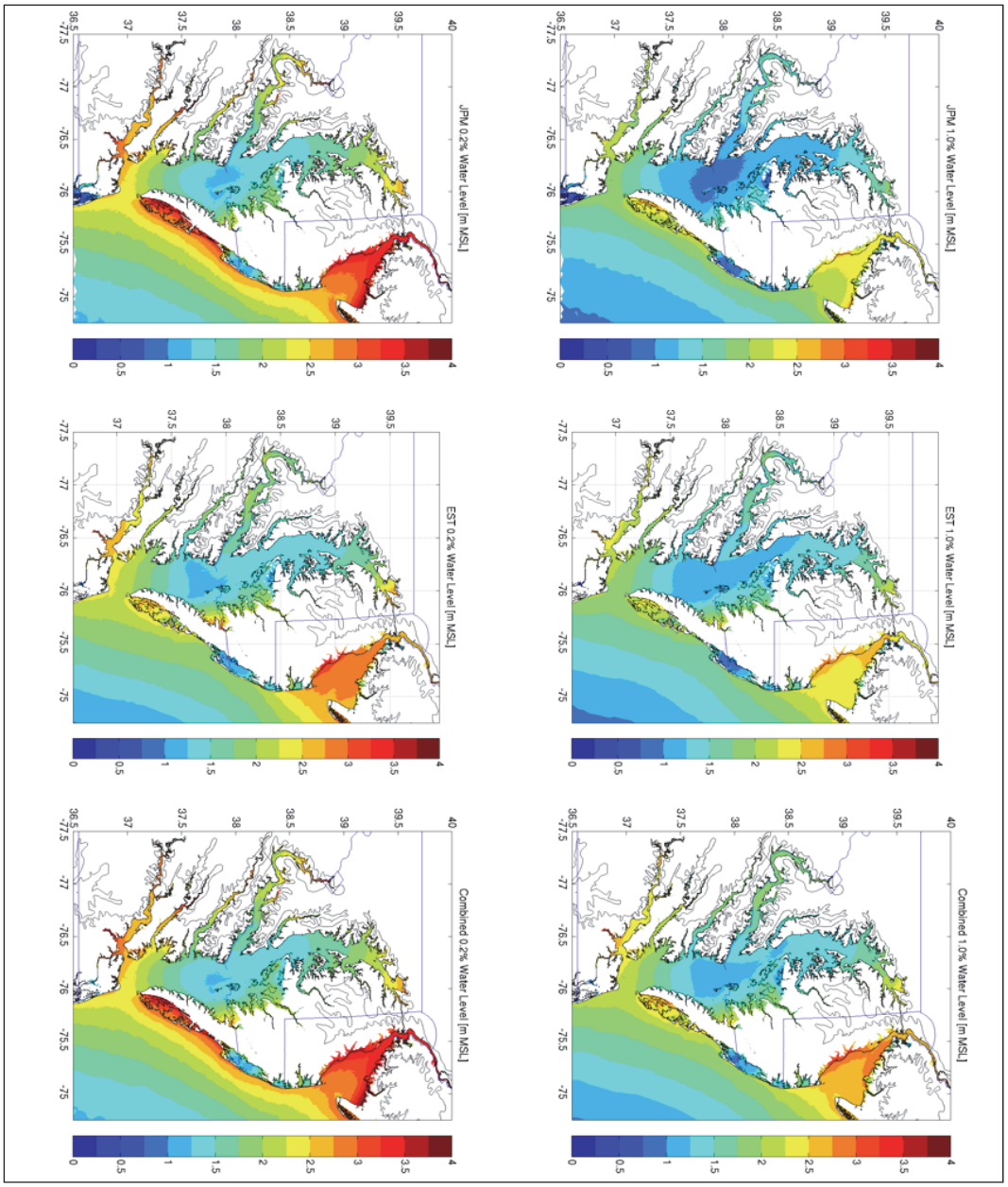

The process at each ADCIRC model node is as follows, referring to Figure 4.6. The 100-yr SWEL value (red dashed line) is used to determine the seven storm surges (black diamonds) closest to that surge level. The corresponding seven wave periods (blue triangles) and wave heights (green squares) are averaged, resulting in the "co-occurring" wave period and height at the 100-yr SWEL level. In the example in Figure 4.6, the starting wave conditions at this example node are 3.9 sec and 1.0 m for period and significant wave height, respectively. In addition to the averaged values, the

standard deviation of the wave conditions is reported for consideration by the mapping groups. The overall process is the same as that used in the FEMA Region II and North Carolina projects.

Figure 4.6. Example of determining the starting wave conditions for the overland wave analysis at a sheltered location in Chesapeake Bay. The black diamonds are the maximum surges for all storms, the green squares are the co-occuring wave heights, and the blue triangles are the co-occurring wave periods. The red line is the 100-yr SWEL value from the combined EST/JPM statistical analysis.

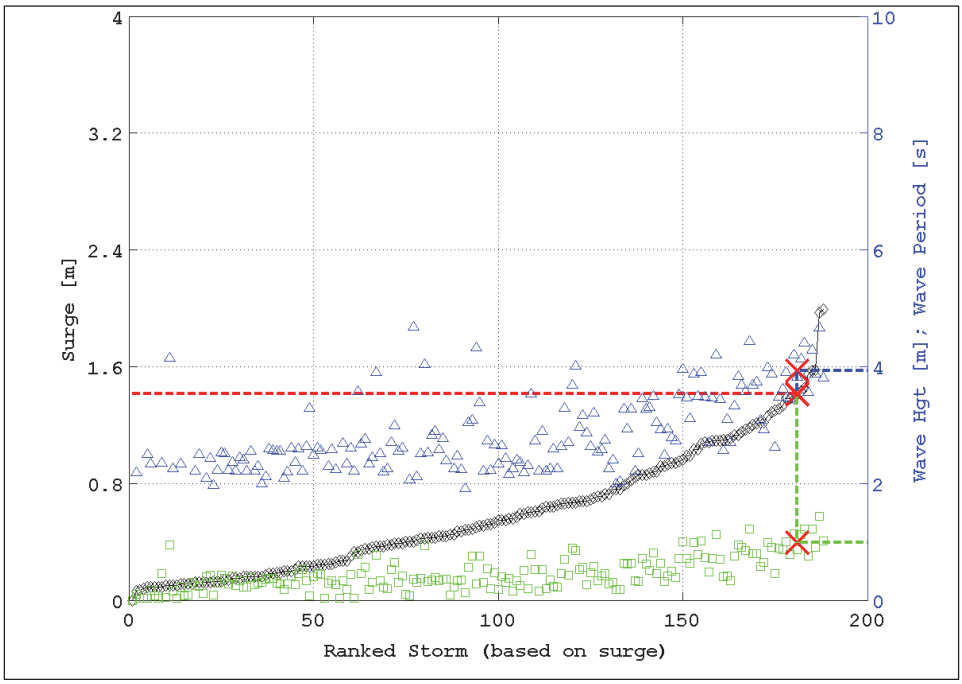

5 Still Water Elevations

This chapter describes the FEMA storm surge results and how they compare to the effective Still Water Elevation Levels (SWEL) throughout Region III. Furthermore, a discussion of Hurricane Irene's impacts to Region III and a preliminary comparison of Region II results in overlapping areas of the Delaware Bay are presented. Finally, analyses of the reduced SWEL levels in the upper Chesapeake Bay are discussed. To be consistent with previous published/effective FEMA SWELs, the next few sections are referenced to English Customary units. The FEMA 100-yr SWEL levels are shown in Figure 5.1 with units of feet relative to mean sea level (MSL).

Comparison with Effective Still Water Elevations (SWEL)

The recurrence interval results from the FEMA Region III Coastal Storm Surge Study were compared to the effective published 100-yr SWELs at select locations throughout Region III. The effective SWELs were developed in a variety of prior Flood Insurance Studies: modeling studies performed by US Army Corps of Engineers (USACE) and the Virginia Institute of Marine Science (VIMS), and analysis of Water Level Gauge data performed by the USACE, National Weather Service (NWS), US Geological Survey (USGS), Dewberry, and Grenier Engineering. These data were provided by Dewberry. The effective SWEL locations and sources were plotted in ESRI Geographic Information Systems (GIS) and are shown in Figure 5.2.

To compare the effective SWELs with the SWELs computed herein, the Region III modeled results, at every mesh node, were also imported into the GIS. For each effective published SWEL point provided by Dewberry and shown in Figure 5.2, the corresponding point(s) from the modeled mesh nodes were selected using a search radius of ~300 ft. (The GIS software extracted all the points within 300 ft from each effective SWEL point.) The file containing all of the extracted points was then imported into Matlab where they were used to determine new values at each effective SWEL point. This was done by interpolating the points contained within the radius of ~300 ft (up to 4 with varying SWEL elevations of +/- 0.25 ft) to the location of the effective SWEL point. The effective SWELs were then subtracted from the modeled SWELs, and their differences are shown in Figures 5.3 through 5.7.

Figure 5.1 FEMA Region III 100-yr combined SWEL results (MSL).

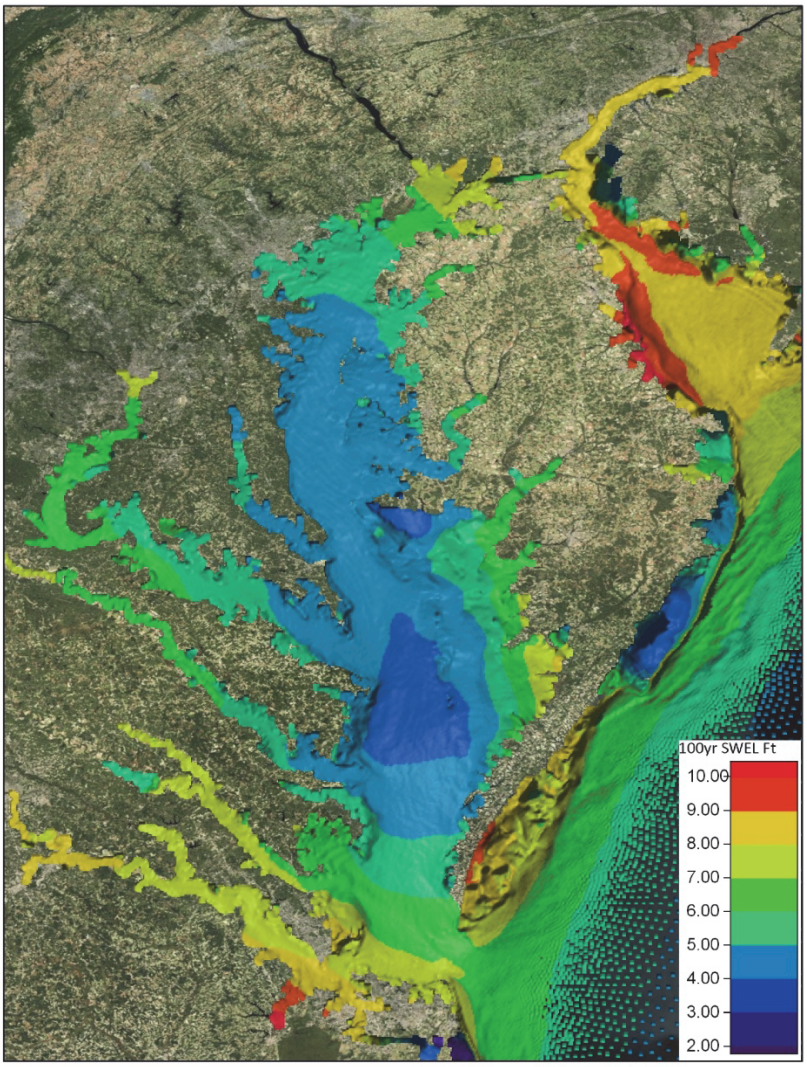

The majority (78 percent) of the effective SWELs were within +/- 1.5 ft when compared to the new SWELs at the 100-yr recurrence interval. However, there are some important differences to note, such as the elevated surge levels (1 percent) in the Delaware Bay and lower Chesapeake Bay with absolute differences ranging from (1.6 to 4.2 ft) and the reduced levels (21 percent) in the upper Chesapeake Bay and Eastern Shore of Virginia with values between (- 1.6 to -4.0 ft). The elevated values found in the Delaware Bay may be attributed to the methodology of the previous studies which utilized historical water-level gauge analysis in this area. With very few hurricanes measured in the historical record, it is not surprising that the present study, which includes hurricanes that track up or near the Delaware Bay, has greater 100-yr SWEL levels in this region. The causes of differences in the Chesapeake Bay are difficult to diagnose due to the varying methodologies used to develop the established SWELs.

Figure 5.2. Effective SWEL locations and elevations (colored dots) from Dewberry and their associated source (black text).

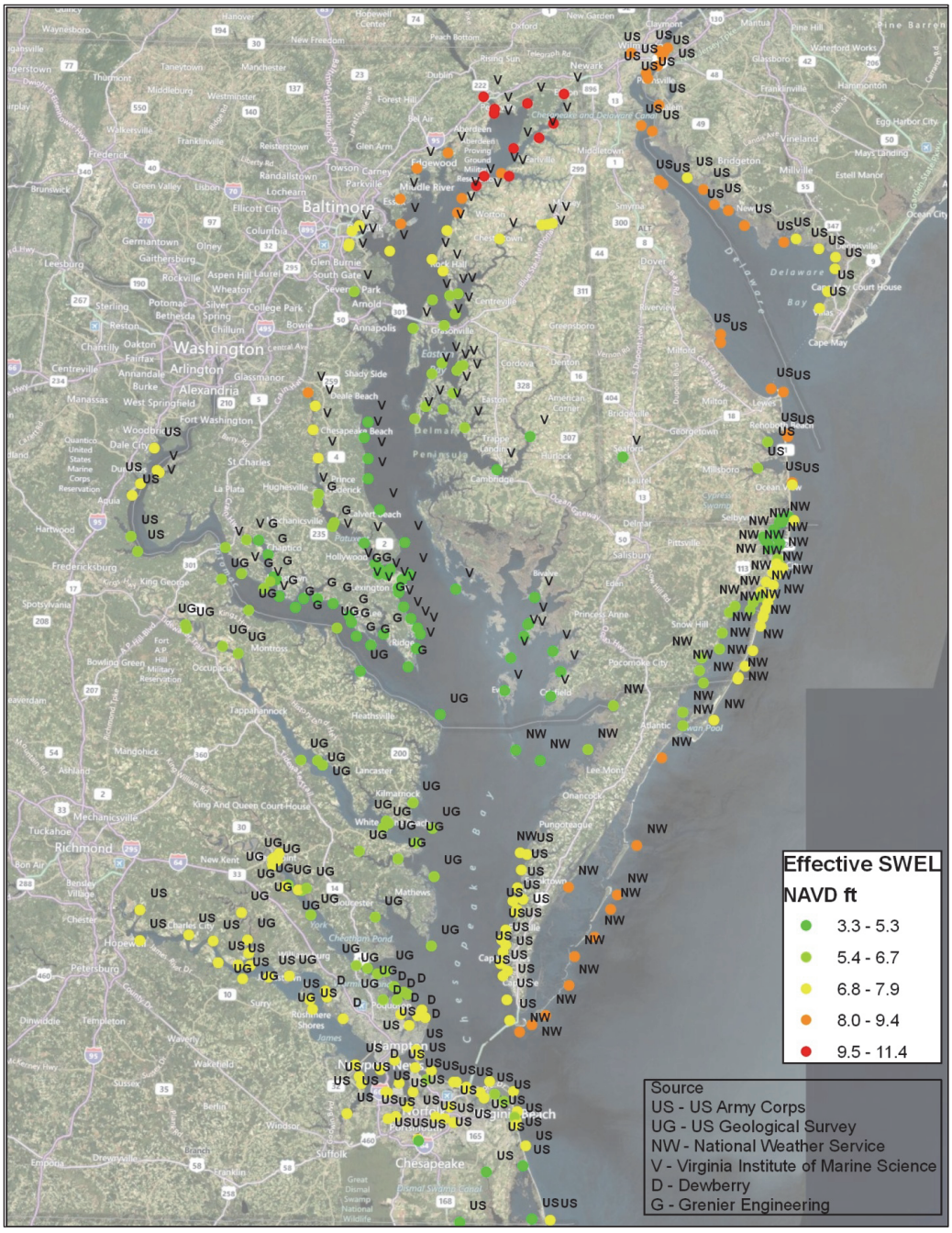

Figure 5.3. Difference between effective SWEL and FEMA Region III modeled (Modeled - Effective) for Delaware Bay.

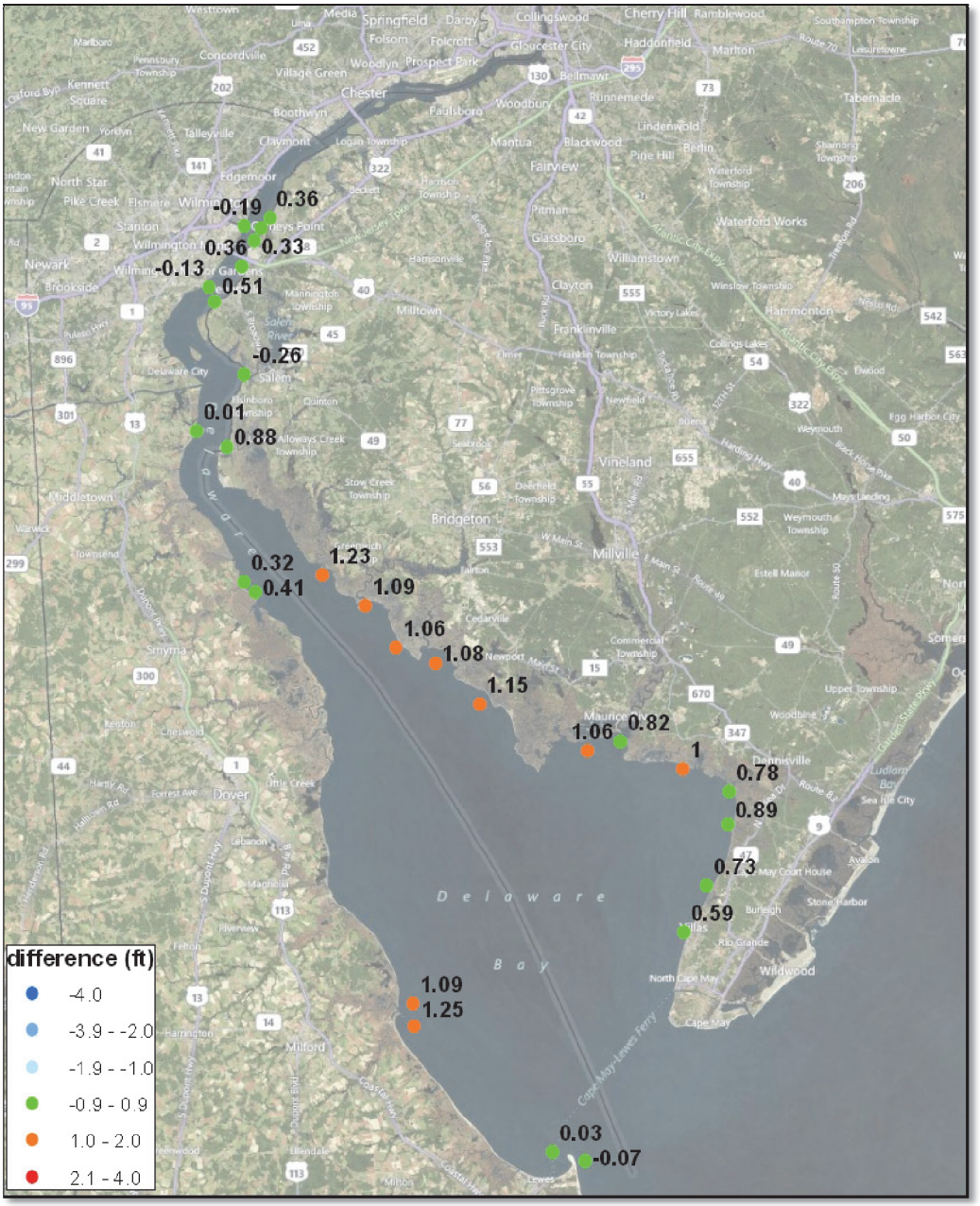

Figure 5.4. Difference between effective SWEL and FEMA Region III modeled (Modeled - Effective) for the Eastern seaboard.

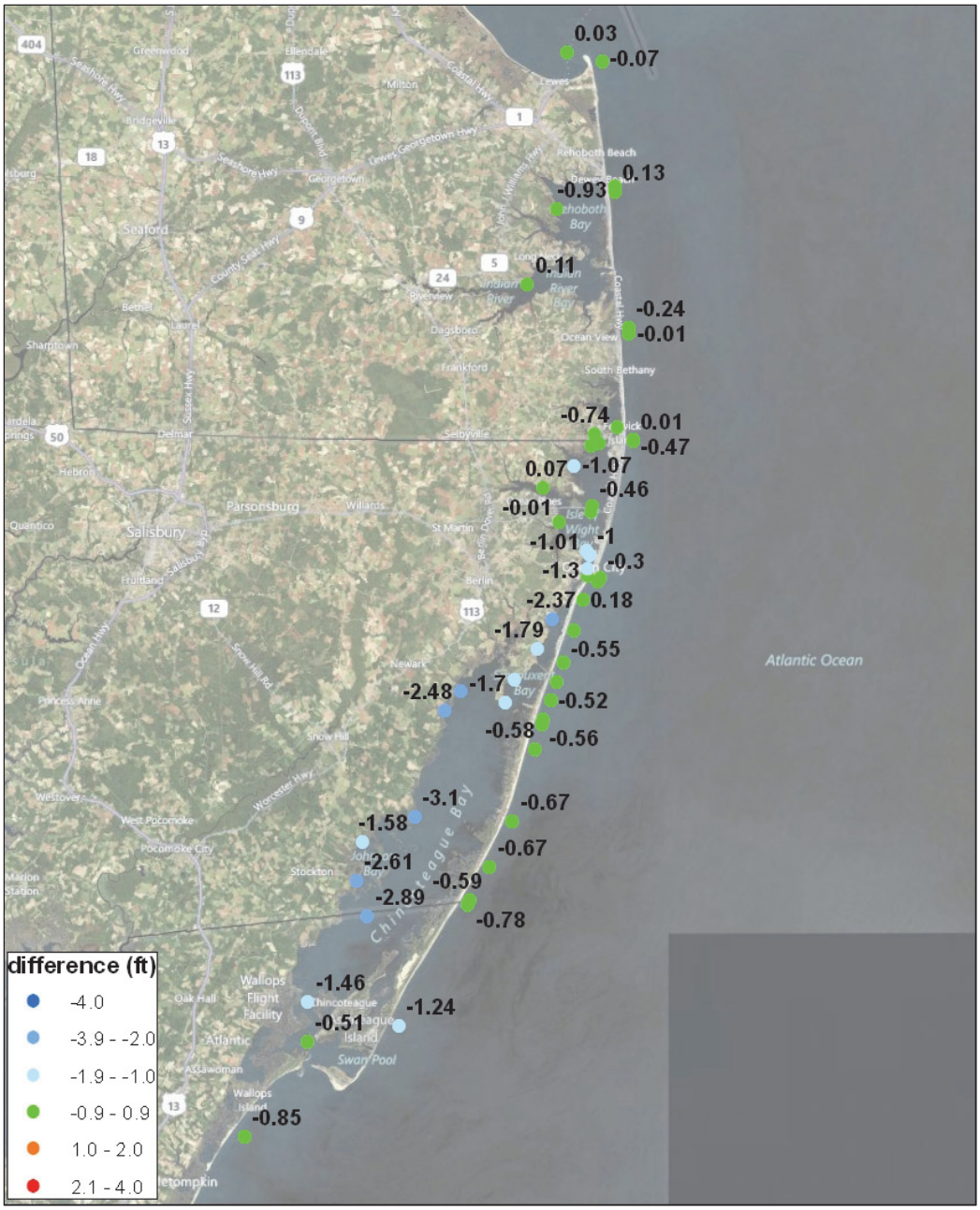

Figure 5.5. Difference between effective SWEL and FEMA Region III modeled (Modeled - Effective) for the Upper Chesapeake Bay.

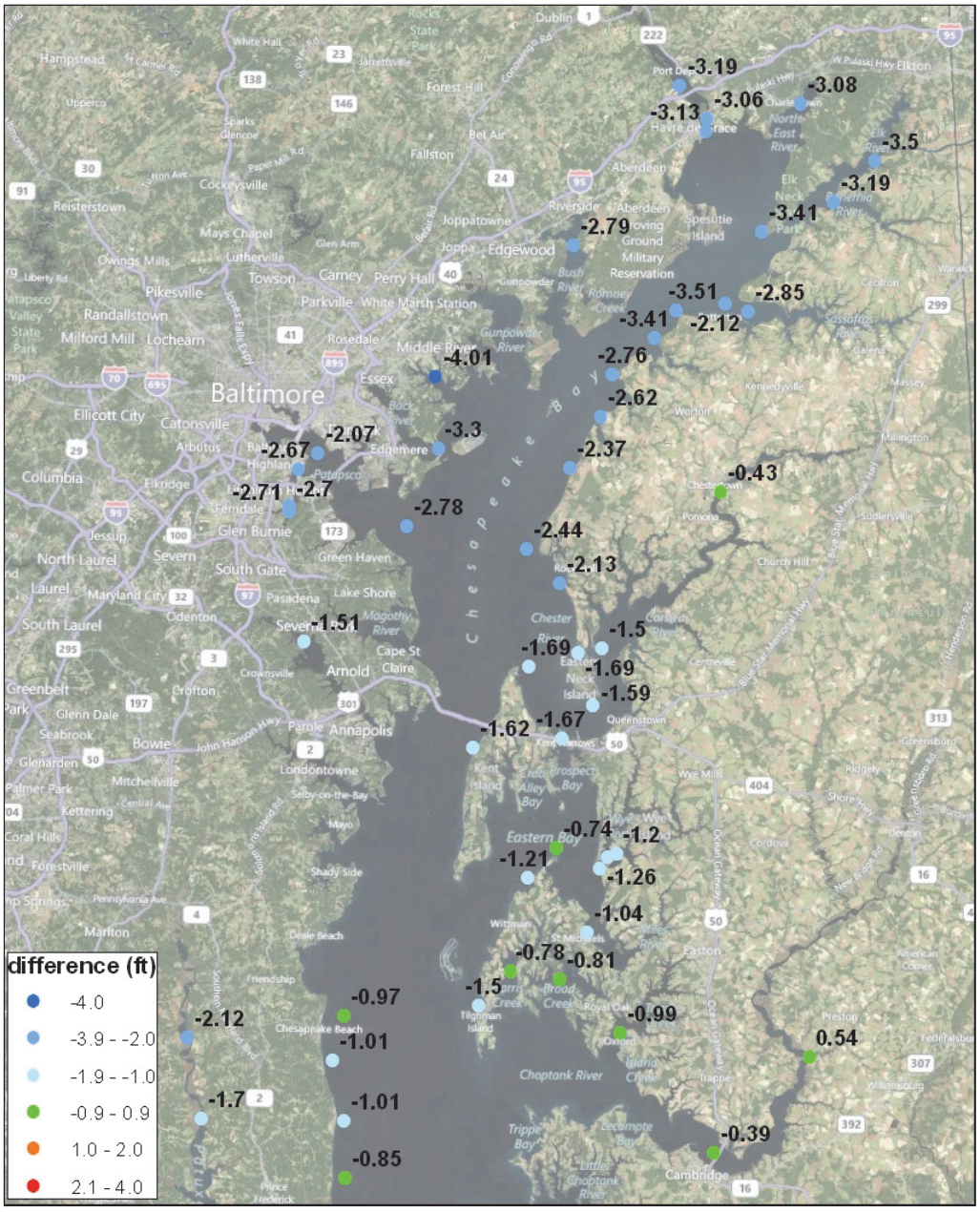

Figure 5.6. Difference between effective SWEL and FEMA Region III modeled (Modeled - Effective) for the mid-Chesapeake Bay.

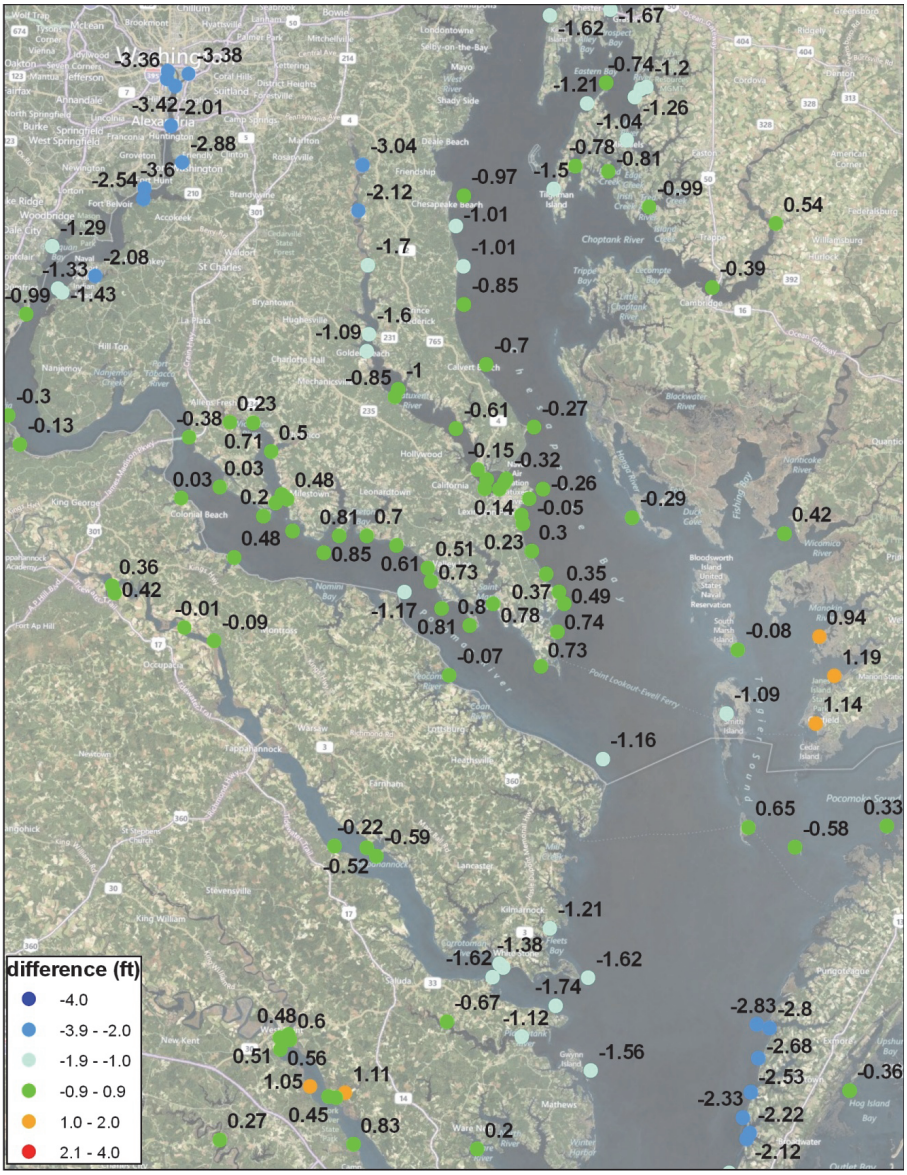

Comparison with FEMA Region II to the North

A preliminary assessment was performed between FEMA Regions II to the North encompassing New Jersey and New York with Region III. The comparison evaluated the Region II preliminary 100-yr SWEL elevations with the Region III results in the overlapping area of the Delaware Bay and Southern Coastline of New Jersey.

For both Regions, the 100-yr SWEL nodal elevations were plotted in GIS and compared by the same approach as described in the previous section. A search radius of 150 ft was employed to find overlapping points. The points

that overlapped were compared by subtracting Region II from Region III with the results shown in Figure 5.8. The comparison results were outstanding with all points (~52,000) falling within +/- 1.12 ft. These encouraging results demonstrate the fidelity of the modeling approach since the 100-yr SWELs were computed on two different model meshes by two separate teams and achieved such similar results.

Figure 5.7. Difference between effective SWEL and FEMA Region III modeled (Modeled - Effective) for the lower Chesapeake Bay.

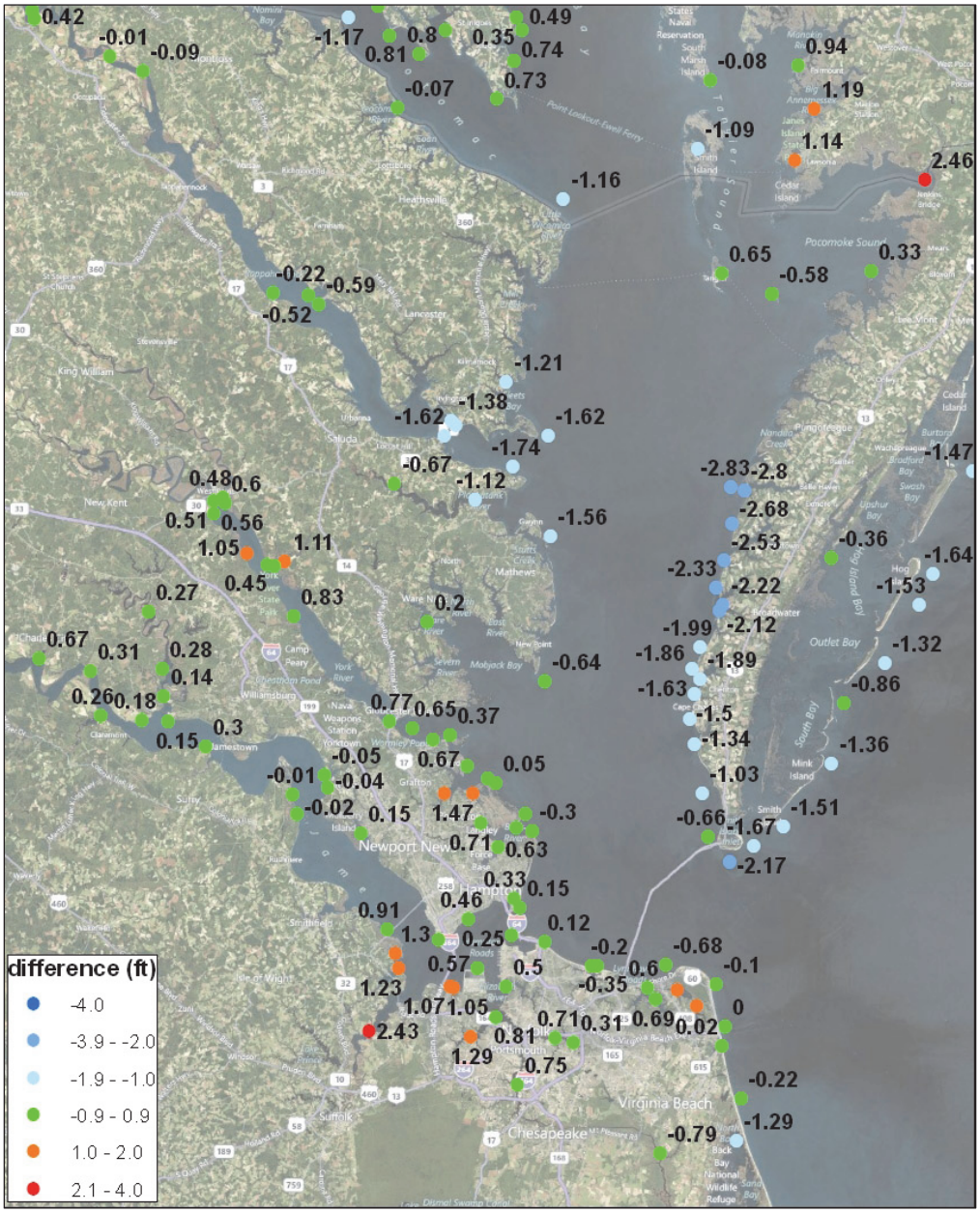

Figure 5.8. Comparison of 100-yr SWEL between FEMA Region III and Region II to the North (Region III-Region II). Green dots represent locations with less than +/- 1ft of change.

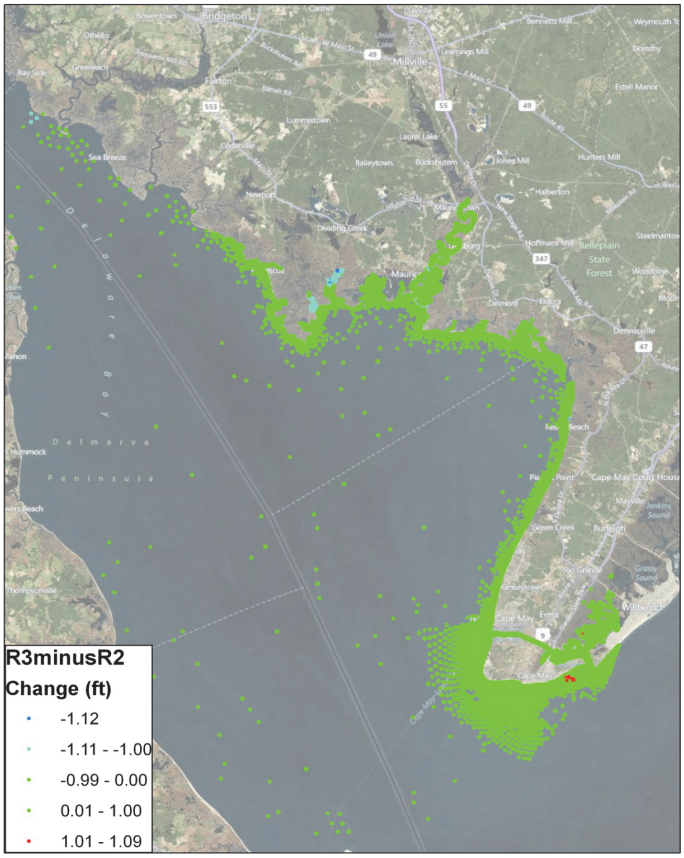

Hurricane Irene's Impact on Region III

Hurricane Irene made landfall on the Outer Banks of North Carolina on August 27, 2011 and then tracked up the eastern seaboard impacting Region III. Figure 5.9 displays Hurricane Irene's track and intensity. Irene's surge impact was measured at 7 NOAA (National Oceanic and Atmospheric Administration) Water level stations throughout Region III with locations shown in Figure 5.10. The measured residual data (observed - predicted tides = total storm surge) from each water-level station are compiled in Table 5.1. These values were then compared to the extratropical storm set extracted using peak over threshold for the full historical record at each gauge. From each water-level station storm set, which is ranked by the highest storm surge having a value/rank of 1 and the smallest surge having the highest value/rank (i.e. 25), Hurricane Irene's surge impacts were evaluated.

Figure 5.9. Hurricane Irene track and intensity throughout Region III.

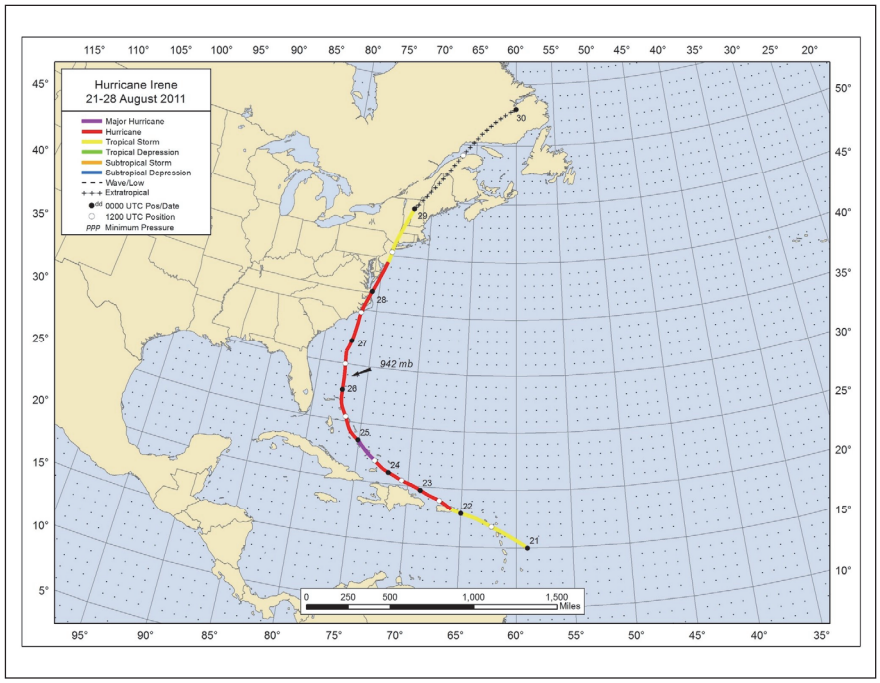

Figure 5.10. NOAA water level station locations and historical record in years.

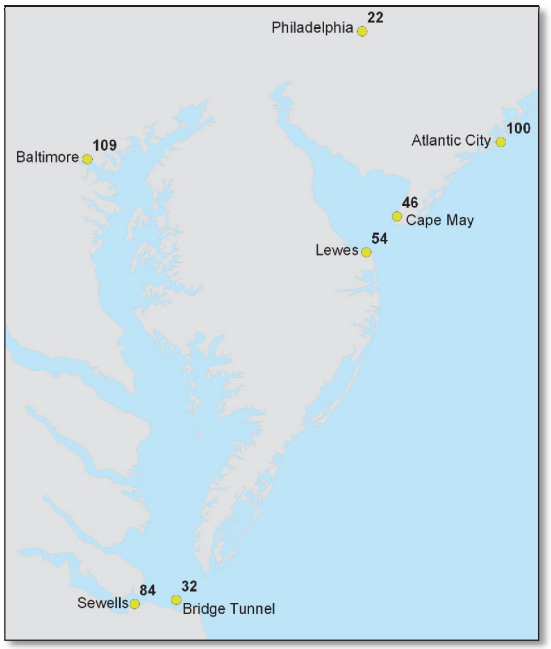

Table 5.1. Hurricane Irene storm surge measurements compared to maximum historical extratropical storm surge at 7 stations throughout FEMA Region III.

NOAA WL Station Name	Hurricane Irene Storm Surge NAVD88 ft (preliminary data)	Historical Max Observed NAVD88 ft	Difference ft	Irene storm rank
Atlantic City	3.22	4.63	-1.41	25
Baltimore	0.72	3.77	-3.05	NA
Sewells Point	4.53	5.68	-1.15	9
Cape May	2.49	5.09	-2.59	NA
Bridge Tunnel	4.13	5.45	-1.31	8
Lewes	2.92	5.54	-2.62	57
Philadelphia	2.69	4.99	-2.30	NA

Hurricane Irene produced minimal coastal surge impacts throughout FEMA Region III. The highest surge measured was 4.53 ft at Sewells point and ranked as the ninth largest of its historical record. The Chesapeake Bridge Tunnel had the second highest surge measured at 4.13 ft and was the eighth largest measured at this location. At stations Lewes and Atlantic City, the surge impacts were ranked 57th and 25th, respectively. At stations Baltimore, Cape May, and Philadelphia, Hurricane Irene did not make the ranking list and thus had very minimal measured storm surge.

Upper Chesapeake Bay and Upper Potomac River Analyses

With the reduced SWEL levels in the upper Chesapeake Bay when compared with the effective SWEL levels, a further investigation was performed using three NOAA water-level gauges in the upper Chesapeake Bay and upper Potomac River located at Chesapeake City, Tolchester Beach, and Washington, DC, with their locations shown in Figure 5.11. For each station the top 10 extreme water levels were plotted with the modeled results. This analysis did not separate tropicals from extratropicals and was intended to be a general look at how the 100-yr modeled results compared to the measurements at the NOAA water level stations. Figures 5.12 through 5.14 display the measured storm surges, and the FEMA Region III 100 and 500-yr SWEL return periods. For both Chesapeake City and Tolchester Beach, Hurricane Isabel was the storm of record with surge values measured at 7.13 and 7.08 ft MSL, respectively. For Washington, DC, Hurricane Isabel was ranked as the third largest event with a tropical storm rainfall in 1942 and a snowmelt in 1936 exceeding the Isabel levels.

Figure 5.11. Upper Chesapeake Bay and Upper Potomac River NOAA Water Level Stations (yellow points).

Figure 5. 12. Chesapeake City gauge showing top ten most extreme water levels (orange bars) and FEMA Region III modeled 100- and 500-yr return SWELs (black bars).

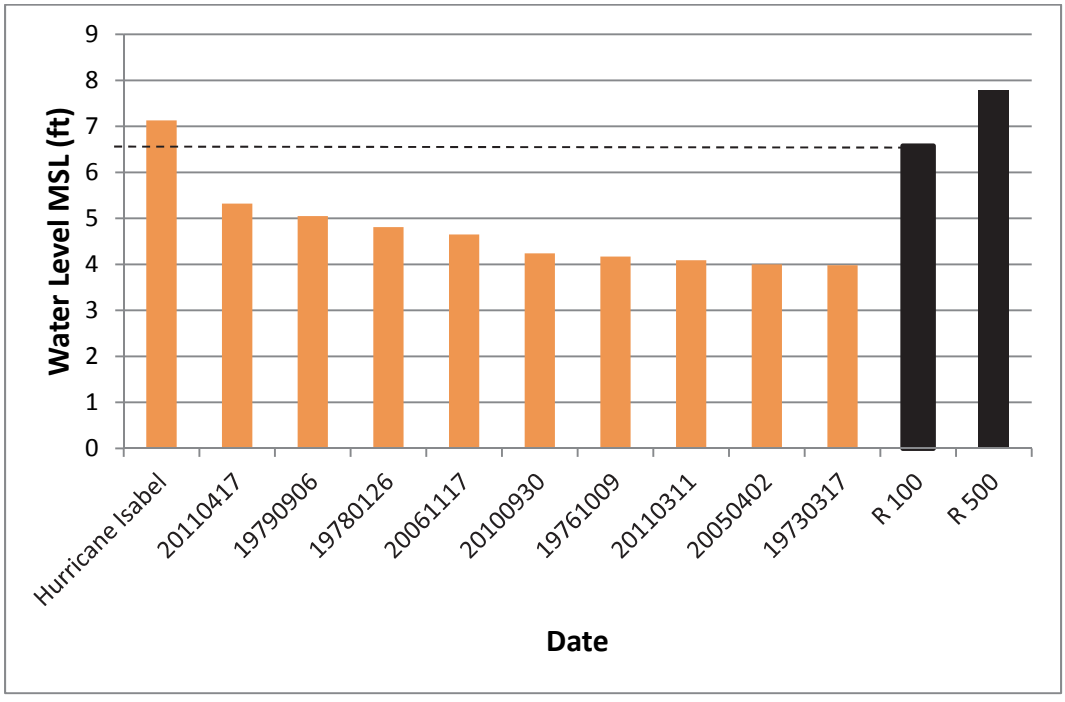

Figure 5.13. Tolchester Beach gauge showing top ten most extreme water levels (orange bars) and FEMA Region III modeled 100- and 500-yr return SWELs (black bars).

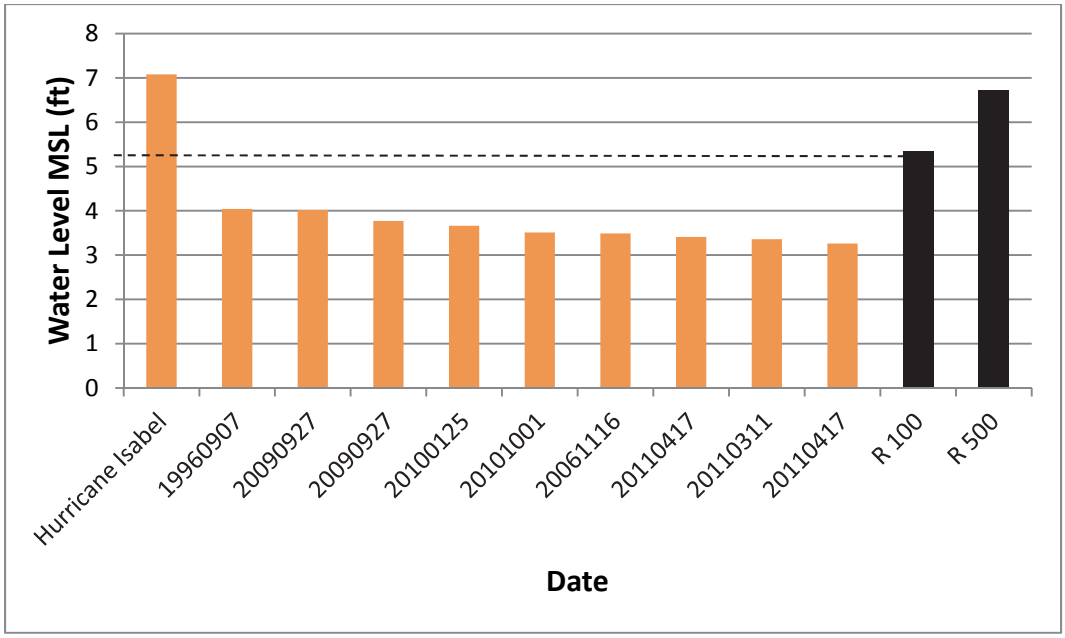

Figure 5.14. Washington, DC gauge showing top ten most extreme water levels (orange bars) and FEMA Region 3 modeled 100- and 500-yr return SWELs (black bars).

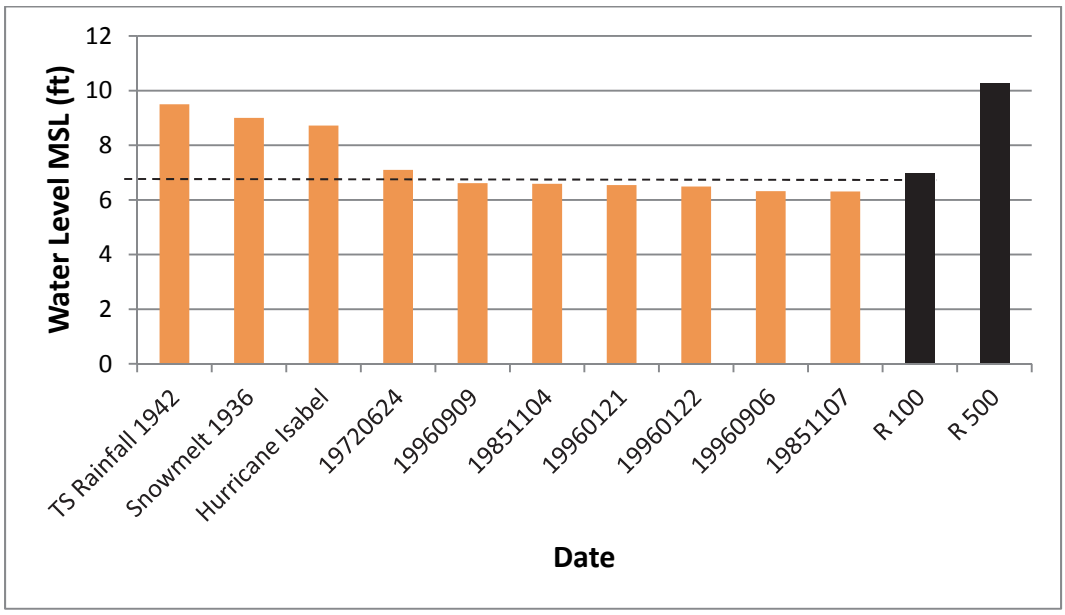

Comparing the Hurricane Isabel response with the top ten previous extreme events as well as the modeled 100-yr and 500-yr SWELs, suggests that Isabel was probably more than a 100-yr event at all three stations in the upper Chesapeake Bay and Upper Potomac River. The Washington, DC, station also demonstrates the susceptibility of this area to both riverine flooding due to rainfall and snowmelt, as well as storm surge. It is important

to note that the current storm surge study did not account for fresh-water inputs in the calculation of total storm surge.

An additional level of verification was performed by comparing the Hurricane Isabel model validation run values with the measured Hurricane Isabel values at each of the three water level stations. The results from this comparison are listed in Table 5.2. At all three stations, the values are within +/- 1.5 ft with an average bias of -0.27 ft.

Table 5.2. Hurricane Isabel Validation Results (Modeled vs. Measured).

NOS Station	Hurricane Isabel Measured (ft) MSL	Hurricane Isabel Modeled (ft) MSL	Difference (ft) Model - Measured
Chesapeake City	7.13	5.83	-1.30
Tolchester Beach	7.08	6.47	-0.61
Washington DC	8.72	9.81	1.09

6 Summary

This report presents an overview of the production phase, statistical analyses, and discussion of results and how they compare to the effective SWEL of the FEMA Region III Flood Insurance Study. During this phase, the project team has conducted a thorough and extensive analysis of the extratropical storm and hurricane storm surge and wave hazard to be used in subsequent mapping activities. The computational system established for the validation study was used without modification. This system, which links together state-of-the-art wind, wave, and surge models into a comprehensive tool for surge- and wave-hazard determination, has been extensively verified and validated in terms of both the individual model components and the networked/coupled system of models. The computational resources required to solve the complete problem specification are considerable, totaling more than 1 million computer hours and 10 terabytes of stored model output.

The methods used to compute the individual storm surge and wave simulations as well as the statistical analyses represent the state-of-the-art in terms of calculation of the surge and wave hazard for a coastal region. While these methods are generally similar to recent, previous studies, several differences are noted. The complexity of the Region III coast includes a large relatively sheltered bay system (Chesapeake) as well as a more exposed bay (Delaware). Large rivers enter into both bays. Both of these features have led to a comprehensive representation of the coastal geometry in both a digital elevation model and the underlying ADCIRC and wave model grids. Substantial effort has been placed in the representation of the rivers and the Intracoastal Waterway. Additionally, two different storm types that define the full storm hazard impact Region III: extratropical storms and tropical storms. This mixture of storm types has required a substantial number of individual simulations and a combination of statistical methods. The levels of detail and effort have resulted in a final product that is both comprehensive and reasonably consistent with effective stillwater levels obtained from previous NFIP studies.

The synthesized results clearly identify the high- and low-risk regions of the mid-Atlantic coast. The coastal storm surge *hot spots*, in order of most extreme to least, are the Delaware Bay (in particular the southwestern

shore), lower Atlantic coast estuary region of the Virginia eastern shore, lower Chesapeake up into the James River, and upper reaches of the Chesapeake Bay leading into the Chesapeake and Delaware Canal.

References

Blanton, B., L. Stillwell, H. Roberts, J. Atkinson, S. Zou, M. Forte, J. Hanson, and R. Luettich. 2011. *Coastal storm surge analysis: Computational system (Intermediate Submission No. 1.2).* ERDC /CHL TR-11-1. Vicksburg, MS: US Army Engineer Research and Development Center.

Borgman, L. E., M. C. Miller, H. L. Butler, and R. D. Reinhard. 1992. *Empirical simulation of future hurricane storm histories as a tool in engineering and economic analysis.* College Station, TX: Fifth International Conference on Civil Engineering in the Oceans, ASCE, 2-5 November 1992.

Forte, M. F., J. L. Hanson, L. Stillwell, M. Blanchard-Montgomery, B. Blanton, R. Luettich, H. Roberts, J. Atkinson, and Jason Miller. 2011. *Coastal storm surge analysis: System digital elevation model (Intermediate Submission No. 1.1).* ERDC/CHL TR-11-1. Vicksburg, MS: US Army Engineer Research and Development Center.

Hanson, J., H. Wadman, B. Blanton, and H. Roberts. 2012. *Coastal storm surge analysis: Modeling system validation (Intermediate Submission No. 2).* ERDC/CHL TR-11-1. Vicksburg, MS: US Army Engineer Research and Development Center.

Niedoroda, A., D. Resio, G. Toro, D. Divoky, H. Das, and C. Reed. 2010: Analysis of the coastal Mississippi storm surge hazard. *Ocean Eng*. 37(1):82–90.

Scheffner, N. W., J. E. Clausner, A. Militello, L. E. Borgman, B. L. Edge, and P. J. Grace. 1999. *Use and application of the empirical simulation technique: User's guide*. ERDC/CHL TR-99-21. Vicksburg, MS: US Army Engineer Waterways Experiment Station, US Army Engineer Research and Development Center.

Vickery, P., D. Wadhera, A. Cox, V. Cardone, J. Hanson, and B. Blanton. 2012. *Coastal storm surge analysis: Storm forcing (Intermediate Submission No. 1.3).* ERDC/CHL TR-11-1. Vicksburg, MS: US Army Engineer Research and Development Center.

Appendix A: USACE Norfolk District Review of Region III SWEL Results

Here are our review comments for the ADCIRC storm surge study results:

1. From our general review, we too did not find any major issues or concerns with the new ADCIRC storm surge results.

For most communities, the effective Flood Insurance Study is based on a historical tide gauge/highwater mark analysis, where the gauge(s) used in the analysis could be located a good distance away. This could possibly mean the 100-year flood elevation is under or overestimated for a community. The ADCIRC modeling provides a more locally and physically based solution, which could be higher or lower than a tide gauge/highwater mark analysis result.

Storm surge models were used/considered in the effective Flood Insurance Studies for Accomack and Northampton Counties and the city of Poquoson. This included the 1976 NOAA Technical Memorandum NWS Hydro-32 analysis along the Atlantic Coast; the 1978 VIMS study for the Chesapeake Bay, and the 1976 Resource Analysis, Inc. two-dimensional unsteady flow model for Chincoteague Bay. The ADCIRC model study provides an overall updated analysis, considering improved modeling, methods, and computer power, where differences with the older effective studies and the new results could occur.

2. There were some places where it appeared the grid could have been extended, but may not be an issue with the final floodplain mapping.

3. With a typical floodplain study, coastal or

riverine, possible modeling errors or issues may surface during the mapping/floodplain delineation phase. This may also be true for the wave height analysis as well.

4. In 2005, our District completed a stillwater frequency analysis for the Sewells Point gauge, for the period 1928 to 2003, including Hurricane Isabel. Although there are additional years of record and other notable storms (Ernesto in 2006, Nor'Ida in 2009, Irene in 2011) that have occurred, it is interesting to see and compare the 2005 study with the ADCIRC results at Sewells Point and the effective 2009 City of Norfolk Flood Insurance Study (gauge analysis based on period of record from 1928 to 1978), elevations in feet and referenced to NAVD88:

ADCIRC Study-
10-year = 5.2
50-year = 6.7
100-year = 7.3
500-year = 8.7

2005 Study-
10-year = 5.0
50-year = 6.4
100-year = 7.0
500-year = 8.4

City of Norfolk Flood Insurance Study-
10-year = 5.5
50-year = 6.9
100-year = 7.6
500-year = 8.9

5. Chris, Jason, and I are familiar with the NOAA/National Hurricane Center's SLOSH model, used in USACE/FEMA Hurricane Evacuation Studies. The SLOSH model is not an accepted storm surge model by FEMA for completing Flood Insurance Studies. It is interesting

to see the general similarities between the ADCIRC and SLOSH model results in terms of the locations with high storm surge levels and those with low storm surge. See the attachments.

Let me know if you have any questions or need more information.

Thanks, Paul
Ph: (757) 201-7778

Appendix B: USACE Baltimore District Review of Region III SWEL Results

We have completed our review of the new calculated 1% annual chance stillwater elevations for the Region III study within our Area of Responsibility.

We did not notice any new elevations calculated that seemed to be outliers compared to the new calculated elevations for surrounding data points.

We also did not notice any new elevations calculated that seemed questionable based on our local knowledge/experience.

We did a check to ensure that our calculated difference between the effective stillwater elevation and the new stillwater elevations for a given area was similar to the differences ERDC calculated. We thought that if our analysis showed a significant difference between old and new that did not match ERDC's calculated difference, it might point us to an anomaly or issue with the newly calculated data. This analysis showed that our calculated difference between the effective elevations and the new elevations is very close to the difference that ERDC calculated, so we did not find any issues or anomalies in the data through this process.

In summary, we did not see anything in the newly calculated stillwater elevations that raised any concerns. We are very confident in the results.

Please let me know if you have any questions or need more information.

Thanks

Christopher Penney
US Army Corps of Engineers
Baltimore District- Planning Division
Phone: 410-962-2941 Fax: 410-962-2948
Email: christopher.penney@usace.army.mil

Appendix C: USACE Philadelphia District Review of Region III SWEL Results

NAP Review of Results

NAP conducted an independent review of the Stillwater Elevation (SWEL) results for the FEMA Region 3 Coastal Domain (henceforth referred to as "R3 Results"). The process chosen by NAP was to look at published effective FEMA data by county and perform a mathematical comparison in order to find areas of interest and further evaluation. Different counties have different information available. The following information was used when available:

1) DFIRM Flood Zone polygons with Static BFEs for AE and VE Zones; some problems inherent are that AE and VE coastal zones may include wave action which are not accounted for in the R3 Results
2) Published Stillwater Elevations in the Flood Insurance Text; these are usually given as points, in some cases as ranges along the coastline
3) Inland Riverine BFEs; this gives us a sense for how well the R3 Results will tie-in with riverine profiles that originate in the tidal zone

Sussex County DE (SC)

Available FEMA Effective information: Coastal/Tidal AE and VE zones with waves; Published SWEL; Inland Riverine BFEs

Kent County DE (KC)

Available FEMA Effective information: Coastal/Tidal AE and VE zones with waves; Published SWEL; Inland Riverine BFEs

New Castle County DE (NCC)

Available FEMA Effective information: Coastal/Tidal AE zone with waves; Published SWEL; Inland Riverine BFEs

Delaware County PA (DC)

Available FEMA Effective information: Tidal AE zones (no waves); Published SWEL; Inland Riverine BFEs

City of Philadelphia PA (P)

Available FEMA Effective information: Tidal AE zones (no waves); Published SWEL; Inland Riverine BFEs

Bucks County PA (BC)

Available FEMA Effective information: Tidal AE zones (no waves); Published SWEL; Inland Riverine BFEs

VE Zone Comparison

The following table shows a comparison between the R3 Results and the Effective VE Zones within Sussex and Kent Counties, DE. As stated above, the Effective VE Zones do include a wave height analysis which is missing from the R3 Results. VE Zones are designated as areas expecting to encounter wave heights in excess of 3-feet. So we can use the 3-feet parameter as a benchmark of sorts in the comparison.

Region 3 Coastal Review: Approach #2 - VE Zone SBFE Revised

No.	VE Zone ID	VE Zones	SBFE	R3 Points	R3 Elev					R3 Mean - VE Zone SBFE
					Count	Min	Max	Mean	SD	
1	Sussex	26		6,047	6,047	3.855	9.463	6.774	1.542	
S1	2007		9.0	1,594	1,594	4.724	6.698	5.606	0.616	-3.4
S2	1911		10.0	259	259	5.495	6.641	6.028	0.332	-4.0
S3	2001		10.0	424	424	4.714	4.928	4.834	0.039	-5.2
S4	1910		14.0	1,020	1,020	6.686	8.371	7.589	0.351	-6.4
S5	1909		13.0	1,234	1,234	7.440	9.463	8.571	0.538	-4.4
S6	1908		11.0	192	192	5.573	6.597	6.085	0.279	-4.9
S7	1907		8.0	239	239	4.759	5.025	4.851	0.066	-3.1
S8	1906		8.0	57	57	3.855	4.305	4.114	0.093	-3.9
S9	1884		12.0	205	205	4.858	8.327	7.823	0.495	-4.2
S10	1905		7.0	33	33	4.229	4.516	4.331	0.065	-2.7
S11	1901		12.0	124	124	5.602	8.545	8.104	0.322	-3.9
S12	1995		10.0	128	128	8.179	9.461	9.191	0.197	-0.8
S13	1903		9.0	138	138	4.599	5.499	4.676	0.131	-4.3
S14	1902		8.0	99	99	4.847	4.944	4.891	0.023	-3.1
S15	1997		13.0	53	53	9.017	9.245	9.147	0.060	-3.9
S16	1889		10.0	114	114	7.796	8.954	8.419	0.279	-1.6
S17	1897		11.0	52	52	7.522	8.080	7.737	0.149	-3.3
S18	1894		12.0	21	21	7.860	8.230	8.058	0.127	-3.9
S19	1891		7.0	5	5	4.029	4.135	4.087	0.036	-2.9
S20	1890		10.0	21	21	8.077	8.300	8.214	0.061	-1.8
S21	1888		10.0	4	4	4.886	5.220	5.038	0.137	-5.0
S22	1887		13.0	12	12	7.250	7.978	7.837	0.192	-5.2
S23	1882		10.0	8	8	6.499	6.958	6.721	0.156	-3.3
S24	1994		11.0	6	6	9.277	9.305	9.295	0.010	-1.7
S25	1992		13.0	4	4	9.266	9.284	9.272	0.007	-3.7
S26	1876		11.0	1	1	8.875	8.875	8.875	0.000	-2.1
2	Kent	14		3,733	3,733	8.021	9.827	8.896	0.349	
K1	1144		11.0	1,021	1,021	8.418	9.514	8.793	0.170	-2.2
K2	1136		13.0	252	252	8.582	9.649	8.986	0.228	-4.0
K3	697		11.0	783	783	8.021	8.830	8.654	0.122	-2.3
K4	1135		11.0	546	546	9.047	9.695	9.420	0.156	-1.6
K5	1142		12.0	453	453	8.970	9.585	9.219	0.143	-2.8
K6	1140		12.0	208	208	8.480	8.897	8.714	0.121	-3.3
K7	1138		12.0	313	313	8.384	8.773	8.513	0.131	-3.5
K8	685		11.0	43	43	8.985	9.827	9.459	0.366	-1.5
K9	682		11.0	34	34	8.174	8.353	8.268	0.048	-2.7
K10	678		11.0	35	35	9.325	9.435	9.361	0.029	-1.6
K11	674		11.0	14	14	8.085	8.196	8.134	0.035	-2.9
K12	670		12.0	14	14	8.134	8.274	8.196	0.044	-3.8
K13	655		11.0	8	8	8.348	8.380	8.365	0.009	-2.6
K14	1133		12.0	9	9	9.249	9.474	9.367	0.061	-2.6

Conclusion: Due to the lack of wave height analysis, there are not too many conclusions that can be drawn from the VE Zone comparison. In all cases, the R3 Results are lower, which is to be expected due to the lack of wave height analysis.

In some cases, where the R3 Results are minimally lower than the Effective VE Zone Elevation (less than 1 ft for example), the addition of wave heights may cause an overall change such that the R3 Results will be 2-feet higher than Effective.

Similarly, where the R3 Results are significantly lower than the Effective VE Zone Elevation (more than 5-feet for example), the addition of wave heights may not bring those R3 Results in line with the Effective. For example, an addition of a 3-foot wave height to the R3 Results would still be 2-feet lower than the Effective VE Zone Elevation.

All of these areas, five VE Zone polygons in total, have been highlighted on the following map. It is interesting to note the location of the two different classifications of highlighted areas; the area where the R3 Results is “too high” is in the somewhat sheltered area of the Bay, and the four areas where the R3 Results are “too low” are on the open coast of the Atlantic Ocean. However, it is worth noting again that it is not appropriate to draw too many conclusions before the wave height analysis is completed.

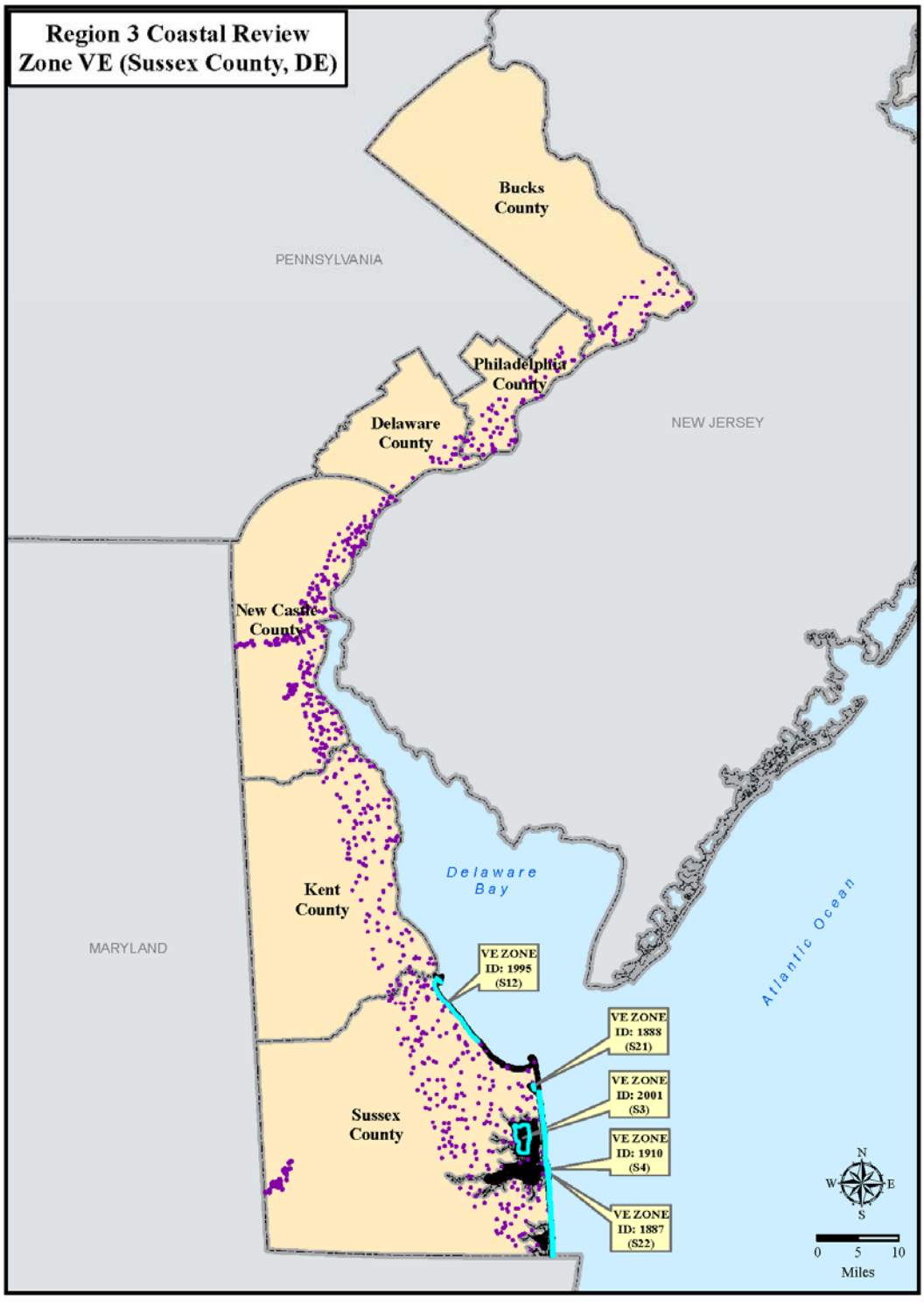
Region 3 Coastal Review
Zone VE (Sussex County, DE)
Bucks County
PENNSYLVANIA
Philadelphia County
Delaware County
NEW JERSEY
New Castle County
Kent County
MARYLAND
Delaware Bay
Atlantic Ocean
Sussex County
VE ZONE ID: 1995 (S12)
VE ZONE ID: 1888 (S21)
VE ZONE ID: 2001 (S3)
VE ZONE ID: 1910 (S4)
VE ZONE ID: 1887 (S22)
N
W
E
S
0 5 10
Miles

AE Zone Comparison

The following table shows a comparison between the R3 Results and the Effective AE Zones within Sussex and Kent Counties, DE; Delaware and Bucks Counties, PA and the City of Philadelphia. As stated above, the Effective AE Zones Sussex and Kent include a wave height analysis which is missing from the R3 Results. AE Zones are designated as areas expecting to see wave heights less than 3-feet. So we can use the 3-feet parameter as a benchmark of sorts in the comparison.

The AE Zones in Delaware, Bucks and Philadelphia do not include a wave height analysis and therefore represents a valid comparison.

Region 3 Coastal Review: Approach #2 - AE Zone SBFE

No.	AE Zone ID	AE Zones	Stillwater	SBFE	R3 Points	R3 Elev					R3 Mean - AE Zone SBFE
						Count	Min	Max	Mean	SD	
1	Sussex	83/56			15,084	15,084	3.546	9.687	6.781	1.719	
S1	1990			10.0	5,674	5,674	7.455	9.647	8.392	0.587	-1.6
S2	1989			9.0	381	381	7.697	9.687	8.546	0.771	-0.5
S3	1869			5.0	352	352	3.546	6.236	4.312	0.667	-0.7
S4	1826			5.0	230	230	5.667	5.961	5.784	0.094	0.8
S5	2008			7.0	587	587	5.493	6.596	6.013	0.195	-1.0
S6	1860			7.0	966	966	4.737	8.189	4.972	0.228	-2.0
S7	1978			9.0	1,316	1,316	4.589	8.365	5.509	1.127	-3.5
S8	1970			6.0	657	657	4.492	5.259	4.829	0.204	-1.2
S9	1867			8.0	377	377	5.474	6.938	6.382	0.394	-1.6
S10	1866			7.0	515	515	6.386	7.236	6.850	0.206	-0.1
S11	1864			7.0	446	446	4.860	6.533	5.524	0.512	-1.5
S12	1863			8.0	284	284	4.775	6.451	5.128	0.351	-2.9
S13	1988			9.0	767	767	7.960	9.022	8.201	0.189	-0.8
S14	1861			6.0	345	345	3.688	6.338	4.499	0.417	-1.5
S15	1862			7.0	215	215	3.786	4.636	4.094	0.174	-2.9
S16	1986			8.0	229	229	4.591	8.394	5.447	1.071	-2.6
S17	1858			8.0	165	165	4.850	5.213	4.959	0.072	-3.0
S18	1857			8.0	162	162	5.060	6.206	5.796	0.213	-2.2
S19	1976			9.0	43	43	9.231	9.479	9.295	0.065	0.3
S20	1756			7.0	26	26	7.018	7.110	7.065	0.026	0.1
S21	1972			7.0	177	177	4.569	5.710	4.722	0.199	-2.3
S22	1980			9.0	158	158	9.270	9.404	9.315	0.021	0.3
S23	1855			6.0	180	180	4.656	5.961	5.350	0.337	-0.6
S24	1846			5.0	371	371	4.045	5.051	4.417	0.209	-0.6
S25	1854			9.0	9	9	6.671	6.715	6.689	0.012	-2.3
S26	1979			8.0	29	29	4.643	4.711	4.673	0.020	-3.3
S27	1853			6.0	18	18	3.774	3.924	3.818	0.039	-2.2
S28	1849			7.0	65	65	4.724	5.189	4.902	0.122	-2.1
S29	1810			8.0	1	1	8.277	8.277	8.277	0.000	0.3
S30	1845			8.0	39	39	6.251	6.590	6.389	0.097	-1.6
S31	1825			7.0	6	6	6.276	6.280	6.278	0.001	-0.7
S32	1749			7.0	5	5	6.177	6.281	6.249	0.041	-0.8
S33	1842			7.0	25	25	5.408	5.633	5.548	0.063	-1.5
S34	1960			10.0	100	100	4.691	4.818	4.751	0.032	-5.2
S35	1841			7.0	23	23	4.841	4.896	4.869	0.014	-2.1
S36	1836			7.0	14	14	7.101	7.239	7.200	0.046	0.2
S37	1969			8.0	26	26	9.289	9.469	9.349	0.044	1.3
S38	1835			7.0	19	19	7.014	7.095	7.057	0.025	0.1
S39	1832			7.0	1	1	3.771	3.771	3.771	0.000	-3.2
S40	1967			9.0	4	4	9.452	9.493	9.480	0.017	0.5
S41	1964			9.0	4	4	9.480	9.492	9.485	0.004	0.5
S42	1827			8.0	6	6	5.039	7.801	6.834	1.270	-1.2
S43	1823			7.0	16	16	7.081	7.093	7.089	0.004	0.1
S44	1804			10.0	5	5	8.143	8.327	8.248	0.059	-1.8
S45	1963			9.0	2	2	8.221	8.232	8.227	0.005	-0.8
S46	1962			9.0	1	1	8.089	8.089	8.089	0.000	-0.9
S47	1820			7.0	12	12	6.940	7.052	6.999	0.034	0.0
S48	1795			7.0	14	14	7.067	7.113	7.089	0.013	0.1
S49	1959			9.0	2	2	9.412	9.417	9.414	0.003	0.4
S50	1814			7.0	1	1	6.612	6.612	6.612	0.000	-0.4
S51	1951			10.0	3	3	7.814	7.848	7.830	0.014	-2.2
S52	1805			7.0	2	2	7.091	7.107	7.099	0.008	0.1

No.	AE Zone ID	AE Zones	Stillwater	SBFE	R3 Points	R3 Elev					R3 Mean - AE Zone SBFE
						Count	Min	Max	Mean	SD	
S53	1801			7.0	3	3	7.094	7.098	7.096	0.002	0.1
S54	1797			10.0	3	3	8.293	8.355	8.334	0.029	-1.7
S55	1790			7.0	1	1	7.087	7.087	7.087	0.000	0.1
S56	1783			7.0	2	2	7.061	7.074	7.067	0.007	0.1
2	Kent	49/33			5,125	5,125	6.548	9.869	8.832	0.668	
K1	632			10.0	4,173	4,173	7.545	9.868	8.885	0.605	-1.1
K2	698			9.0	67	67	7.768	9.069	8.278	0.342	-0.7
K3	694			9.0	52	52	9.234	9.542	9.345	0.111	0.3
K4	696			9.0	68	68	8.726	8.765	8.745	0.007	-0.3
K5	695			9.0	75	75	8.222	8.419	8.274	0.040	-0.7
K6	693			9.0	68	68	6.548	6.852	6.709	0.084	-2.3
K7	691			9.0	28	28	9.139	9.701	9.512	0.133	0.5
K8	690			10.0	71	71	6.837	7.656	7.318	0.247	-2.7
K9	688			9.0	28	28	8.866	9.847	9.126	0.374	0.1
K10	687			11.0	58	58	8.326	9.314	8.658	0.229	-2.3
K11	686			11.0	39	39	8.972	9.829	9.499	0.229	-1.5
K12	684			9.0	14	14	7.712	8.011	7.879	0.109	-1.1
K13	680			11.0	24	24	8.114	8.403	8.295	0.099	-2.7
K14	679			9.0	19	19	8.690	9.766	8.899	0.289	-0.1
K15	662			11.0	39	39	9.130	9.546	9.348	0.149	-1.7
K16	676			11.0	76	76	7.754	8.622	8.317	0.194	-2.7
K17	675			11.0	42	42	9.133	9.272	9.206	0.039	-1.8
K18	673			9.0	5	5	9.516	9.869	9.727	0.170	0.7
K19	672			11.0	21	21	7.558	7.758	7.647	0.054	-3.4
K20	671			11.0	37	37	9.586	9.692	9.641	0.025	-1.4
K21	668			11.0	18	18	9.445	9.704	9.614	0.050	-1.4
K22	665			9.0	6	6	8.880	8.909	8.892	0.011	-0.1
K23	1134			9.0	34	34	9.318	9.473	9.416	0.046	0.4
K24	664			9.0	29	29	9.515	9.691	9.619	0.042	0.6
K25	656			9.0	2	2	8.388	8.389	8.388	0.001	-0.6
K26	654			11.0	6	6	9.304	9.316	9.309	0.005	-1.7
K27	653			9.0	1	1	9.123	9.123	9.123	0.000	0.1
K28	652			11.0	3	3	9.333	9.415	9.370	0.034	-1.6
K29	646			9.0	1	1	8.707	8.707	8.707	0.000	-0.3
K30	647			11.0	4	4	9.074	9.101	9.085	0.010	-1.9
K31	640			9.0	5	5	9.070	9.099	9.081	0.011	0.1
K32	633			9.0	9	9	9.183	9.315	9.258	0.046	0.3
K33	625			9.0	3	3	8.601	8.771	8.675	0.071	-0.3
4	DelCo	10/1			1,341	1,341	8.301	8.842	8.523	0.141	
D1	1445			8.5	1,341	1,341	8.301	8.842	8.523	0.141	0.0
5	Phila*	10/3			2,654	2,654	7.746	9.388	8.352	0.467	
P1	40			8.9	2	2	8.052	8.054	8.053	0.001	-0.9
P2	888			8.9	1,990	1,990	8.825	9.979	9.206	0.313	0.3
P3	889			9.3	64	64	9.967	10.065	10.003	0.020	0.7
6	Bucks	22/1			2,610	2,610	10.404	12.510	11.947	0.571	
B1	2315			13.0	2	2	12.119	12.122	12.121	0.002	-0.9

Conclusion: In comparing the results for this analysis, we were looking for areas where the R3 results were greater than the Effective AE Elevations by 1-foot or more. This applies to areas with and without waves. For areas with waves, this would identify areas where the R3 Results would be 1-foot greater than Effective PLUS the wave height. For areas with no waves, this would identify areas where the R3 Results would higher by 1-foot or more. We only found one instance that met this criteria, which was in Sussex County.

We were also looking for areas with waves where the R3 Results were lower than the Effective by 4-feet or more. With the potential addition of a wave less than 3-feet high, this analysis would identify areas that would have a resulting R3 Result greater than 1-foot lower than the Effective. For areas with no waves, we were looking for areas where the R3 Results were lower than the Effective by 1-foot or more. Again, there was only one instance meeting this criterion, which was also in Sussex County.

The two areas in Sussex County that resulted from this analysis are highlighted on the following map. It is interesting to note the location of the two different classifications of highlighted areas; the area where the R3 Results is “too high” is in the somewhat sheltered area of the Bay, and the area where the R3 Result is “too low” is on the open coast of the Atlantic Ocean. However, it is worth noting again that it is not appropriate to draw too many conclusions before the wave height analysis is completed.

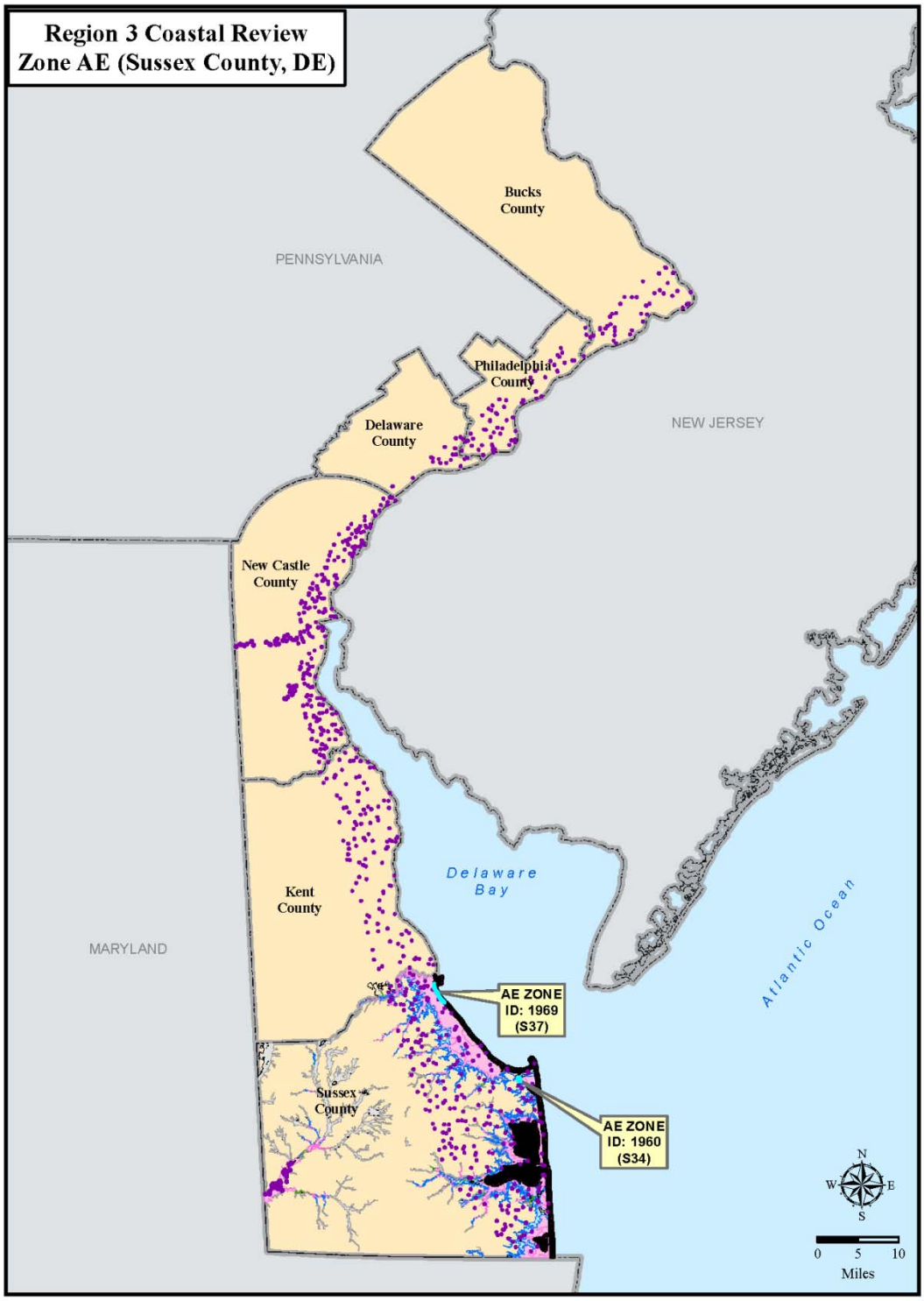
Region 3 Coastal Review
Zone AE (Sussex County, DE)
Bucks County
PENNSYLVANIA
Philadelphia County
Delaware County
NEW JERSEY
New Castle County
Kent County
MARYLAND
Delaware Bay
Atlantic Ocean
AE ZONE ID: 1969 (S37)
Sussex County
AE ZONE ID: 1960 (S34)
N
W
E
S
0 5 10
Miles

Stillwater Elevation Comparison

The following table shows a comparison between the R3 Results and the published Stillwater Elevations (SWEL) within Sussex and New Castle Counties, DE; Bucks County, PA and the City of Philadelphia. SWELs do not include a wave height analysis and represent a straight, valid comparison with the R3 Results. The SWELs are not a regulatory elevation but are used as the basis for generating the Regulatory Base Flood Elevations (BFEs). In counties where a previous wave analysis was performed (Sussex, Kent and New Castle Counties, DE), the Regulatory BFE includes the wave heights, but the SWEL gives us a better idea of how the final results will compare instead of the vague idea of adding up to a 3-foot wave in an AE Zone or something greater than a 3-foot wave in a VE Zone.

Region 3 Coastal Review: Approach #2 - AE Zone SBFE

No.	AE Zone ID	AE Zones	Stillwater	SBFE	R3 Points	R3 Elev					R3 Mean - AE Zone SBFE
						Count	Min	Max	Mean	SD	
SSW1	SSW1		8.4		1,173	1,173	4.569	8.394	5.176	0.630	-3.2
SSW2	SSW2		8.1		254	254	5.474	8.257	5.809	0.287	-2.3
SSW3	SSW3		7.8		202	202	4.661	8.327	5.054	0.662	-2.7
SSW4	1826_SSW4		5.0		230	230	5.667	5.961	5.784	0.093	0.8
SSW5	SSW5		8.5		8,508	8,508	4.589	9.687	7.906	1.318	-0.6
SSW6	SSW6		6.7		1,887	1,887	4.860	7.239	6.356	0.521	-0.3
SSW7	SSW7		6.2		1,805	1,805	4.492	5.703	4.918	0.192	-1.3
SSW8	SSW8		5.2		680	680	3.727	4.999	4.215	0.236	-1.0
SSW9	SSW9		5.2		495	495	3.546	6.236	4.379	0.566	-0.8
3	New Castle	12/1									
NS	88		8.6		11,280	11,280	6.572	8.870	8.348	0.225	-0.3
NSW1	88_NSW1		8.8		2861	2861	7.887	8.373	8.298	0.093	-0.5
NSW2	88_NSW2		8.8		749	749	8.139	8.360	8.319	0.025	-0.5
NSW3	88_NSW3		8.7		1932	1932	8.287	8.451	8.363	0.028	-0.3
NSW4	88_NSW4		8.7		3452	3452	7.771	8.599	8.330	0.174	-0.4
NSW5	88_NSW5		8.6		1,671	1,671	6.572	8.870	8.369	0.471	-0.2
NSW6	88_NSW6		8.7		566	566	8.562	8.750	8.658	0.030	0.0
NSW7	88_NSW7		8.6		49	49	8.018	8.150	8.095	0.037	-0.5
5	Phila*	10/3			2,654	2,654	7.746	9.388	8.352	0.467	
PSW1	PSW1		8.8		1,183	1,183	8.948	9.288	9.112	0.102	0.3
PSW2	PSW2_888		8.9		1,990	1,990	8.825	9.979	9.206	0.313	0.3
PSW3	PSW3_889		9.0		64	64	9.967	10.065	10.003	0.020	1.0
6	Bucks	22/1			2,610	2,610	10.404	12.510	11.947	0.571	
BSW1	BSW1_1636		9.1		512	512	10.634	11.481	11.044	0.227	1.9
BSW2	BSW2_1636		10.1		1,150	1,150	10.404	12.485	11.980	0.376	1.9

** Stillwater elevations converted to NAVD*

Conclusion: Since the SWEL is a straight comparison to the R3 Results, in this comparison we were looking for areas with +/- 1-foot of difference. This would flag any areas where one would expect a significant deviation from the Published SWEL.

There were six such areas identified during this analysis. Four were in Sussex County and all four show areas where the Published SWEL was significantly lower than the R3 Results. These ranged from 1.3-feet less to 3.2-feet less than the R3 Results.

Two of the areas were in Bucks County and both areas showed that the R3 Results were 1.9-feet higher than the Published SWEL.

All six of the areas identified in this comparison are shown on the following map.

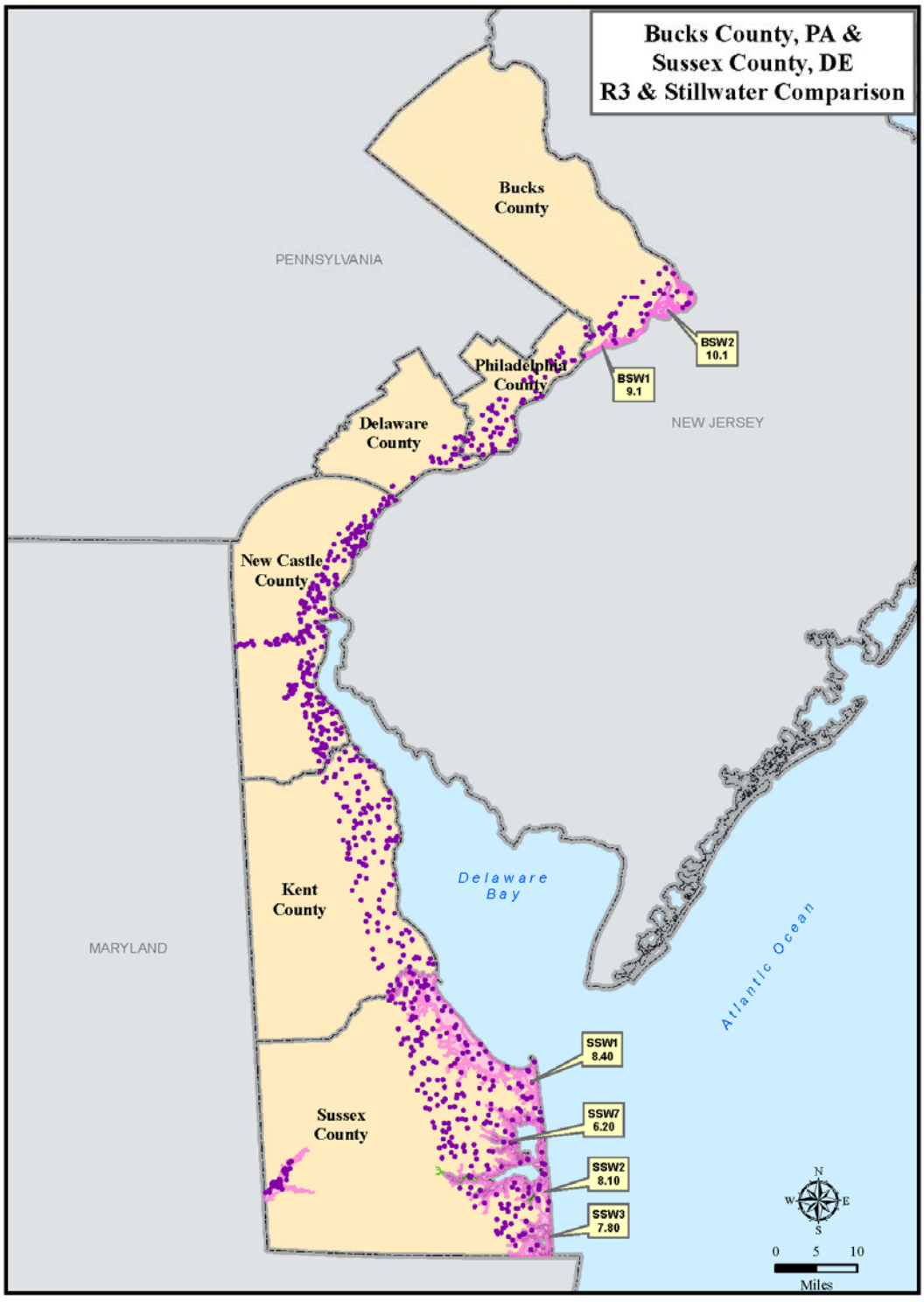
Bucks County, PA &
Sussex County, DE
R3 & Stillwater Comparison
Bucks County
PENNSYLVANIA
BSW2
10.1
BSW1
9.1
Philadelphia County
Delaware County
NEW JERSEY
New Castle County
Kent County
Delaware Bay
MARYLAND
Atlantic Ocean
SSW1
8.40
SSW7
6.20
SSW2
8.10
SSW3
7.80
Sussex County
N
W
E
S
0
5
10
Miles

Riverine BFE Analysis

The following maps show some of the results of the riverine BFE analysis. For this analysis we were primarily looking for one area of potential concern; locations where the R3 Results do not extend out to the most downstream riverine BFE and the riverine BFE is lower than the adjacent R3 Results. Two examples of this scenario are shown on the following map, and their generalized locations are shown on the subsequent location map. During the mapping process, these areas would require that the elevations from the R3 Results extend inland further than what is shown in the effective. The tidal elevation will intersect with the riverine profile at a point further inland than the effective.

Conclusion: While the two areas identified on the maps will need to be addressed during mapping of the floodplain, they do not represent any areas of further concern for the R3 Results.

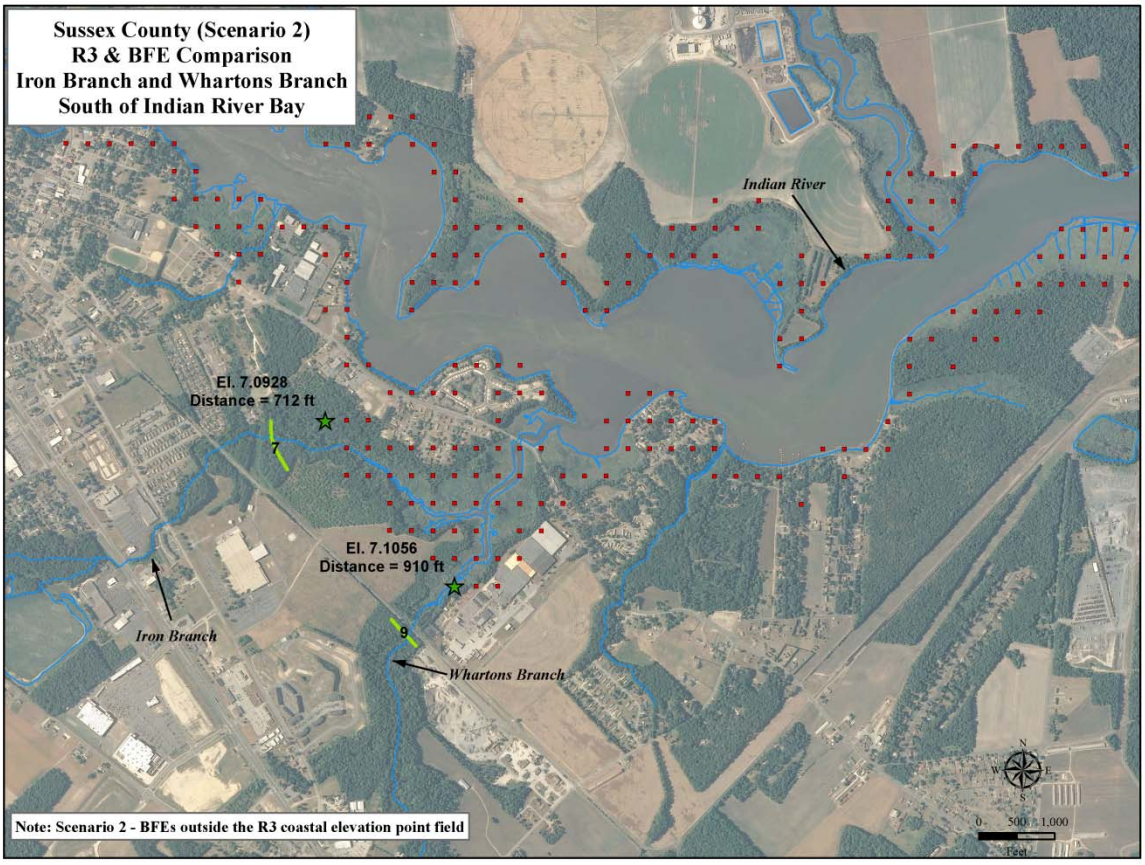
Sussex County (Scenario 2)
R3 & BFE Comparison
Iron Branch and Whartons Branch
South of Indian River Bay
Indian River
El. 7.0928
Distance = 712 ft
7
El. 7.1056
Distance = 910 ft
9
Iron Branch
Whartons Branch
Note: Scenario 2 - BFEs outside the R3 coastal elevation point field
N
W
E
S
0
500
1,000
Feet

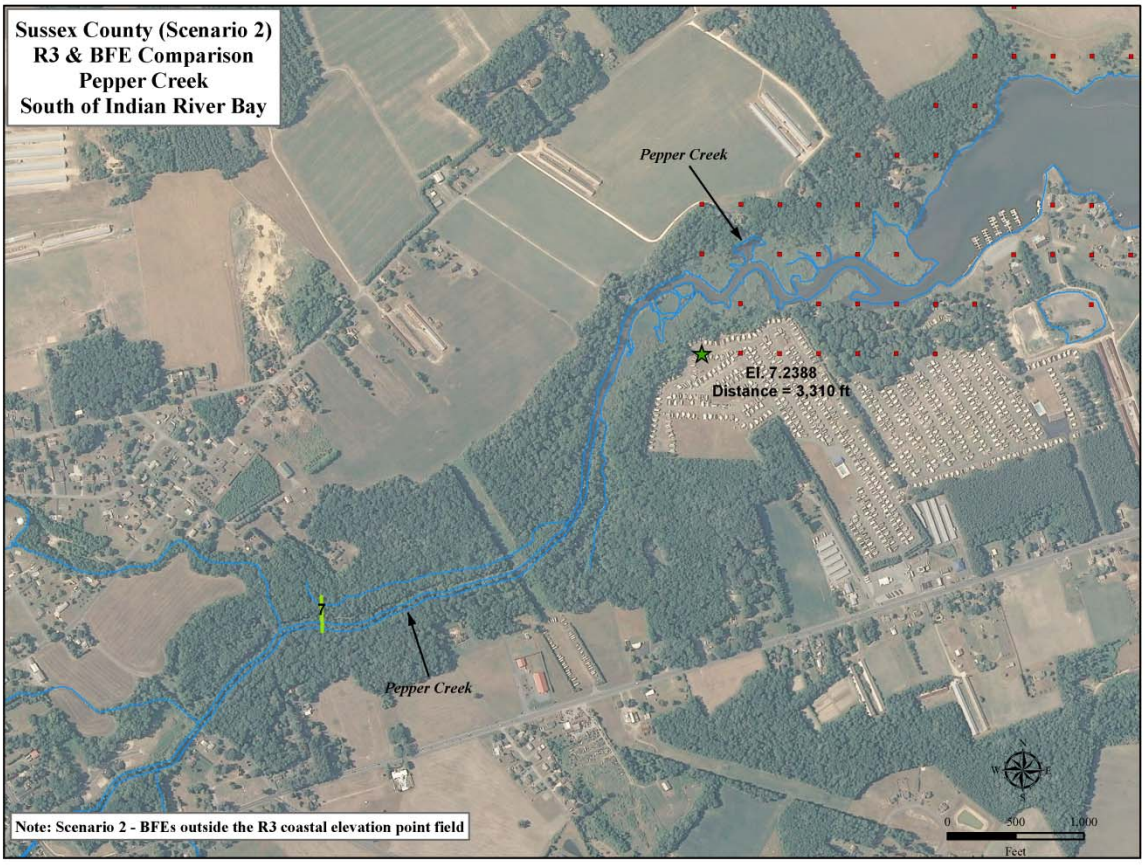
Sussex County (Scenario 2)
R3 & BFE Comparison
Pepper Creek
South of Indian River Bay
Pepper Creek
El. 7.2388
Distance = 3,310 ft
7
Pepper Creek
Note: Scenario 2 - BFEs outside the R3 coastal elevation point field
N
W
E
S
0
500
1,000
Feet

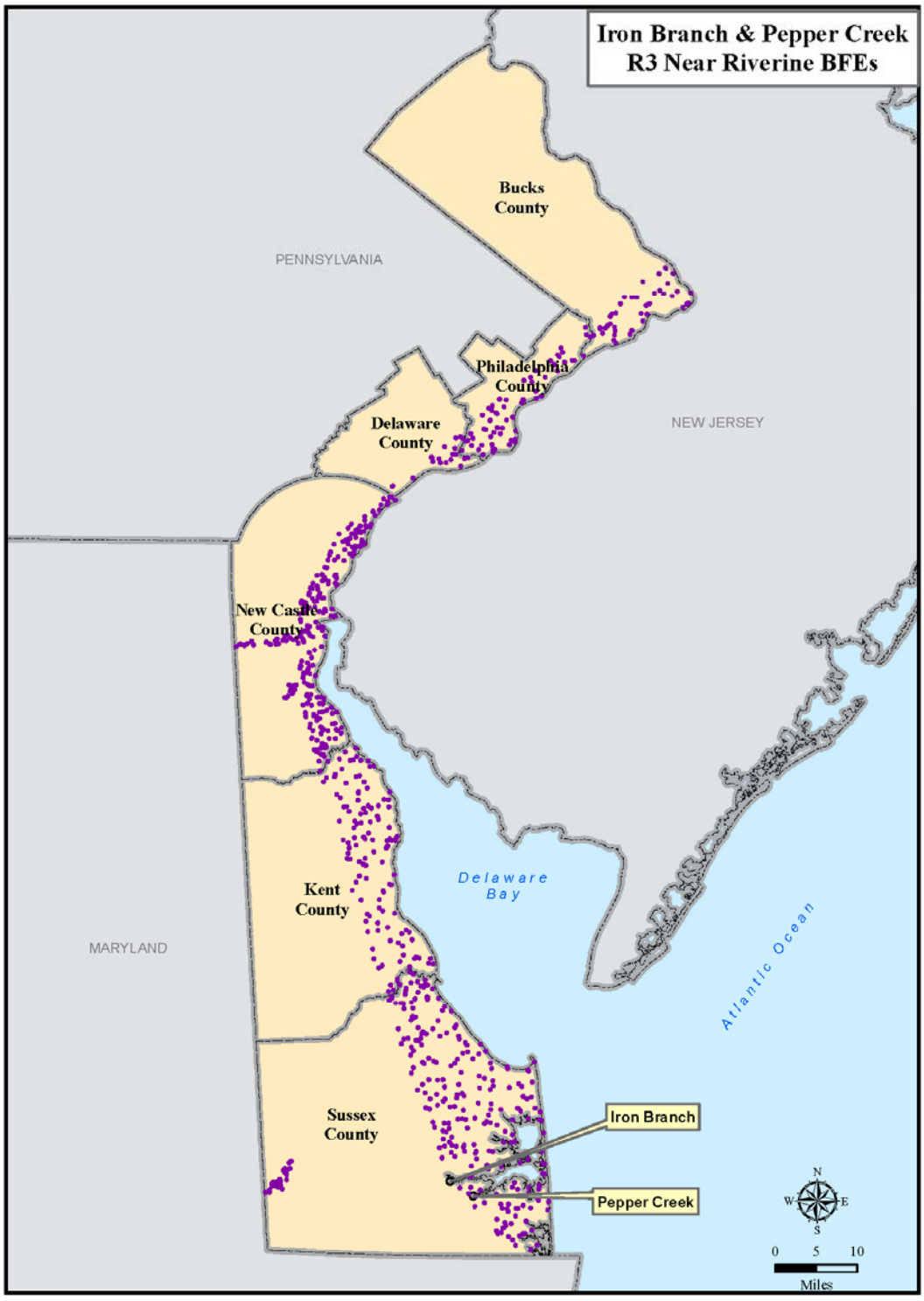
Iron Branch & Pepper Creek
R3 Near Riverine BFEs
Bucks County
PENNSYLVANIA
Philadelphia County
Delaware County
NEW JERSEY
New Castle County
Kent County
MARYLAND
Delaware Bay
Atlantic Ocean
Sussex County
Iron Branch
Pepper Creek
N
W
E
S
0 5 10
Miles

Overall Conclusions

The map on the following page shows a compilation of all areas identified during this review. While it is interesting to see that the majority of the areas of concern are located in Sussex County, it is also important to note that the results are consistent with the SWEL differences that have been presented up to now by the modeling team (meaning, slightly higher results expected within the Delaware Bay and slightly lower results on the open coast).

However, the one area of concern is the uppermost reaches of the tidal Delaware River in Bucks County, PA. The SWEL differences as you travel upstream along the Delaware River show a very good correlation until you reach the northern boundary of the City of Philadelphia and Bucks County. At that point, the R3 Results are almost 2-feet higher than previous SWELs. This review concludes that this area should be looked at further for explanation as questions may arise during the remainder of the study process.

Additional Effective Profile Comparison

An additional analysis was performed for Bucks County based on the findings above. Since this area of the Delaware River represents the transition from tidally controlled elevations to fluvial, the comparison of R3 Results to SWEL elevations was not valid here. During the SWEL comparison, a single SWEL value was assigned to rather large areas of the River. The problem with this type of analysis in this area of the River is that the comparison is of a large area with a static SWEL to a River which is transitioning to a fluvial condition, and therefore changing much faster than in areas closer to the Bay.

In order to better compare effective elevations to the R3 Results, this report looked at the effective tidal profiles in Bucks County by municipality, moving from Downstream to Upstream (all elevations referenced are in NAVD ’88 vertical datum).

The effective tidal profile for Bensalem Township averages about 10.1 throughout the Township. The R3 Results average about 10.9; an average difference of about 0.8-foot, which would not otherwise be flagged for further investigation.

The effective tidal profile for Bristol Township ranges from about 10.1 to 11.3 throughout the Township. The R3 Results range from about 11.3 to 11.7; an average difference of about 0.8-foot, which would not otherwise be flagged for further investigation.

The effective tidal profile for Bristol Borough ranges from about 10.2 to 11.1 throughout the Borough. The R3 Results average about 11.6; an average difference of about 0.8-foot, which would not otherwise be flagged for further investigation.

The effective tidal profile for Tullytown Borough averages about 11.6 throughout the Borough. The R3 Results average about 11.7; an average difference of about 0.1-foot, which would not otherwise be flagged for further investigation.

Upstream of Tullytown, fluvial conditions begin to control and the R3 Results will not be used.

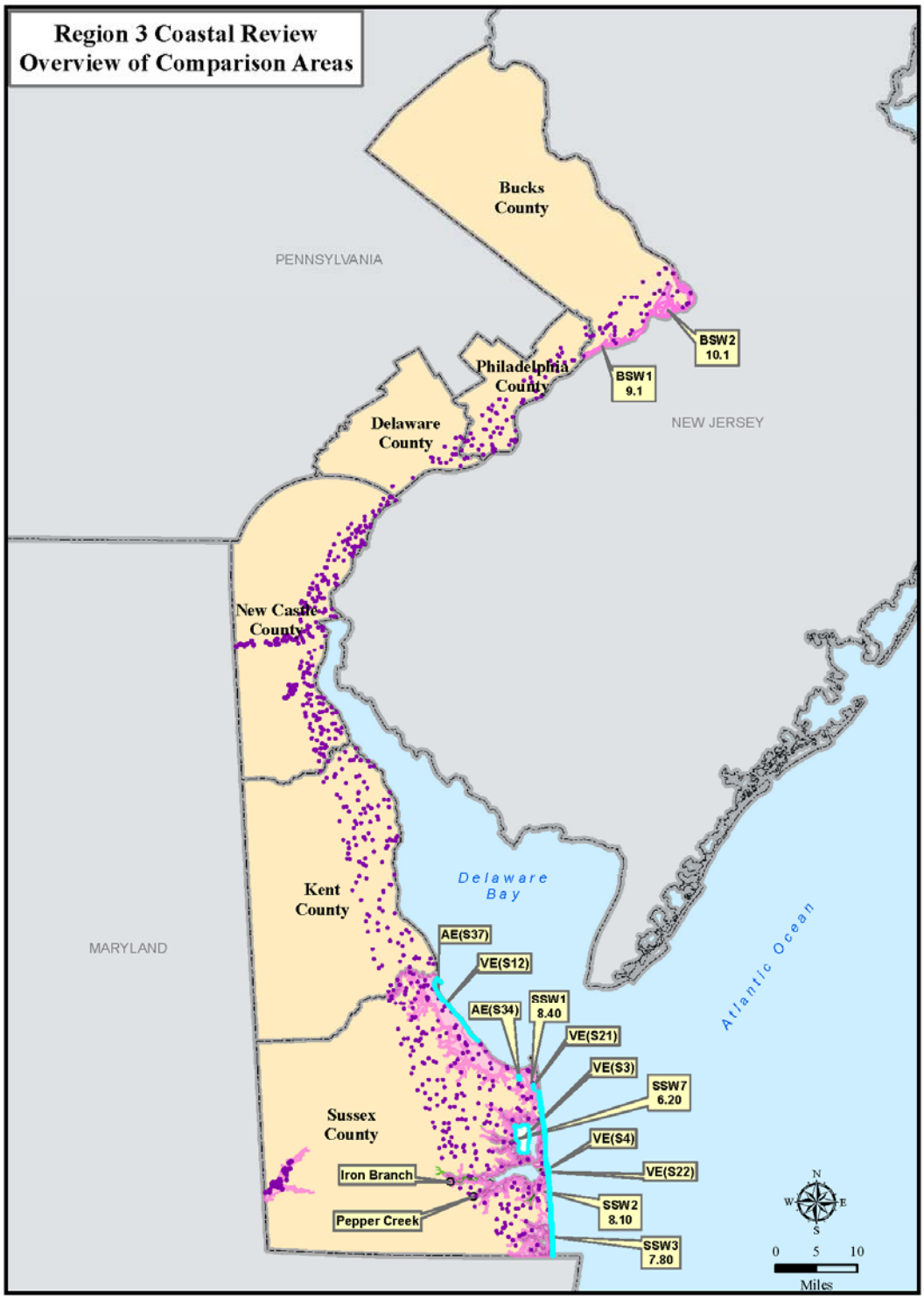
Region 3 Coastal Review
Overview of Comparison Areas
Bucks County
PENNSYLVANIA
Philadelphia County
Delaware County
NEW JERSEY
New Castle County
Kent County
MARYLAND
Sussex County
Delaware Bay
Atlantic Ocean
BSW2 10.1
BSW1 9.1
AE(S37)
VE(S12)
AE(S34)
SSW1 8.40
VE(S21)
VE(S3)
SSW7 6.20
VE(S4)
VE(S22)
SSW2 8.10
SSW3 7.80
Iron Branch
Pepper Creek
N
W
E
S
0 5 10
Miles

Appendix D: Assessment of the SDERL Pre-Processing Error for the Region III FIS Project

Assessment of the Surface Directional Effective Roughness Length (SDERL) pre-processing error for the Region 3 FIS project.

Date: 7 Mar 2012

Brian Blanton and Rick Luettich

Overview: Standard wind velocity input to ADCIRC is assumed to represent wind conditions at 10m above a marine (water) surface. ADCIRC can optionally read in a node-based, roughness length that is used to adjust the wind velocity to account for differences between the roughnesses of a land surface and a marine surface. (Generally, land is rougher than water and therefore winds blowing over land are reduced compared to their value if they are blowing over water.) It is assumed that the atmospheric boundary layer adjusts to the surface roughness over a finite horizontal distance (boundary layer adjustment length) and therefore the effective roughness at any node reflects the roughness conditions in the upwind direction over the boundary layer adjustment length. Thus the roughness length at any node may vary depending on the upwind direction.

The ADCIRC nodal attribute ***surface_directional_effective_roughness_length*** (sderl) allows the user to specify a directionally dependent roughness length. Typically, the USGS National Land Cover Database (NLCD) is used to determine the directional roughness at each model node. Since sderl is only a function of the grid, the land cover and the wind direction, it is computed as a pre-processing step prior to an ADCIRC model run. ADCIRC is configured to use 12 30-deg directional bins, centered at 0, 30, … 330 degrees. Currently there are several, independently developed, utility programs available that compute and store 12 roughness lengths for each node in the ADCIRC grid. This information is communicated to ADCIRC as a table in the nodal attribute (fort.13) file in which each row corresponds to a specified node number in the grid and there is one column for the roughness length in each of the 12 directional bins. Generally, open water nodes that are not influenced by land roughnesses (i.e., land is farther away than the boundary layer adjustment length) are not recorded to the fort.13 file. Figure 1 displays the 12 directional bins as well as the roughness lengths at one selected node in the grid.

Recently an inconsistency was discovered between the column ordering in the directional roughness utility program developed at UNC and posted to the adcirc.org website and the column ordering used by ADCIRC to read in this information. The details of this inconsistency are described below.

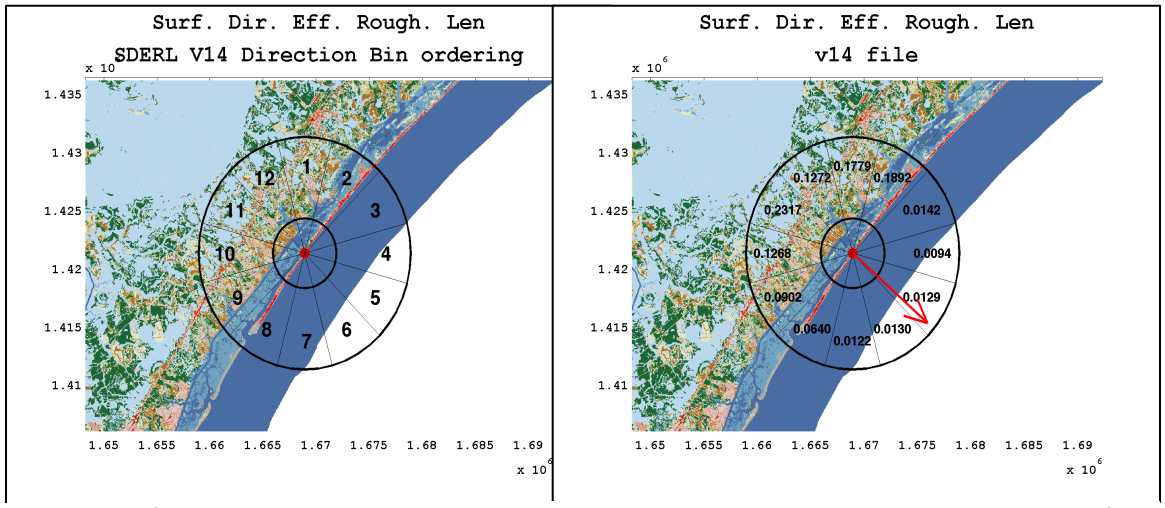

Figure 1: Left) Bin ordering in the pre-processing code that builds the SDERL nodal attribute. Right) the resulting roughness coefficients in the 12 bins at the node location (red dot). Note that the roughness lengths are larger over land.

In version 14 and earlier versions of the directional roughness utility program, a wind blowing from true north is assumed to be coming from 0 degrees; increasing angles proceed clockwise around the compass. This is shown in Figure 1 (left), where the actual NLCD data is shown for coastal NC. The 12 directional sectors are drawn, centered at a node on the coast. Note that bin 1 is pointing to true north, and the bin numbering proceeds *clockwise*.

Consider a wind vector pointing offshore at this coastal node (red arrow in Figure 1, right). Since the wind is blowing over land toward the open water, one expects that the effective wind speed should be reduced by an amount that is a function of the land roughness UPSTREAM of the direction to which the wind is blowing. Thus, in this example, the roughness length of 0.2317 should be used in the reduction process, since it is in the bin opposite to the bin containing the wind direction.

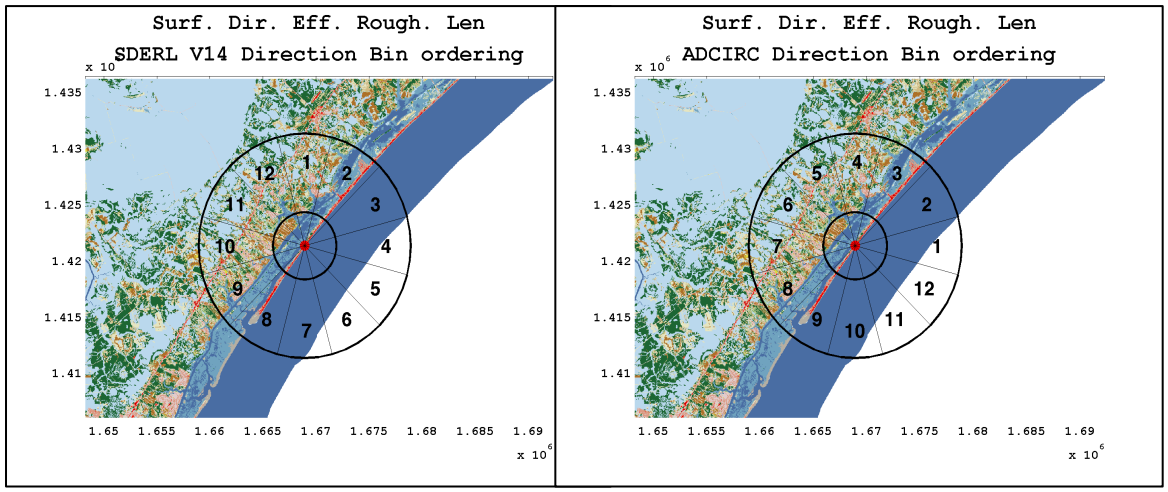

Figure 2: Directional bin ordering for the v14 SDERL code (left) and ADCIRC's assumptions about the bin ordering (right).

However, ADCIRC computes the wind direction as atan2(y,x), which assumes that 0 degrees is true EAST, and that increasing angle values proceed COUNTERclockwise. This is shown in Figure 2 (right). In addition to this compass issue, ADCIRC uses the direction the wind is blowing TOWARDS, instead of the direction the wind is blowing FROM, as a reference direction to identify the proper roughness value.

To account for these three issues (True North vs. True East as 0 deg, CW vs CCW as bin ordering, and TOWARD vs. FROM bin selection), the pre-processing code has been modified to output the 12 roughness coefficients in an order consistent with ADCIRC's bin determination and selection. Figure 3 shows the results of this modification, where Roughness length values for the node shown with the red dot, for the v14 and v16 SDERL nodal attribute. The red arrow represents a wind blowing in the offshore direction. The expectation is that the roughness length that affects this wind direction should be higher since the wind is blowing from land to open water. In the v16 case, the resulting roughness length is 0.2317. Note that this value (0.2317) is in the opposite land sector in the v14 ordering (see right panel of Figure 1).

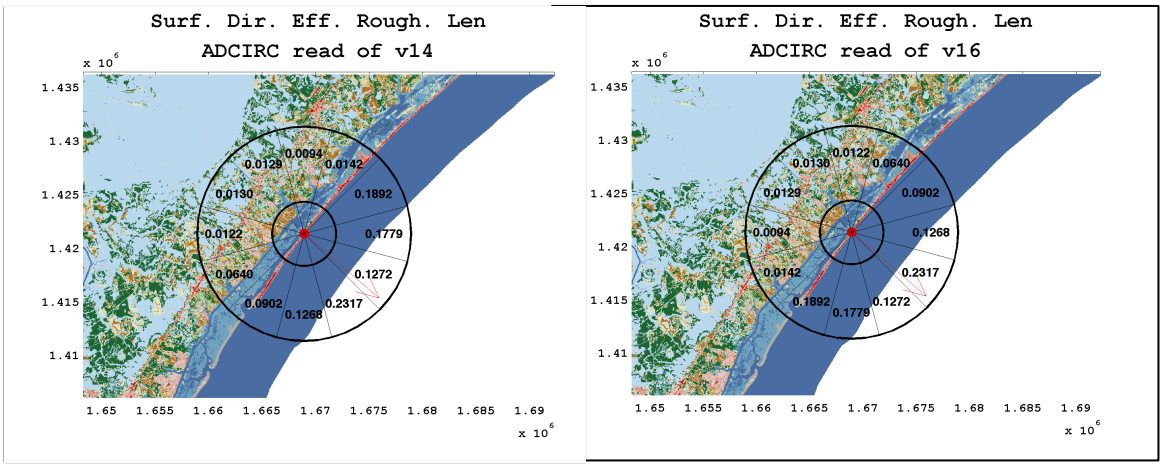

Figure 3: Roughness length values for the node shown with the red dot, for the v14 and v16 SDERL nodal attribute.

Effect on 10-meter winds.

In areas affected by land**,** ADCIRC uses the roughness length to compute a wind velocity that is reduced from the standard marine wind velocity. This is shown in the equations below, in which the wind velocity used to compute the wind stress (tau) is scaled by the ratio of marine and land roughness lengths.

$$
\begin{aligned}
\tau &= \rho_a c_d |\mathbf{W}_{10}| \mathbf{W}_{10} \\
c_d &= (0.75 + 0.067|\mathbf{W}_{10}|) \times 10^{-3} \quad \text{(Garrett 1977) } c_d \leq \text{ upper limit} \\
\mathbf{W}_{10} &= \mathbf{W}_{10,marine} \quad \text{10 meter wind velocity over water} \\
\mathbf{W}_{10} &= \mathbf{W}_{10,land} \quad \text{10 meter wind velocity over land and shadows} \\
\mathbf{W}_{10,land} &= \mathbf{W}_{10,marine} \left[\frac{Z_{0,marine}}{Z_{0,land}} \right]^{0.0706} \quad \text{(BL similarity)}
\end{aligned}
$$

Table 1 shows the ratio between roughness lengths in the V16 and V14 version of the SDERL code and the resulting ratio in the 10-meter wind speed. This table indicates that a two fold error in the roughness length causes 5 percent error in wind speed, while an order of magnitude error in the roughness length causes a 15 - 18 percent error in wind speed.

Table 1: Ratio of roughness lengths between V16 and V14 and resulting ratio of 10-meter wind speed.

$\frac{Z_{0,land,v16}}{Z_{0,land,v14}}$	$\frac{\lvert\mathbf{W}_{10,land,v16}\rvert}{\lvert\mathbf{W}_{10,land,v14}\rvert}$
0.1	**0.85**
0.5	**0.95**
2	**1.05**
5	**1.12**
10	**1.18**

Effect on simulated water levels.

To understand the effect of this issue on the simulated water levels, particularly in light of ongoing FEMA coastal FISs, the 29 extra tropical storms were recomputed with the revised (v16) sderl nodal attribute. The exact same computational system as was used in the FIS, and the grid version was the same (FEMA_R3_20110303_MSL). All other parameters are the same between the FIS (v14) simulations and the v16 simulations. The resulting maximum water level files were processed in the same way as in the FIS. Figure 5 shows the difference between the maximum across all simulations (MAAS) for the v16 and v14 simulations. Note that this difference is shown in ***FEET.*** Generally, the overall difference is less than 0.1 ft. The differences are also generally larger (0.2 to 0.4 ft) near the coast in Delaware Bay and up the narrow rivers in Chesapeake Bay. The largest difference occurs in the Indian River. However, the differences are still less than one foot. The distribution of the maximum differences is shown in Figure 4. The mean and standard deviation are .09 and .11 ft respectively, although the distribution is not gaussian.

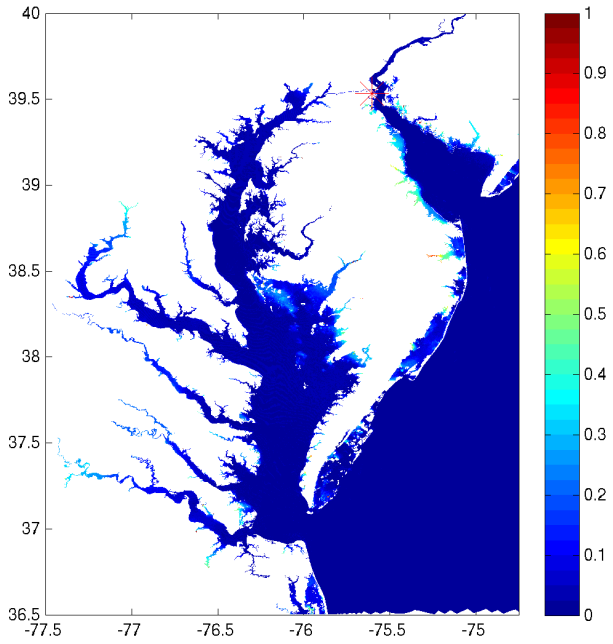

Figure 5: Difference in *FEET* between the V16 and V16 water level maximum across all storms (MAAS) for extra-tropicals.

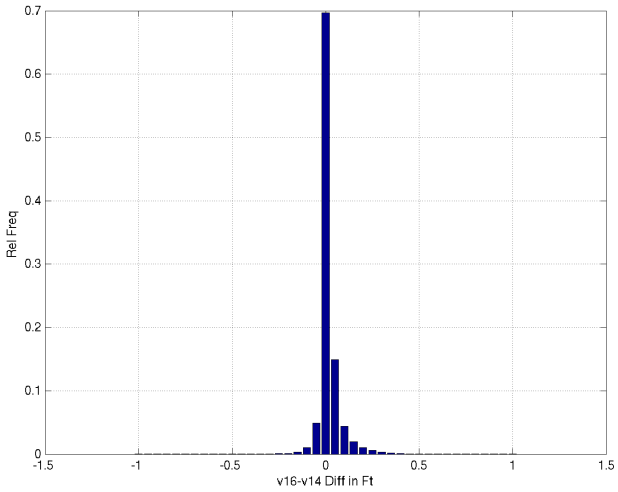

Figure 4: Distribution of differences in MAAS water levels between V16 and V14 extra-tropical simulations. The units are in *FEET*.

It is important to keep in mind that this difference is at the individual simulation level. A more relevant issue is the impact of this sderl issue on the statistical analysis. To address this aspect, the Empirical Simulation Technique (EST) analysis was recomputed for the V16 extra-tropicals and the EST analysis was recomputed. The resulting 1% return levels were then compared between the two data sets. An example of the EST analysis is shown in Figure 6 for one node on the western Delaware Bay coast.

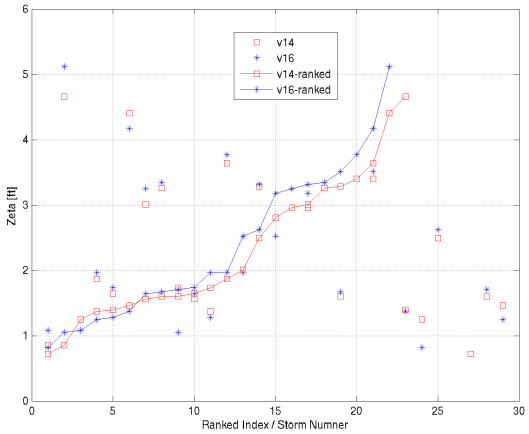

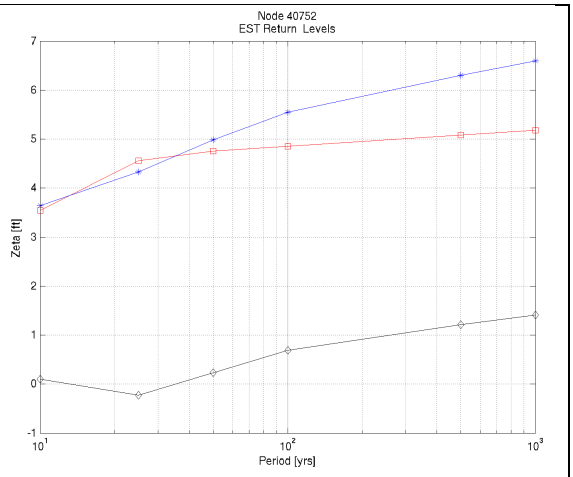

Figure 6: Example of extra-tropical surge response (left) and EST analysis (right) for one node in western Delaware Bay. The left panel shows both raw and ranked surge. Note that the v16 responses are generally higher by about .1-.2 feet. The right panel shows the computed EST return levels. The 1% return level difference is about .6 feet.

Figure 7 shows the difference in 1% levels between the V16 and V14 EST analyses. The units are in *FEET*. The VA and MD open coast is generally unaffected, as is the open water within the bays and on the continental shelf. The largest differences are along the western Delaware Bay coast, where the differences reach about .6 ft. Areas in the middle, eastern Chesapeake Bay also reach 0.4 – 0.5 ft.

The distribution of the differences is shown in Figure 8. Only nodes within the depth range of 1 meter up to the inland extent of the 1000-year surface are considered, to remove the effect of the large number of open-water nodes for which the differences are near zero. Since these locations are generally not used in subsequent overland analyses, it seems appropriate to eliminate them from the statistics. The mean and standard deviation of this difference is .06 and .10 ft, respectively.

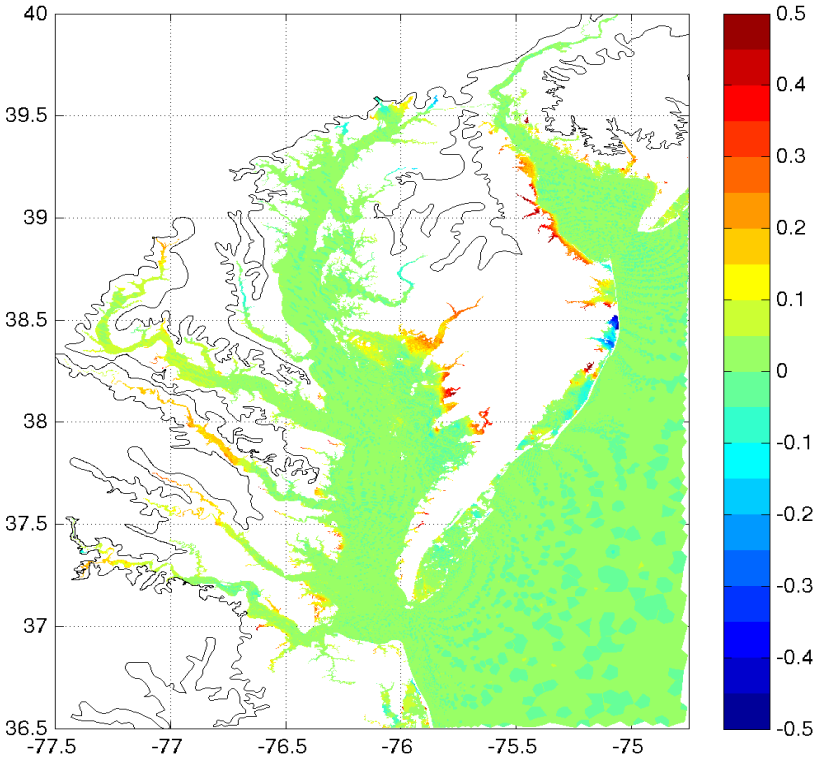

Figure 7: Difference in *FEET* at the 1% level between the V16 and V14 EST analysis.

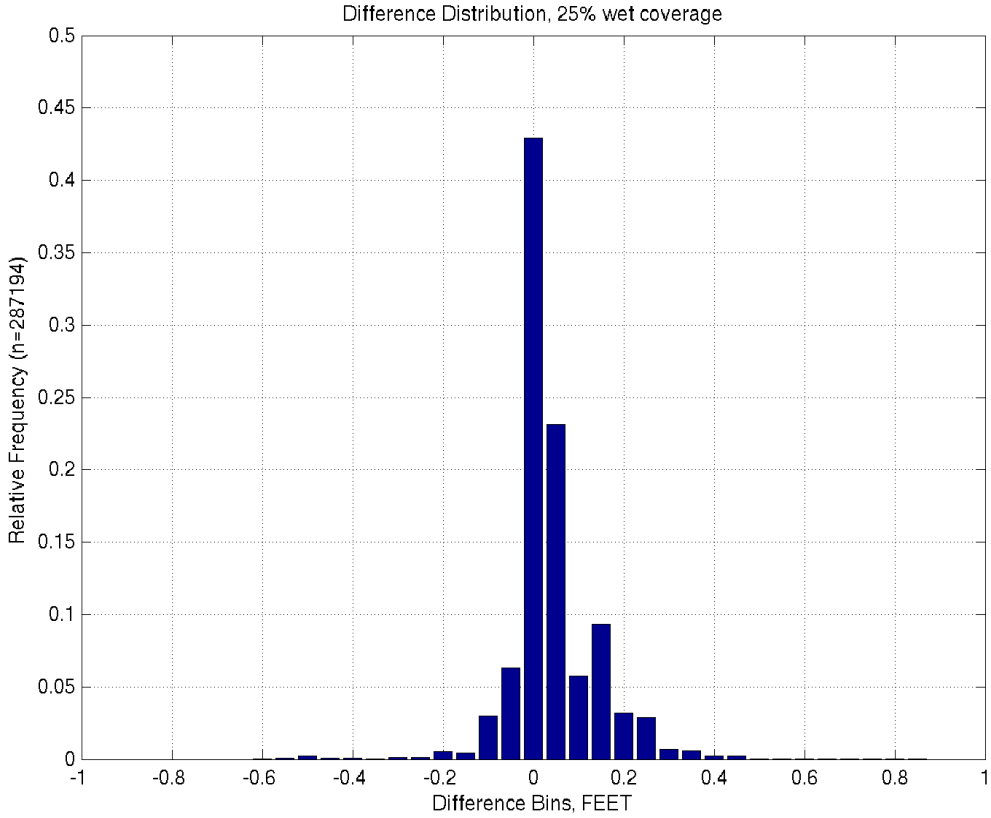

Figure 8: Distribution of differences between the V16 and V14 1% levels within the study region.

There are two areas that have larger than 0.5 ft (in absolute value), as can be seen in Figure 7 and Figure 8. The first area is in the upper end of Newport Bay (which is itself in at the upper end of Chincoteague Bay). The differences here are positive, meaning that the V16 results are higher than the V14 results. This particular area is one in which not all of the ET storms wet the ADCIRC nodes (for ADCIRC nodes on land). In this case (which is also typical of the other areas with relatively larger differences over land), the EST results are subject to larger uncertainties. This is illustrated in Figure 9 for a node on land in upper Newport Bay. The V14 results are shown with the 99, 95, and 90% confidence limits (blue, red, green, and magenta, respectively) along with the V16 results (black). Eight of the 29 storms wet this node, and the width of the 95% confidence interval at the 100-yr level is about .4 meters (1.3 ft). Note that the V16 results (black line) are higher than the V14 results (as indicated in the spatial plot in Figure 7) from about 50 years and greater, and that above about 90 years, the V16 results are at or above the V14 EST uncertainty estimates.

This can be compared to results at an open-coast node where there is little difference in the 1% values Figure 10 shows the same quantities as in Figure 9 except for an open-coast node along the northern MD shore. The 1% values are 1.60 and 1.61 m for the V16 and V14 results, respectively.

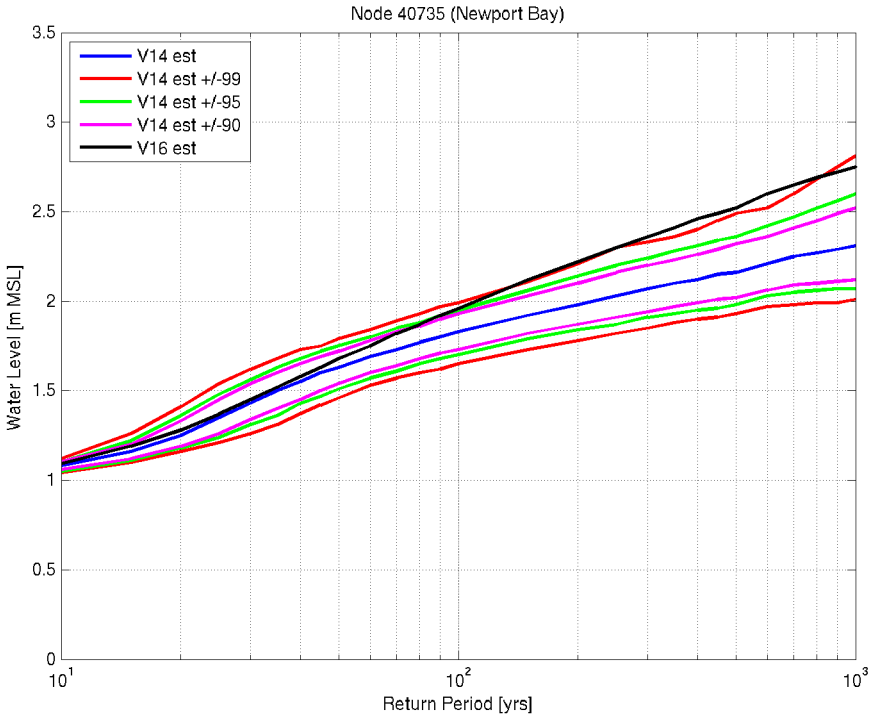

Figure 9: EST analysis with uncertainty estimates for a Newport Bay node on land. V16 results are shown with the black line. The other lines are V14 results with associated 99, 95, and 90% confidence limits.

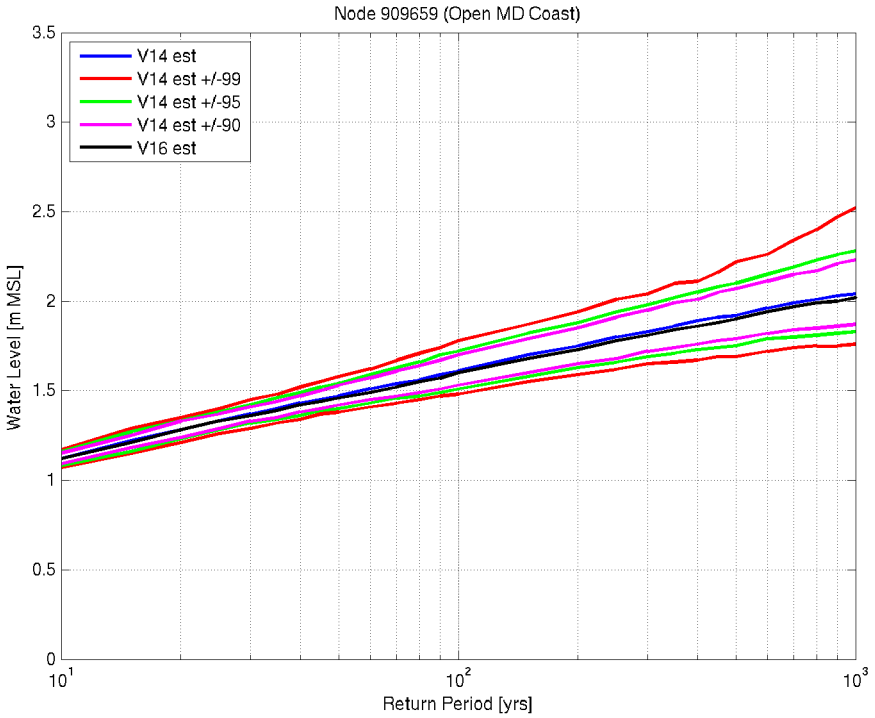

Figure 10: EST analysis with uncertainty estimates for an open-coast node along the northern MD shore. V16 results are shown with the black line. The other lines are V14 results with associated 99, 95, and 90% confidence limits.

REPORT DOCUMENTATION PAGE

Form Approved
OMB No. 0704-0188

Public reporting burden for this collection of information is estimated to average 1 hour per response, including the time for reviewing instructions, searching existing data sources, gathering and maintaining the data needed, and completing and reviewing this collection of information. Send comments regarding this burden estimate or any other aspect of this collection of information, including suggestions for reducing this burden to Department of Defense, Washington Headquarters Services, Directorate for Information Operations and Reports (0704-0188), 1215 Jefferson Davis Highway, Suite 1204, Arlington, VA 22202-4302. Respondents should be aware that notwithstanding any other provision of law, no person shall be subject to any penalty for failing to comply with a collection of information if it does not display a currently valid OMB control number. **PLEASE DO NOT RETURN YOUR FORM TO THE ABOVE ADDRESS.**

1. REPORT DATE *(DD-MM-YYYY)*	2. REPORT TYPE	3. DATES COVERED *(From - To)*
November 2013	Report 5 in a series	

4. TITLE AND SUBTITLE
Coastal Storm Surge Analysis: Storm Surge Results;
Report 5: Intermediate Submission No. 3

5a. CONTRACT NUMBER

5b. GRANT NUMBER

5c. PROGRAM ELEMENT NUMBER

6. AUTHOR(S)
Jeffrey L. Hanson, Michael F. Forte, Brian Blanton, Mark Gravens, and Peter Vickery

5d. PROJECT NUMBER

5e. TASK NUMBER

5f. WORK UNIT NUMBER

7. PERFORMING ORGANIZATION NAME(S) AND ADDRESS(ES)

Coastal and Hydraulics Laboratory
US Army Engineer Research and Development Center
3909 Halls Ferry Road
Vicksburg, MS 39180-6199

8. PERFORMING ORGANIZATION REPORT NUMBER

ERDC/CHL TR-11-1

9. SPONSORING / MONITORING AGENCY NAME(S) AND ADDRESS(ES)
Federal Emergency Management Agency
615 Chestnut Street
One Independence Mall, Sixth Floor
Philadelphia, PA 19106-4404
Under US Army Corps of Engineers Work Unit J64C87

10. SPONSOR/MONITOR'S ACRONYM(S)

11. SPONSOR/MONITOR'S REPORT NUMBER(S)

12. DISTRIBUTION / AVAILABILITY STATEMENT
Approved for public release; distribution is unlimited.

13. SUPPLEMENTARY NOTES

14. ABSTRACT

The Federal Emergency Management Agency (FEMA), Region III office, has initiated a study to update the coastal storm surge elevations within the states of Virginia, Maryland, and Delaware, including the Atlantic Ocean, Chesapeake Bay (including its tributaries), and the Delaware Bay. This effort is one of the most extensive coastal storm surge analyses to date, encompassing coastal floodplains in three states and including the largest estuary in the world. The study will replace outdated coastal storm surge stillwater elevations for all Flood Insurance Studies in the study area, and serve as the basis for new coastal hazard analyses and ultimately updated Flood Insurance Rate Maps (FIRMs). Study efforts were initiated in August of 2008, and were concluded in 2013.

The storm surge study utilized the ADvanced CIRCulation Model for Oceanic, Coastal, and Estuarine Waters (ADCIRC) for simulation of two-dimensional hydraulics. ADCIRC was coupled with two-dimensional wave models to calculate the combined effects of surge and wind-induced waves. A seamless modeling grid was developed to support the storm surge modeling efforts.

This report is the fifth and final in a series for the project. It provides a detailed overview of the extratropical and tropical storm statistical analyses, treatment of tidal influences, and final water level recurrence interval results. Furthermore, the similarities and differences between the new results and earlier study findings are explored.

15. SUBJECT TERMS

FEMA Region III	Hurricane	ADCIRC
Extratropical Storm	Tropical Storm	Region III DEM
	Storm Surge SWAN	

16. SECURITY CLASSIFICATION OF:			17. LIMITATION OF ABSTRACT	18. NUMBER OF PAGES	19a. NAME OF RESPONSIBLE PERSON
a. REPORT	b. ABSTRACT	c. THIS PAGE			19b. TELEPHONE NUMBER *(include area code)*
Unclassified	Unclassified	Unclassified		104	